AD-A087 403 MCDONNELL DOUGLAS RESEARCH LABS ST LOUIS MO F/G 20/14
RADIATION AND SCATTERING FROM BODIES OF TRANSLATION, VOLUME II,--ETC(U)
APR 80 L N MEDGYESI-MITSCHANG, J M PUTNAM F30602-77-C-0233
UNCLASSIFIED RADC-TR-80-142-VOL-2 NL

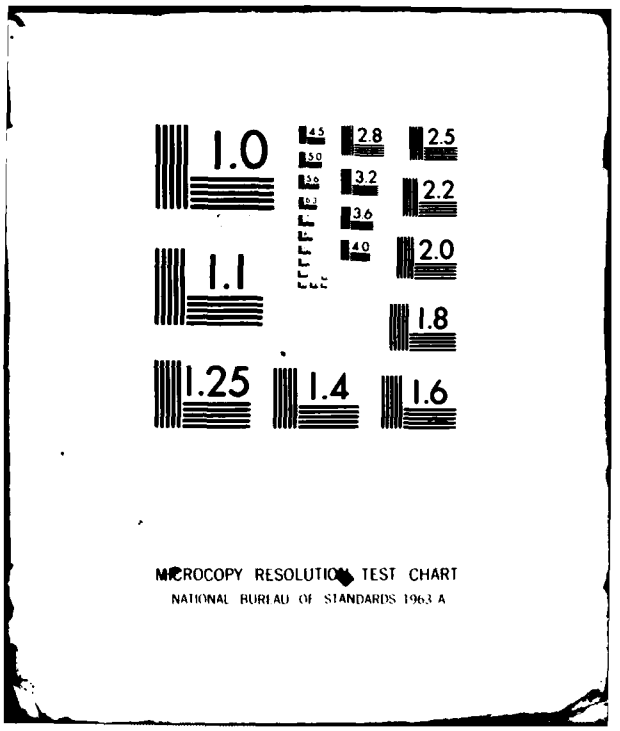
1.0
1.1
1.25
1.4
1.6
1.8
2.0
2.2
2.5
2.8
3.2
3.6
4.0
4.5
5.0
5.6
6.3
MICROCOPY RESOLUTION TEST CHART
NATIONAL BUREAU OF STANDARDS 1963 A

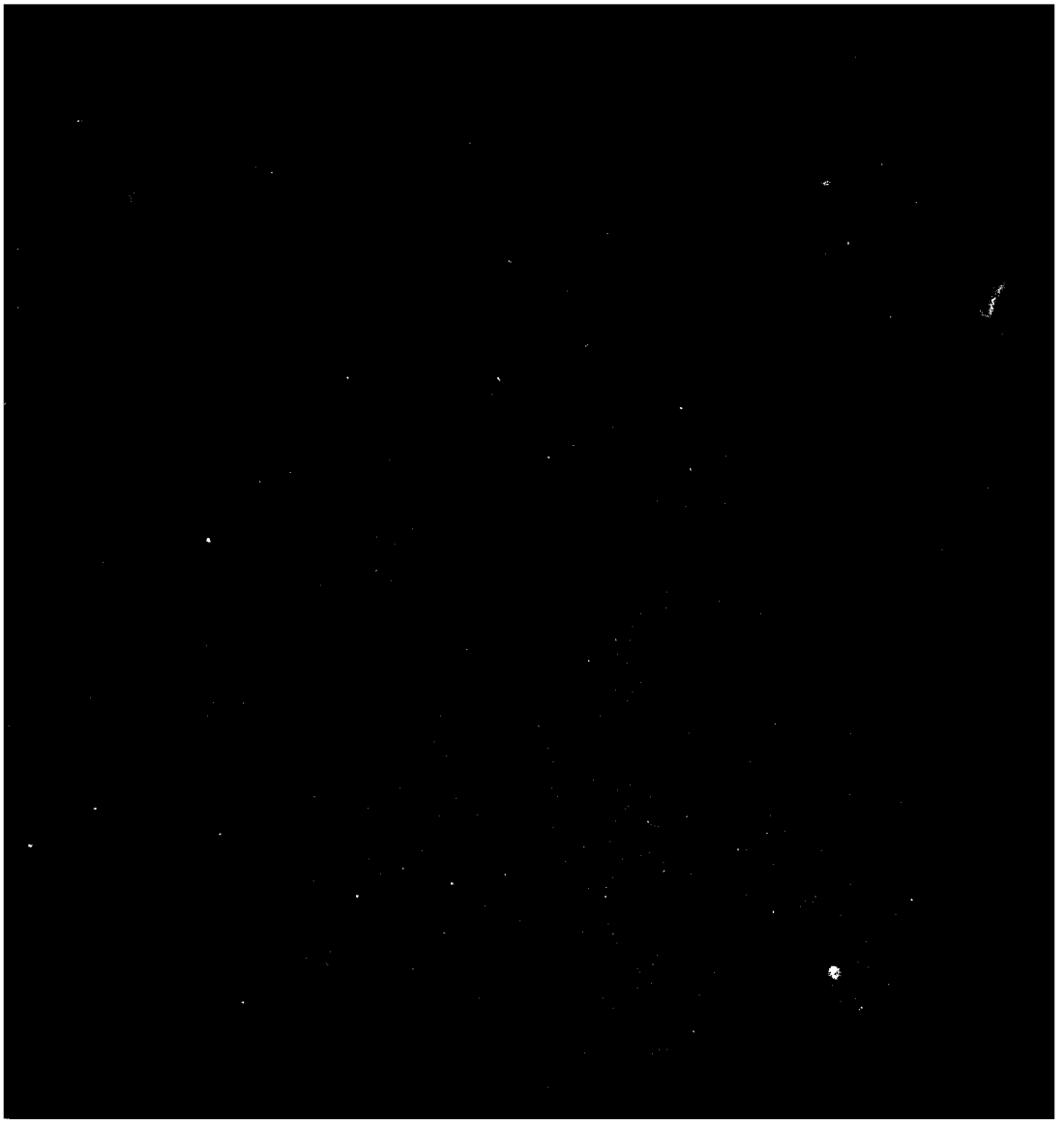

DISCLAIMER NOTICE

THIS DOCUMENT IS BEST QUALITY PRACTICABLE. THE COPY FURNISHED TO DTIC CONTAINED A SIGNIFICANT NUMBER OF PAGES WHICH DO NOT REPRODUCE LEGIBLY.

(19) TR-80-142-Vol-2

UNCLASSIFIED

SECURITY CLASSIFICATION OF THIS PAGE (When Data Entered)

REPORT DOCUMENTATION PAGE

READ INSTRUCTIONS BEFORE COMPLETING FORM

(18) 1. REPORT NUMBER: RADC-TR-80-142, Vol II (of three)

2. GOVT ACCESSION NO.: AD-A084 403

3. RECIPIENT'S CATALOG NUMBER:

(6) 4. TITLE (and Subtitle): RADIATION AND SCATTERING FROM BODIES OF TRANSLATION, Volume II, User's Manual, Computer Program Documentation

(9) 5. TYPE OF REPORT & PERIOD COVERED: Final Technical Report, 26 Sep 77 — 26 Jul 79

6. PERFORMING ORG. REPORT NUMBER: N/A

(10) 7. AUTHOR(s): L. N. Medgyesi-Mitschang, J. M. Putnam

(15) 8. CONTRACT OR GRANT NUMBER(s): F30602-77-C-0233

9. PERFORMING ORGANIZATION NAME AND ADDRESS: McDonnell Douglas Corporation, McDonnell Douglas Research Laboratories, St. Louis MO 63166

10. PROGRAM ELEMENT, PROJECT, TASK AREA & WORK UNIT NUMBERS: 62702F; (16) 23380308; (17) 23

11. CONTROLLING OFFICE NAME AND ADDRESS: Rome Air Development Center (RBCT), Griffiss AFB NY 13441

12. REPORT DATE: Apr 1980

13. NUMBER OF PAGES: 126

14. MONITORING AGENCY NAME & ADDRESS (if different from Controlling Office): Same (12) 126

15. SECURITY CLASS. (of this report): UNCLASSIFIED

15a. DECLASSIFICATION/DOWNGRADING SCHEDULE: N/A

16. DISTRIBUTION STATEMENT (of this Report)

Approved for public release; distribution unlimited.

17. DISTRIBUTION STATEMENT (of the abstract entered in Block 20, if different from Report)

Same

18. SUPPLEMENTARY NOTES

RADC Project Engineer: Daniel E. Warren (RBCT)

19. KEY WORDS (Continue on reverse side if necessary and identify by block number)

Radiation	Method of moments
Scattering	Near field analysis
Conducting surfaces	Aperture coupling

20. ABSTRACT (Continue on reverse side if necessary and identify by block number)

A hierarchy of computer programs implementing the method of moments for bodies of translation (MM/BOT) is described. The algorithm treats the far-field radiation and scattering from finite-length open cylinders of arbitrary cross section as well as the near fields and aperture-coupled fields for rectangular apertures on such bodies. The theoretical development underlying the algorithm is described in Volume I of this report. (Cont'd)

DD FORM 1 JAN 73 1473 EDITION OF 1 NOV 65 IS OBSOLETE

UNCLASSIFIED

SECURITY CLASSIFICATION OF THIS PAGE (When Data Entered)

40-315

Item 20 (Cont'd)

The structure of the computer algorithm is such that no a priori knowledge of the method of moments technique or detailed FORTRAN experience are presupposed for the user. A set of carefully drawn example problems illustrates all the options of the algorithm. For more detailed understanding of the workings of the codes, special cross referencing to the equations in Volume I is provided. For additional clarity, comment statements are liberally interspersed in the code listings, summarized in ~~Volume II.~~ the present volume.

TABLE OF CONTENTS

TABLE OF CONTENTS

LIST OF ILLUSTRATIONS

LIST OF ILLUSTRATIONS

LIST OF TABLES

1. INTRODUCTION

This manual is divided into two parts. Section 2 constitutes the user section, describing the overall flow of the codes, input data requirements, and parameter relations. At the end of the section, a series of sample problems is given to illustrate the use of the codes. Sample problem 1 exercises all parts of the computer algorithm and serves as a check case for the installation of the codes on a given machine. Section 3 provides a detailed description of all the codes and subroutines. The user need not make reference to Section 3 or to the analysis in Volume I of this report to successfully install and execute the algorithm on a particular computer system.

A brief synopsis of the main program features and options are listed below:

Flexible body geometry - The algorithm can treat a finite-length BOT of any asymmetric cross section. The analysis assumes that the body is open on the ends. Certain degenerate forms of the BOT configuration have also been analyzed with this algorithm such as flat plates, parabolic and square cylinders.

Arbitrary antenna placement and excitation - The algorithm treats single or multiple rectangular aperture (slot) antennas embedded in the BOT surface. Location of the antennas can be anywhere on the BOT. Spacing between adjacent apertures can be electrically small. All apertures can be asymmetric.

Surface currents - The algorithm outputs the surface currents on the BOT surface in spatial and modal form. Both the magnitude and the phase of the t- and z-directed components are given.

Choice of polarization and radiation planes - The radiated fields and the power gain, normalized to an isotropic radiator, are given in the user-specified planes for θ and ϕ polarization.

Arbitrary choice of sampling points for near fields - The electric and magnetic fields (six components in all) resulting from currents induced by antennas on the BOT or by incident fields are computed at user-specified points in the vicinity of the BOT surface.

Calculation of aperture-coupled fields - All the field components for the electromagnetic waves penetrating a passive rectangular aperture on the BOT are computed at user-specified sampling points. The size and location of the aperture are also user specified.

The foregoing features of the algorithm are demonstrated in the sample problems of Section 2.6. These features have been tested, and the corresponding results are in good agreement with available data. As in all modeling, caution must be exercised in applying this analysis to certain problems such as the computation of the edge diffraction from the BOT ends and the fields coupled through small apertures. To achieve sufficient accuracy, a large number of modes may be necessary in these problems.

2. USER SECTION

The MM/BOT computer codes are written in FORTRAN IV, consisting of five main-line programs (i.e., BOTZSS, BOTINV, BOTRA, BOTSCM, and BOTSCB) and one small utility program (BOTSEG) as shown in Figure 1. The five main-line programs use the same coordinate data file with minor deletions, depending on which of the above programs are run. In addition, two binary disk files, ZBOT and YBOT, are generated by the programs BOTZSS and BOTINV. All the programs have user-oriented inputs, which can be easily generated for a given problem. Examples demonstrating the input data requirements are discussed in Section 2.6.

2.1 Implementation of Computer Codes

All of the BOT computer codes are written in USA Standard FORTRAN IV, with the exception of end-of-file (EOF) checks in programs BOTINV, BOTRA, BOTSCM, and BOTSCB. The EOF checks given in the listings in Appendix C are specific to the compiler used in the program development (i.e., CDC CYBER 175 system). The functioning of the EOF checks in the present listings is as follows:

IF (EOF(u)) a,b

u - unit number to check.

a - statement label to branch to if an EOF is encountered.

b - statement label to branch to if an EOF is not encountered.

This EOF check occurs in the listings (Appendix C) at the following places:

BOTINV	line numbers 480, 1310, and 1870
BOTRA	line number 1500
BOTSCM	line number 1300
BOTSCB	line numbers 1330, 2125, 8310, and 8970

The device unit numbering convention is as follows:

unit number 5 - card reader

unit number 6 - line printer

unit number 1 - binary input disk file containing alternating records of lengths 2 and $2(NP-3)^2$ words, respectively. NP is the number of data points describing the BOT generating curve discussed in Section 2.2.

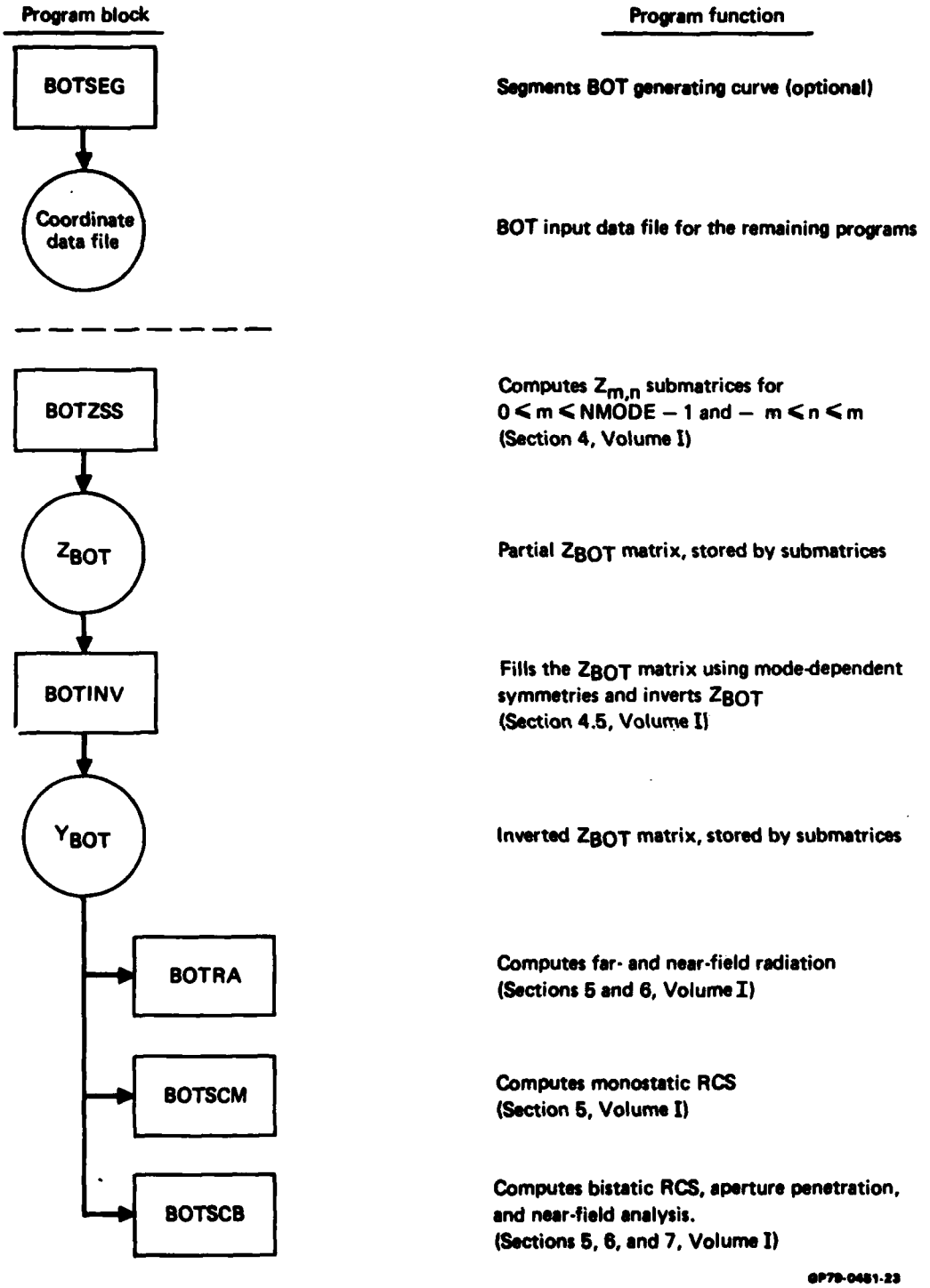

Figure 1. Overall flow diagram for MM/BOT algorithm.

unit number 2 - binary output disk file containing alternating records of lengths 2 and $2(NP-3)^2$ words, respectively.

2.2 BOTSEG Description

BOTSEG is a utility program, which can be used to segment the BOT generating curve using a limited set of data points (see coordinate geometry in Figure 2). The required input data and formats are described below.

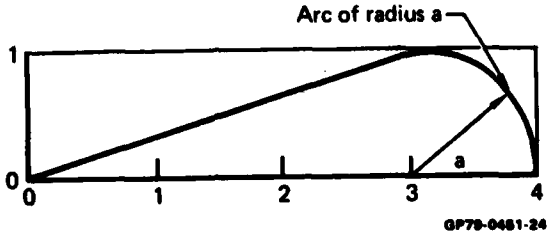

Figure 2. Representation of a BOT with a cross section formed by a wedge and arc segment.

```
      READ(5,1)NPTS,NP
1     FORMAT(2I3)
```

NPTS - Number of input data points used to describe the BOT generating curve.

NP - Number of equally spaced BOT generating curve data points to be calculated. (The calculated data are used as input to the remaining BOT programs.)

```
      DO 100 I = 1, NPTS
100   READ(5,2)XTAB(I),YTAB(I),XC(I),YC(I)
2     FORMAT(4E10.4)
```

XTAB(I) - x coordinate of the I-th point on the input curve (meters).

YTAB(I) - y coordinate of the I-th point on the input curve (meters).

XC(I),YC(I) - (meters) Indicate whether the points [XTAB(I), YTAB(I)] and [XTAB(I+1),YTAB(I+1)] are connected by a straight-line segment or an arc with changing radius. If XC(I) = YC(I) = 0, the segment is straight. Otherwise, [XC(I),YC(I)] is assumed to be the center of an arc

with the above end-points, where the radius changes linearly with angle from [XTAB(I),YTAB(I)] to [XTAB(I+1), YTAB(I+1)], subtending the angle of the triangle formed by the three points. Note, if the three points are colinear, the direction of the arc will be clockwise.

For example, consider a cylinder with a cross-section given in Figure 2. The generating curve for this body can be represented with three points (NPTS = 3) as follows:

0	0	0	0
3	1	3	0
4	0	0	0

BOTSEG is currently dimensioned to handle 100 points on the input curve and 83 points on the output curve. The NP data points used to represent the BOT generating curve determines the location and number of triangle functions and its derivatives (denoted by arrays T and TP in the codes), used to discretize the unknown currents on the BOT surface. As an example, Figure 2b shows a portion of a BOT generating curve defined by points τ_1, τ_2, τ_3 . . . τ_i with the triangle functions centered at τ_3, τ_5, etc. Note the triangle functions span five data points, with adjacent functions overlapping each other.

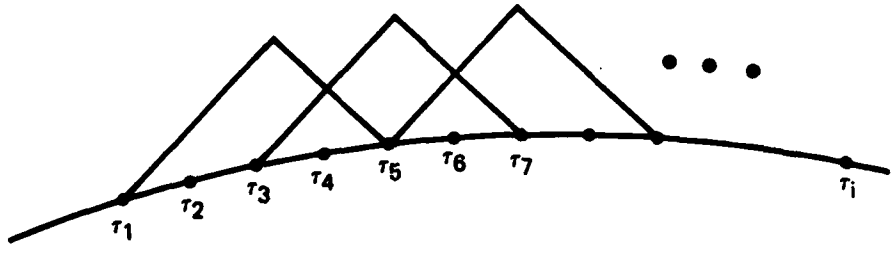

GP79-0461-106

Figure 2b. Triangle functions on BOT surface.

2.3 Input Data Description and Formats

A detailed description of the input data required by the five main-line MM/BOT codes is provided below. READ statements and formats are listed in the order in which they appear within the programs, followed by a description of the required data for each of the main-line MM/BOT codes.

2.3.1 Primary Data Set

This data set is read and required by all the programs.

```
READ(5,1)NMODE
1   FORMAT(I3)
```

NMODE - Number of non-negative modes to be considered (i.e., there will be 2*NMODE-1 total modes).

```
READ(5,2)NPT,NBAND
2   FORMAT(2I3)
```

NPT - Number of diagonal bands to be used in each $Z^{tt}_{m,n}$, $Z^{zt}_{m,n}$, $Z^{tz}_{m,n}$, and $Z^{zz}_{m,n}$ submatrix. NPT=1 indicates that only the diagonal terms are nonzero in each submatrix, NPT=2 indicates that only diagonal and off-diagonal terms are nonzero, etc. If NPT $\geq$ (NP-3)/2, each submatrix is full, where NP is described below.

NBAND - Number of submatrix diagonal bands to be used during the inversion of Z_{BOT}. NBAND=1 indicates that only the diagonal $Z_{m,n}$ submatrices are to be used during inversion. NBAND=2 indicates that diagonal and off-diagonal $Z_{m,n}$ submatrices are to be used, etc. If NBAND $\geq$ 2*NMODE-1, the entire Z_{BOT} matrix is inverted.

```
READ(5,3)NP,MC,BK
3   FORMAT(2I3,E14.7)
```

NP - Number of points used to describe the BOT generating curve. (NP must be odd.) If the BOT generating curve is closed (i.e., the first and last points coincide), the programs will increase NP by two and add two points to the generating curve (i.e., the YH and XH arrays described below). This new NP should be used in all definitions involving NP (i.e., dimensions, etc.).

MC - Number of terms to be used in the numerical integration of the Green's function [Equation (34) of Volume I].

BK - Wave number for the problem (meters^{-1}).

```
READ(5,4)(YH(I),I=1,NP)
4   FORMAT(10F8.4)
```

YH - Array of y coordinates for the generating curve (meters).

```
READ(5,5)(XH(I),I=1,NP)
```

5 FORMAT(10F8.4)

XH - Array of x coordinates for the generating curve (meters).

READ(5,6)L

6 FORMAT(F8.4)

L - Half length of the BOT (meters).

2.3.2 Scattering and Radiation Analysis Data Set

This data set is read by the BOTRA, BOTSCM, and BOTSCB programs. Additional data are required by some of the above programs as specified later.

READ(5,7)NANG,NT,PHII,THI

7 FORMAT(2I3,2F8.4)

NANG - Number of fixed radiation or scattering angles, as defined by IPLANE below. NANG radiation or scattering patterns will be calculated.

NT - Number of varied radiation or scattering angles, as defined by IPLANE below.

PHII - ϕ angle of incident wave (degrees). Used only in BOTSCB program.

THI - θ angle of incident wave (degrees). Used only in BOTSCB program.

READ(5,8)(ANG(I),I=1,NANG)

8 FORMAT(10F8.4)

ANG - Array of fixed radiation or scattering angles, as defined by IPLANE below.

READ(5,9)(IPLANE(I),I=1,NANG)

9 FORMAT(10I8)

IPLANE - Array indicating whether the corresponding element of array ANG is a ϕ or θ angle. IPLANE(I)=1 indicates that ANG(I) is a fixed ϕ angle. In this case, ϕ is fixed at ANG(I) and θ varies between 0° and 180° at NT equally spaced angles. (The only exception is program BOTSCM, where θ varies between 0° and 90° at NT equally spaced angles.) IPLANE(I)=2 indicates that ANG(I) is a fixed θ angle. In this case, θ is fixed at ANG(I) and ϕ varies between 0° and 180°.

2.3.3 Antenna Related Data Set

This data set is read only by the BOTRA program and should be deleted when running the BOTSCB program.

```
      READ(5,10)NSA
10    FORMAT(I3)
```

NSA - Number of slot antennas on the BOT.

```
      READ(5,11)(IS(K),K=1,NSA)
11    FORMAT(10I8)
```

IS(K) - Triangle function at which slot antenna K is located (centered).

```
      READ(5,12)(ZO(K),K=1,NSA)
12    FORMAT(10F8.4)
```

ZO(K) - Starting Z coordinate for antenna K (meters).

```
      READ(5,13)(Z1(K),K=1,NSA)
13    FORMAT(10F8.4)
```

Z1(K) - Ending Z coordinate for antenna K (meters). (ZO(K) < Z1(K) for all K.)

```
      READ(5,14)(EO(K),K=1,NSA)
14    FORMAT(10F8.4)
```

EO(K) - Constant excitation across slot antenna K [Equation (59) of Volume I]. (EO(K) is complex.)

```
      READ(5,15)(TEXC(K),K=1,NSA)
15    FORMAT(10F8.4)
```

TEXC(K) - Indicates t excitation on slot antenna K when TEXC(K) $\neq$ 0. This is the $(U^t)_i$ term in Equation (47) of Volume I.

```
      READ(5,16)(ZEXC(K),K=1,NSA)
16    FORMAT(10F8.4)
```

ZEXC(K) - Indicates z excitation on slot antenna K when ZEXC(K) $\neq$ 0. This is the $(U^z)_i$ term in Equation (47) of Volume I.

2.3.4 Aperture Analysis Data Set

This data set is read only by the BOTSCB program and should be deleted when running the BOTRA program.

```
      READ(5,17)ZO,Z1,YO,XO,Y1,X1
```

17 FORMAT(6F8.4)

ZO - Starting z coordinate for the aperture (meters).

Z1 - Ending z coordinate for the aperture (meters). If Z1 $\leq$ ZO, an aperture is not present, and the remaining parameters in this data set are ignored.

YO - Starting y coordinate for the aperture (meters).

XO - Starting x coordinate for the aperture (meters). If the start of the aperture is on generating curve segment I, the point (XO,YO) should be approximately on the line segment joining (XH(I),YH(I)) and (XH(I+1),YH(I+1)). To be specific, XO must lie between XH(I) and XH(I+1), and YO must lie between YH(I) and YH(I+1).

Y1 - Ending y coordinate for the aperture (meters).

X1 - Ending x coordinate for the aperture (meters). If the end of the aperture is on generating curve segment J, the point (X1,Y1) must satisfy the same conditions as (XO,YO) above with J replacing I. The aperture is assumed to start at (XO,YO) and extend to (X1,Y1) in the t direction (i.e., in the direction of the generating curve). If the aperture does not cover the peaks of at least two triangle functions, the program will print an error message and stop execution.

2.3.5 Near-Field Analysis Data Set

This data set is read by the BOTRA and BOTSCB programs.

READ(5,18)NTEST

18 FORMAT(I3)

NTEST - Number of test points at which near-field radiation or scattering is to be calculated. NTEST may be set to zero.

Repeat the following NTEST times:

READ(5,19)ZTEST,YTEST,XTEST

19 FORMAT(3F8.4)

ZTEST - z coordinate of the test point (meters).

YTEST - y coordinate of the test point (meters).

XTEST - x coordinate of the test point (meters).

2.4 Parameter Selection

The choice of most of the parameters in Section 2.3 is specified by the user depending upon the explicit requirements of the problem. For example, NSA is set by the number of slot antennas on the BOT. Similarly, BK is determined by the frequency at which the MM/BOT analysis is carried out. On the other hand, the choice of the parameters NP, MC, and NMODE is based upon the requirements of the MM/BOT theory, as explained below.

The parameter NP specifies the number of coordinate points used to describe the BOT generating curve in the t-direction. These points in turn define the segmentation (strips) of the BOT surface. In general, the separation of the points should not exceed 0.15 λ. If the BOT has a rapidly changing surface geometry with sharp curvatures, a higher density of points may be necessary. The resulting number of triangle functions used to expand the surface currents on the BOT is determined by NM = (NP-3)/2. Since at least one half of a triangle function should subtend an active aperture antenna in BOTRA and at least two triangle functions must intercept a passive aperture in BOTSCB, the value of NP is specified by these conditions as well as the strip width. As a general principle, the accuracy of the analysis is improved by increasing NP.

The parameter MC is used in the numerical evaluation of the integrated Green's kernel G_{mn} [Equation (26) in Volume I). A necessary condition for the approximations used in obtaining G_{mn} is that MC > 8(NMODE-1).

The parameter NMODE is set by the length of the BOT. In general, the minimum requirement is that NMODE $\gtrsim 2L/\lambda$, where L is the (axial) half-length of the BOT. This requirement is comparable to the MM/BOR analysis requirement that the maximum circumferential modes used be $n \sim \pi D/\lambda$, where D is the largest diameter of the BOR. As a general observation, the accuracy of the analysis increases and the spatial resolution of the surface currents on the BOT is improved as NMODE is increased. This is particularly true for the edge currents. However, practical computer main memory limitations usually set the upper limit on NMODE.

2.5 Program Dimensions

The MM/BOT programs (Appendix C) are currently set up to handle problems with the following set of parameters. (Some of the arrays are overdimensioned in the listings.)

NMODE $\leq$ 4

NBAND $\leq$ 2*NMODE-1

NP $\leq$ 19 (17 for a closed generating curve)

MC $\leq$ 50

NANG $\leq$ 6

NT $\leq$ 91

NSA $\leq$ 20

NAM $\leq$ 12 (NAM is the number of triangle function peaks subtended by an aperture).

For a different set of input parameters, the minimum dimensions required for each program are listed below. Table 1 contains definitions of the parameters used as the subscripts in the arrays enumerated in the dimension statements.

TABLE 1. DEFINITION OF DIMENSION STATEMENT INDICES

Parameter	Definition
LS	NP-3
MC	Input
NAM	Number of triangle function peaks subtended by an aperture
NANG	Input
NM	(NP-3)/2
NMODE	Input
NP	Number of points on the generating curve (input). If the curve is closed, use NP+2 in place of NP in all definitions.
NSA	Input
NT	Input

GP79-0461-106

BOTZSS Minimum Dimensions

```
COMPLEX Z(LS*LS),G((NP-1)*NP/2)
DIMENSION YH(NP),XH(NP),DH(NP-1)
DIMENSION SV(NP-1),CV(NP-1),XS(NP-1),YS(NP-1)
```

```
      DIMENSION UMN(MC),JK(4)
      DIMENSION TP(4*NM),T(4*NM),TZ(4*NM)
```

BOTINV Minimum Dimensions

```
      DIMENSION YH(NP),XH(NP)
      COMPLEX Z(K1),ZI(K2),WORK(K3)
      DIMENSION NZ(K4)
      COMMON NM,JK(4),LR(K5)
```

where K1 through K5 depend on NBAND and are defined below.

NBAND	1	<2*NMODE-1	>2*NMODE-1
K1	0	$LS^2*\{(2*NMODE-1)*(2*NBAND-1)-(NBAND-1)*NBAND\}$	$\{LS*(2*NMODE-1)\}$
K2	LS^2	$LS^2*(2*NMODE-1)$	LS^2
K3	0	LS	0
K4	0	2*NMODE-1	0
K5	LS	LS	LS*(2*NMODE-1)

BOTRA Minimum Dimensions

```
      DIMENSION IS(NSA),ZO(NSA),Z1(NSA),TEXC(NSA),ZEXC(NSA)
      COMPLEX EO(NSA)
      COMPLEX VM(LS),VN(LS)
      COMPLEX GT(NT),GP(NT)
      COMPLEX ESC(3),HSC(3),CUR(LS*(2*NMODE-1))
      COMPLEX Y(LS*LS),RT(LS),RP(LS)
      COMMON/BODY/DH(NP-1),R(NP-1),SP(NP-1),CP(NP-1),SV(NP-1),CV(NP-1),
                  BK,L,NP,T(4*NM),TZ(4*NM)
      COMMON/TEST/MC,GAMMA,TP(4*NM),XS(NP-1),YS(NP-1)
      DIMENSION YH(NP),XH(NP),THR(NT),PHIR(NT)
      DIMENSION ANG(NANG),IPLANE(NANG)
```

Subroutine PLANE dimensions are as follows:

```
      COMMON/BODY/DH(NP-1),R(NP-1),SP(NP-1),CP(NP-1),SV(NP-1),CV(NP-1),
                  BK,L,NP,T(4*NM),TZ(4*NM)
```

Subroutine NEARB dimensions are as follows:

```
      COMPLEX G(NP-1),HO(NP-1),H1(NP-1)
      COMMON/BODY/DH(NP-1),R(NP-1),SP(NP-1),CP(NP-1),SV(NP-1),CV(NP-1),
                  BK,L,NP,T(4*NM),TZ(4*NM)
      COMMON/TEST/MC,GAMMA,TP(4*NM),XS(NP-1),YS(NP-1)
```

BOTSCM Minimum Dimensions

```
COMPLEX STT(NT),SPP(NT),STP(NT),SPT(NT)
COMPLEX YT(LS),YP(LS)
COMPLEX Y(LS*LS),RT(NT*LS),RP(NT*LS)
COMMON/BODY/DH(NP-1),R(NP-1),SP(NP-1),CP(NP-1),SV(NP-1),CV(NP-1),
          BK,L,NP,T(4*NM),TZ(4*NM)
DIMENSION YH(NP),XH(NP),THS(NT),PHIS(NT)
DIMENSION ANG(NANG),IPLANE(NANG)
```

Subroutine PLANE dimensions are given under BOTRA dimensions.

BOTSCB Minimum Dimensions

```
COMPLEX STT(NT),SPP(NT),STP(NT),SPT(NT)
COMPLEX ESCT(3),HSCT(3),CURT(LS*(2*NMODE-1))
COMPLEX ESCP(3),HSCP(3),CURP(LS*(2*NMODE-1))
COMPLEX Y(LS*LS),RT(LS),RP(LS)
COMMON/BODY/DH(NP-1),R(NP-1),SP(NP-1),CP(NP-1),SV(NP-1),CV(NP-1),
          BK,L,NP,T(4*NM),TZ(4*NM)
COMMON/TEST/MC,GAMMA,TP(4*NM),XS(NP-1),YS(NP-1)
COMMON/S/LT(NAM),VLOW(NAM),VHGH(NAM),IT(NAM)
DIMENSION YH(NP),XH(NP),THS(NT),PHIS(NT)
DIMENSION ANG(NANG),IPLANE(NANG)
```

Subroutine PLANE dimensions are given under BOTRA dimensions.

Subroutine NEARB dimensions are given under BOTRA dimensions.

Subroutine ASYMAC dimensions are as follows:

```
COMPLEX YA(NAM*NAM),CAT(2*NAM),CAP(2*NAM),EVT(2*NAM),EVP(2*NAM)
DIMENSION FPP(3,NAM)FPPZ(3,NAM),LR(2*NAM)
COMMON/S/LT(NAM),VLOW(NAM),VHGH(NAM),IT(NAM)
```

Subroutine APPAR dimensions are as follows:

```
COMMON/S/LT(NAM),VLOW(NAM),VHGH(NAM),IT(NAM)
```

2.6 Sample Problems

In this section, four sample problems are considered to illustrate the use of the MM/BOT algorithm. Sample problem 1 exercises all the main-line programs given in Figure 1. The inputs, outputs, and selected intermediate results are reproduced here to provide a check case for the proper function-

ing of the codes. Problem 2 demonstrates the radiation analysis for aperture antennas embedded in an asymmetric BOT (i.e., wing section). Problem 3 considers the scattering from a square cylinder of finite length. Finally, problem 4 demonstrates the use of the codes to compute the aperture-coupled electric and magnetic fields inside a BOT, approximating a fuselage equipment compartment when subject to electromagnetic illumination.

2.6.1 Problem 1a

Consider a right-circular cylinder of 2.76 λ length and 0.216 λ radius, with an embedded ϕ-polarized aperture antenna at $\phi = 0°$. The aperture is fed uniformly, subtends a 45° opening, and is 2.06 λ long in the axial direction (see Figure 3a).

a) Calculate the power gain patterns in the horizontal ($\phi = 0, 180°$) plane and the roll ($\theta = \pm 90°$) planes in the θ and ϕ polarizations.

b) Compute the currents on the cylinder surface.

c) Compute the electric and magnetic field components (near fields) at test points on a line bisecting the aperture, i.e., at XTEST = 14.256, 19.44, 71.28, 150, and 300 m where the corresponding YTEST = ZTEST = 0.0.

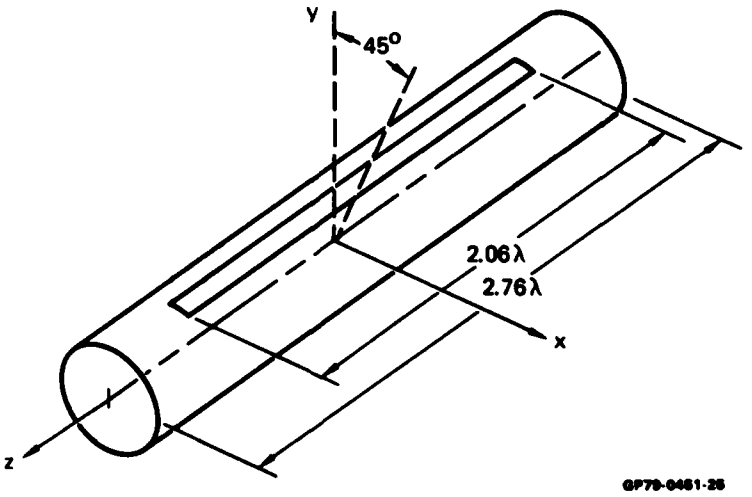

Figure 3a. Slotted cylinder for problem 1.

Solution - The problem was solved by running the programs BOTSEG, BOTZSS, BOTINV, and BOTRA in sequence. The calculations were carried out at 10 MHz (λ = 30 m). The cylinder was represented by NP = 17 points around the circumference.

Execution of BOTSEG is shown in Figure 3b, together with the data file for the coordinates of the problem and a plot of the NP data points and triangle functions for the cylinder cross section. (Note Figure 3b was generated in a time-share mode. The question marks at the beginning of each line are prompt signs used in the time-share mode.) The generated file was used as the basic input file for the programs BOTZSS, BOTINV, and BOTRA. Four modes were used in the calculations, i.e., NMODE = 4. Partial listings of the inputs and outputs from these programs are shown in the subsequent figures. Specifically, the input data for execution of the programs are given in Figure 4. For reference, the variable of the data set are labeled with the applicable format statements in parenthesis. Note the aperture coincided with the fourth triangle function (IS = 4) and only one triangle function was used to span the aperture (NSA = 1). If a non-uniform aperture excitation is desired, then more triangle functions should be used to span the aperture each with a different E_o. Partial outputs from BOTZSS, BOTINV, and BOTRA are shown in Figures 5, 6, and 7, respectively. The radiation power gain for the slotted cylinder for the horizontal and roll planes normalized to an isotropic radiator is summarized in Figure 7b. (The comparison of these results with the MM/BOR analysis is given in Figure 10 of Volume I.) Partial output of the currents on the cylinder is plotted in Figure 7c. The electric and magnetic fields computed in the near-field analysis are listed in Figure 7d. (For further discussion of these results, see Section 8 of Volume I.)

The foregoing calculations were carried out at 10 MHz. If the dimensions of the body (BOT) and the antenna are given initially in terms of wavelength, any convenient frequency can be chosen in the setup procedure for carrying out the computations. If the data are to be compared with range measurements at a given frequency, for ease of data interpretation, the calculations are also done at that frequency.

```
RNH BOTSEG
? 3 17                                          (2I3)
? 0.0          0.0        6.48        0.0   }
?12.96         0.0        6.48        0.0   } (4E10.4)
? 0.0          0.0

PERIMETER =  40.7150

NP = 17

YH
     0.0000    2.4798    4.5821    5.9867    6.4800    5.9867    4.5821    2.4798    0.0000   -2.4798

    -4.5821   -5.9867   -6.4800   -5.9867   -4.5821   -2.4798    0.0000

XH
     0.0000     .4933    1.8979    4.0002    6.4800    8.9598   11.0621   12.4667   12.9600   12.4667

    11.0621   8.9598    6.4800    4.0002    1.8979     .4933    0.0000

BODY COORDINATES + INDICATES TRIANGLE PEAK
```

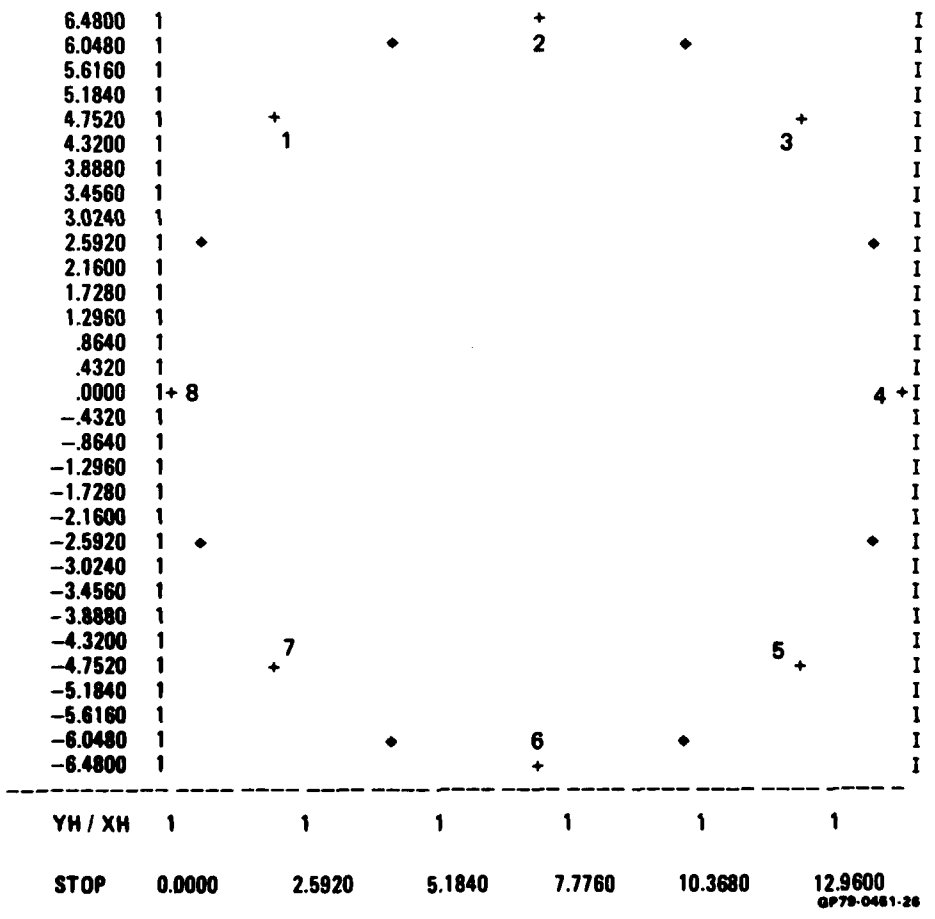


```
YH / XH    1         1         1         1         1         1

STOP     0.0000    2.5920    5.1840    7.7760   10.3680   12.9600
```

GP79-0461-26

Figure 3b. Execution of BOTSEG for problem 1, with triangle functions numbered on the plot.

```
NMODE      4
NPT, NBA  20  14
NP, MC, BK  17  50   .2094397E+00
        YH  0.0000   2.4798   4.5821   5.9867   6.4800   5.9867   4.5821   2.4798   -.0000  -2.4798
            -4.5821  -5.9867  -6.4800  -5.9867  -4.5821  -2.4798   0.0000                          } Primary BOT data set
        XH  0.0000    .4933   1.8979   4.0002   6.4800   8.9598  11.0621  12.4667  12.9600  12.4667
            11.0621   8.9598   6.4800   4.0002   1.8979    .4933   0.0000
         L  41.4
NANG, NT    4  46
       ANG      0.0     180.0      90.0     -90.0   } Radiation angles
    IPLANE        1         1         2         2
       NSA  1
        IS        4
        ZO -31.0500
        ZI  31.0500
        EO   1.0000    .0000
      TEXC   1.0000                                 } Slot antenna
      ZEXC    .0000
     NTEST  5
     ZTEST  0.0000   0.0000  14.2560
     YTEST  0.0000   0.0000  19.4400
     YTEST  0.0000   0.0000  71.2800                } Near-field points
     XTEST  0.0000   0.0000150.0000
     XTEST  0.0000   0.0000300.0000
```

Figure 4. Input data for execution of programs used in problem 1a.

GP79-0481-27

```
   NPT     NBAND    NMODE     NP       MC      BK
   20       14        4       17       90   .2094397E+00

YH
  0.0000  2.4798  4.5821  5.9867  6.4800  5.9867  4.5821  2.4798  0.0000 -2.4798
 -4.5821 -5.9867 -6.4800 -5.9867 -4.5821 -2.4798  0.0000

XH
  0.0000   .4933  1.8979  4.0002  6.4800  8.9598 11.0621 12.4667 12.9600 12.4667
 11.0621  8.9598  6.4800  4.0002  1.8979   .4933  0.0000

BODY COORDINATES, + INDICATES TRIANGLE PEAK
```

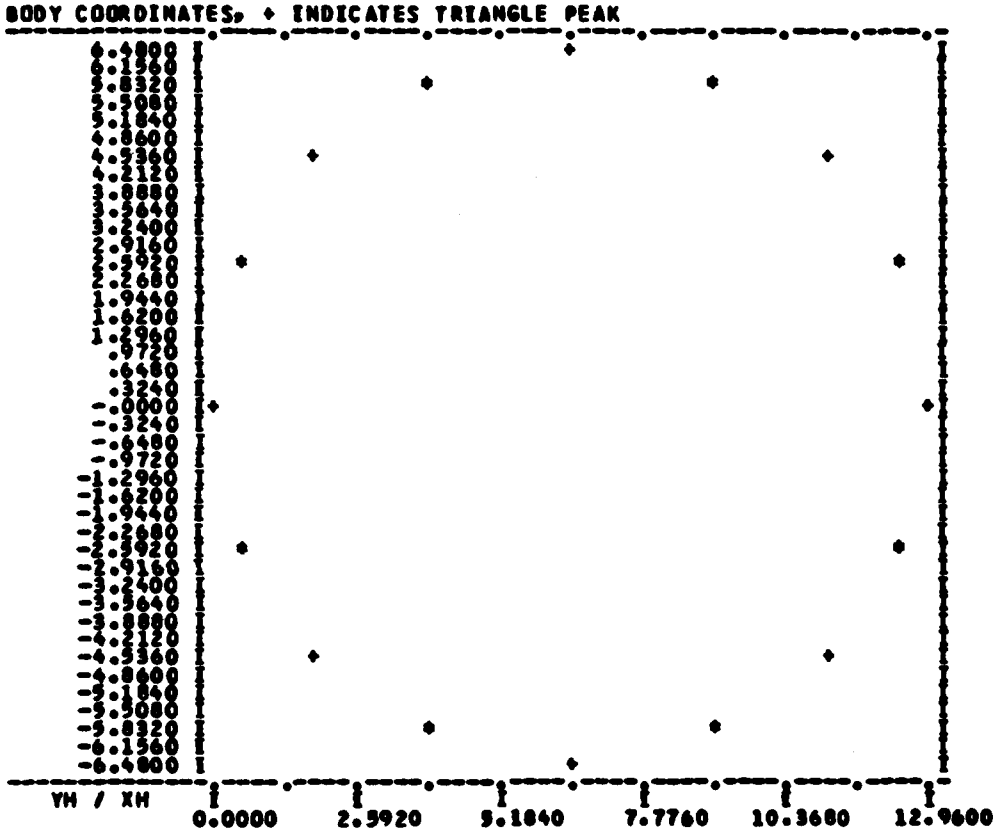


```
HALF-LENGTH OF BOT =      41.4000
```

GP78-0481-28

Figure 5a. Partial output of BOTZSS for problem 1a.

Impedance matrices for mode numbers M,N are input by columns. In output below, Z1 is a complex 8 x 8 matrix.

M= 1 N= 1 NO= 19 NC= 50 SK= .2094297E+00

Z1

[illegible]

26.42	74.99	30.10	81.48	
33.83	80.08	26.42	74.99	
69.48	146.3	33.83	80.08	
95.30	-213.5	69.48	146.3	$Z^{tt}_{1,1}$
69.48	146.3	95.30	-213.5	
33.83	80.08	69.48	146.3	
26.42	74.99	33.83	80.08	
30.10	81.48	26.42	74.99	

Z2

[illegible]

1.542	-12.94	-.2046E-12	.3021E-12	
16.43	-23.22	1.542	-12.94	
55.85	-20.16	16.43	-23.22	
.3200E-05	-.1516E-05	55.85	-20.16	
-55.85	20.16	.9974E-05	-.2944E-05	$Z^{zt}_{1,1}$
-16.43	23.22	-55.85	20.16	
-1.542	12.94	-16.43	23.22	
-.6440E-12	-.5777E-13	-1.542	12.94	

Z3

[illegible]

1.542	-12.94	.1129E-11	-.2666E-12	
16.43	-23.22	1.542	-12.94	
55.85	-20.16	16.43	-23.22	
-.3200E-05	.1516E-05	55.85	-20.16	
-55.85	20.16	-.9974E-05	.2944E-05	$Z^{tz}_{1,1}$
-16.43	23.22	-55.85	20.16	
-1.542	12.94	-16.43	23.22	
.5304E-13	-.4262E-13	-1.542	12.94	

Z4

[illegible]

20.95	-81.23	4.527	-82.12	
67.95	-61.61	20.95	-81.23	
126.1	28.35	67.95	-61.61	
153.5	126.9	126.1	28.35	
126.1	28.35	153.5	126.9	$Z^{zz}_{1,1}$
67.95	-61.61	126.1	28.35	
20.95	-81.23	67.95	-61.61	
4.528	-82.12	20.95	-81.23	

GP79-0461-29

Figure 5b. Partial output of BOTZSS - impedance matrices for problem 1a.

```
N= 2 M= 1 MP= 19 MC= 90 BK= .2094397E+00

Z1
 3.984      -10.90       2.556      -2.798       1.894       3.251       4.281       7.931       6.034       9.784
 6.034       9.784       4.281       7.931       1.894       3.251       2.556      -2.798       3.984      -10.90
 4.281       7.931       1.894       3.251       2.556      -2.798       3.984      -10.90       2.556      -2.798
 1.894       3.251       2.556      -2.798       3.984      -10.90       2.556      -2.798       1.894       3.251
 2.556      -2.798       3.984      -10.90       2.556      -2.798       1.894       3.251       4.281       7.931
 3.984      -10.90       2.556      -2.798       1.894       3.251       4.281       7.931       6.034       9.784
 2.556      -2.798       1.894       3.251       4.281       7.931       6.034       9.784       4.281       7.931
 1.894       3.251       4.281       7.931       6.034       9.784       4.281       7.931       1.894       3.251
 4.281       7.931       6.034       9.784       4.281       7.931       1.894       3.251       2.556      -2.798
 6.034       9.784       4.281       7.931       1.894       3.251       2.556      -2.798       3.984      -10.90

Z2
 .4883E-06  -.2059E-06   3.179      -2.615       1.465      -3.337       .1126      -2.082      -.3561E-12  -.4030E-12
-.1126       2.082      -1.465       3.337      -3.179       2.615
-3.180       2.615      -.2059E-06   .1095E-06   3.180      -2.615       1.465      -3.337       .1126      -2.082
-.4490E-12  -.3284E-12   -.1126       2.082      -1.465       3.337       3.179      -2.615       1.465      -3.337
-1.465       3.337      -3.179       2.615       .4883E-06  -.2059E-06   3.179      -2.615       1.465      -3.337
 .1126      -2.082       .1344E-12  -.5038E-12   -.1126       2.082
 1.465      -3.337       .1126      -2.082       -3.180       2.615       .2055E-06  -.1095E-06   3.180      -2.615
-.2428E-11   .5759E-12   -.1126       2.082      -1.465       3.337       .3478E-13   .1740E-13
 3.179      -2.615       1.465      -3.337       .1126      -2.082      -3.179       2.615       .4883E-06  -.2059E-06
 .1126      -2.082       .2140E-12   .6630E-14   -.1126       2.082      -1.465       3.337      -3.180       2.615
 .2055E-06  -.1095E-06   3.180      -2.615       1.465      -3.337       .1126      -2.082      -1.465       3.337
-1.465       3.337       .1126      -2.082       -.1003E-11   .3953E-12   -.1126       2.082      -1.465       3.337
-3.179       2.615       .4883E-06  -.2059E-06   3.179      -2.615
 3.180      -2.615       1.465      -3.337       .1126      -2.082      -.1042E-12   .4072E-13   -.1126       2.082
-1.465       3.337      -3.180       2.615       .2055E-06  -.1095E-06

Z3
-.2441E-06   .1029E-06   1.590      -1.308       .7326      -1.668       .5629E-01  -1.041       .1214E-11  -.2879E-12
-.5629E-01   1.041      -.7326       1.668      -1.590       1.308
-1.590       1.308      -.1028E-06   .9476E-07   1.590      -1.308       .7326      -1.668       .5630E-01  -1.041
-.1079E-12  -.3114E-14   -.5630E-01   1.041      -.7326       1.668
-.7326       1.668      -1.590       1.308      -.2441E-06   .1029E-06   1.590      -1.308       .7326      -1.668
-.2441E-01   1.041      -.9016E-12  -.1676E-12   -.5629E-01   1.041
-.2430E-01   1.041      -.7326       1.668      -1.590       1.308      -.1028E-06   .9476E-07   1.590      -1.308
 .7326      -1.668       .5630E-01  -1.041       .2209E-13  -.2036E-13
 .1781E-12   .2413E-12   -.2430E-01   1.041      -.7326       1.668      -1.590       1.308      -.2441E-06   .1029E-06
 1.590      -1.308       .7326      -1.668       .2629E-01  -1.041
-.5630E-01   1.041      -.4742E-12   .1643E-12   -.5630E-01   1.041      -.7326       1.668      -1.590       1.308
-.1029E-06   .9476E-07   1.590      -1.308       .7326      -1.668
 .7326      -1.668       .5629E-01  -1.041       -.6110E-13   .2511E-12   -.5629E-01   1.041      -.7326       1.668
-1.590       1.308      -.2441E-06   .1029E-06   1.590      -1.308
 1.590      -1.308       .7326      -1.668       .5630E-01  -1.041       .1989E-13  -.8997E-14   -.5630E-01   1.041
-.7326       1.668      -1.590       1.308      -.1028E-06   .9476E-07

Z4
 6.468      -2.805       4.982      -4.951       1.619      -7.564      -1.401      -8.316      -2.944      -8.323
-1.401      -8.316       1.619      -7.564       4.982      -4.951       1.619      -7.564      -1.401      -8.316
 4.982      -4.951       6.468      -2.805       4.982      -4.951
-2.944      -8.323       -1.401      -8.316       1.619      -7.564
-1.619      -7.564       4.982      -4.951       6.468      -2.805       4.982      -4.951       1.619      -7.564
-1.401      -8.316       -2.944      -8.323       -1.401      -8.316
-1.401      -8.316       1.619      -7.564       4.982      -4.951       6.468      -2.805       4.982      -4.951
 1.619      -7.564       -1.401      -8.316       -2.944      -8.323

-2.944      -8.323       -1.401      -8.316       -1.619      -7.564       4.982      -4.951       6.468      -2.805
 4.982      -4.951       1.619      -7.564       -1.401      -8.316
-1.401      -8.316       -2.944      -8.323       -1.401      -8.316       1.619      -7.564       4.982      -4.951
 6.468      -2.805       4.982      -4.951       1.619      -7.564
 1.619      -7.564       -1.401      -8.316       -2.944      -8.323       -1.401      -8.316
 4.982      -4.951       6.468      -2.805       4.982      -4.951
 4.982      -4.951       1.619      -7.564       -1.401      -8.316       -2.944      -8.323       -1.401      -8.316
 1.619      -7.564       4.982      -4.951       6.468      -2.805
```

$Z^{tt}_{2,1}$ $Z^{zt}_{2,1}$ $Z^{tz}_{2,1}$ $Z^{zz}_{2,1}$

GP79-0461-30

Figure 5c. Partial output of BOTZSS - impedance matrices for problem 1a.

```
      NP          NNODE       NBAND
      17            4           14

YH
  0.0000  2.4798  4.5821  5.9867  6.4800  5.9867  4.5821  2.4798  0.0000 -2.4798
 -4.5821 -5.9867 -6.4800 -5.9867 -4.5821 -2.4798  0.0000

XH
  0.0000   .4933  1.8979  4.0002  6.4800  8.9598 11.0621 12.4667 12.9600 12.4667
 11.0621  8.9598  6.4800  4.0002  1.8979   .4933  0.0000

THE MINIMUM BOTINV ARRAY DIMENSIONS FOR THIS
PROBLEM ARE AS FOLLOWS:

      Z          ZI        WORK          NZ          LR
  12544         256           0           0         112
```

GP79-0481-31

Figure 6a. Partial output of BOTINV for problem 1a.

Admittance matrices for mode numbers M, N are output by columns. In output below, Y1 in a complex 8 x 8 matrix.

M= -3 N= -3

Y1

```
 .9070E-04 -.4701E-03  .6824E-04 -.5931E-03  .1753E-04  .1402E-03 -.2040E-04 -.6361E-03 -.3618E-04  .2877E-03
-.2040E-04 -.6361E-03  .1753E-04  .1402E-03 -.5931E-03  .6824E-04 -.4701E-03  .9070E-04
 .6824E-04 -.5931E-03  .9070E-04 -.4701E-03  .6824E-04 -.5931E-03  .1753E-04  .1402E-03 -.2040E-04 -.6361E-03
-.3618E-04  .2877E-03 -.2040E-04 -.6361E-03  .1753E-04  .1402E-03  .6824E-04 -.5931E-03  .1753E-04  .1402E-03
-.2040E-04 -.6361E-03 -.3618E-04  .2877E-03 -.2040E-04 -.6361E-03  .9070E-04 -.4701E-03  .6824E-04 -.5931E-03
-.2040E-04 -.6361E-03  .1753E-04  .1402E-03 -.6361E-03 -.3618E-04  .2877E-03  .6824E-04 -.5931E-03  .9070E-04 -.4701E-03
 .1753E-04  .1402E-03 -.2040E-04 -.6361E-03 -.3618E-04  .2877E-03  .6824E-04 -.5931E-03  .1753E-04  .1402E-03
-.3618E-04  .2877E-03 -.2040E-04 -.6361E-03  .1753E-04  .1402E-03 -.2040E-04 -.6361E-03  .6824E-04 -.5931E-03  .9070E-04 -.4701E-03
 .6824E-04 -.5931E-03  .1753E-04  .1402E-03 -.2040E-04 -.6361E-03  .1753E-04  .1402E-03  .6824E-04 -.5931E-03
-.2040E-04 -.6361E-03 -.3618E-04  .2877E-03 -.2040E-04 -.6361E-03  .1753E-04  .1402E-03 -.2040E-04 -.6361E-03
 .9070E-04 -.4701E-03  .6824E-04 -.5931E-03  .1753E-04  .1402E-03 -.2040E-04 -.6361E-03 -.3618E-04  .2877E-03
 .1753E-04  .1402E-03 -.2040E-04 -.6361E-03 -.3618E-04  .2877E-03 -.2040E-04 -.6361E-03  .1753E-04  .1402E-03
 .6824E-04 -.5931E-03  .9070E-04 -.4701E-03  .6824E-04 -.5931E-03  .1753E-04  .1402E-03 -.2040E-04 -.6361E-03
 .6824E-04 -.5931E-03  .1753E-04  .1402E-03 -.2040E-04 -.6361E-03 -.3618E-04  .2877E-03 -.2040E-04 -.6361E-03
 .1753E-04  .1402E-03  .6824E-04 -.5931E-03  .9070E-04 -.4701E-03  .6824E-04 -.5931E-03  .1753E-04  .1402E-03
```

$Y^{tt}_{-3,-3}$

Y2

```
-.1226E-08 -.8726E-10  .3402E-02 -.8071E-04 -.1881E-02 -.7677E-04  .1194E-02  .4113E-04 -.3217E-08  .6403E-09
-.1194E-02 -.4113E-04 -.1881E-02 -.7677E-04 -.3402E-02 -.8071E-04
-.3402E-02 -.8071E-04 -.1705E-08 -.7936E-10 -.3402E-02 -.8071E-04 -.1881E-02 -.7677E-04  .1194E-02  .4113E-04
-.3178E-08 -.6873E-09 -.1194E-02 -.4113E-04 -.1881E-02 -.7677E-04
-.1881E-02 -.7677E-04 -.3402E-02 -.8071E-04 -.7798E-08 -.3533E-09  .3402E-02  .8070E-04 -.1881E-02 -.7677E-04
-.1194E-02 -.4113E-04 -.2123E-08 -.3293E-09 -.1194E-02 -.4113E-04
-.1194E-02 -.4113E-04 -.1881E-02 -.7677E-04 -.3402E-02 -.8071E-04 -.1212E-08  .2662E-09  .3402E-02  .8071E-04
-.1881E-02 -.7677E-04 -.1194E-02 -.4113E-04 -.3088E-08 -.3869E-09
-.3268E-08  .5289E-09 -.1194E-02 -.4113E-04 -.1881E-02 -.7677E-04 -.3402E-02 -.8071E-04 -.1211E-08  .1049E-09
-.3402E-02 -.8070E-04 -.1881E-02 -.7677E-04 -.1194E-02 -.4113E-04
-.1194E-02 -.4113E-04 -.3179E-08 -.5956E-09 -.1194E-02 -.4113E-04  .1881E-02 -.7677E-04 -.3402E-02 -.8071E-04
-.1442E-08 -.3604E-11 -.3402E-02 -.8071E-04 -.1881E-02 -.7677E-04
-.1881E-02 -.7677E-04 -.1194E-02 -.4113E-04 -.2331E-08 -.2193E-09 -.1194E-02 -.4113E-04  .1881E-02 -.7677E-04
-.3402E-02 -.8071E-04 -.2481E-08 -.3599E-09 -.3402E-02 -.8070E-04
-.3402E-02 -.8071E-04 -.1881E-02 -.7677E-04 -.1194E-02 -.4113E-04 -.3794E-08  .3322E-09 -.1194E-02 -.4113E-04
-.1881E-02 -.7677E-04 -.3402E-02 -.8071E-04 -.2790E-08 -.5727E-09
```

Y3

```
-.1226E-08 -.8726E-10  .3402E-02 -.8071E-04 -.1881E-02 -.7677E-04  .1194E-02  .4113E-04  .3268E-08 -.5289E-09
-.1194E-02 -.4113E-04 -.1881E-02 -.7677E-04 -.3402E-02 -.8071E-04
-.3402E-02 -.8070E-04 -.1705E-08 -.7936E-10 -.3402E-02 -.8071E-04 -.1881E-02 -.7677E-04  .1194E-02  .4113E-04
-.3178E-08 -.6873E-09 -.1194E-02 -.4113E-04 -.1881E-02 -.7677E-04
-.1881E-02 -.7677E-04 -.3402E-02 -.8071E-04 -.7798E-08 -.3533E-09  .3402E-02  .8071E-04 -.1881E-02 -.7677E-04
-.1194E-02 -.4113E-04 -.2123E-08 -.3293E-09 -.1194E-02 -.4113E-04
-.1194E-02 -.4113E-04 -.1881E-02 -.7677E-04 -.3402E-02 -.8071E-04 -.1212E-08  .2662E-09  .3402E-02  .8071E-04
-.1881E-02 -.7677E-04 -.1194E-02 -.4113E-04 -.3796E-08 -.3922E-09
-.3217E-08 -.6403E-09 -.1194E-02 -.4113E-04 -.1881E-02 -.7677E-04 -.3402E-02 -.8071E-04 -.1211E-08  .1049E-09
-.3402E-02 -.8071E-04 -.1881E-02 -.7677E-04 -.1194E-02 -.4113E-04
-.1194E-02 -.4113E-04 -.3179E-08 -.6672E-09 -.1194E-02 -.4113E-04  .1881E-02 -.7677E-04 -.3402E-02 -.8071E-04
-.1442E-08 -.3604E-11 -.3402E-02 -.8071E-04 -.1881E-02 -.7677E-04
-.1881E-02 -.7677E-04 -.1194E-02 -.4113E-04 -.2123E-08 -.3293E-09 -.1194E-02 -.4113E-04  .1881E-02 -.7677E-04
-.3402E-02 -.8071E-04 -.2481E-08 -.3599E-09 -.3402E-02 -.8071E-04
-.3402E-02 -.8071E-04 -.1881E-02 -.7677E-04 -.1194E-02 -.4113E-04 -.3098E-08 -.3869E-09 -.1194E-02 -.4113E-04
-.1881E-02 -.7677E-04 -.3402E-02 -.8071E-04 -.2790E-08 -.5727E-09
```

$Y^{tz}_{-3,-3}$

Y4

```
 .2281E-03 -.1632E-01  .2471E-03 -.1752E-01 -.6974E-04  .2486E-01  .3227E-04 -.2873E-01 -.1372E-03  .2984E-01
-.6972E-04  .2486E-01  .3227E-04 -.2873E-01  .2471E-03 -.1752E-01 -.6974E-04  .2486E-01 -.1372E-03  .2984E-01
 .2471E-03 -.1752E-01 -.6974E-04  .2486E-01  .3227E-04 -.2873E-01  .2281E-03 -.1632E-01  .2471E-03 -.1752E-01
 .2281E-03 -.1632E-01  .2471E-03 -.1752E-01 -.6974E-04  .2486E-01  .3227E-04 -.2873E-01 -.1372E-03  .2984E-01
-.6972E-04  .2486E-01  .3227E-04 -.2873E-01  .2471E-03 -.1752E-01 -.6974E-04  .2486E-01 -.1372E-03  .2984E-01
 .2471E-03 -.1752E-01 -.6974E-04  .2486E-01  .3227E-04 -.2873E-01  .2281E-03 -.1632E-01  .2471E-03 -.1752E-01
 .2281E-03 -.1632E-01  .2471E-03 -.1752E-01 -.6974E-04  .2486E-01  .3227E-04 -.2873E-01 -.1372E-03  .2984E-01
 .3227E-04 -.2873E-01 -.1372E-03  .2984E-01 -.6972E-04  .2486E-01  .2471E-03 -.1752E-01 -.6974E-04  .2486E-01
 .2471E-03 -.1752E-01 -.6974E-04  .2486E-01  .3227E-04 -.2873E-01  .2281E-03 -.1632E-01  .2471E-03 -.1752E-01
-.6972E-04  .2486E-01  .3227E-04 -.2873E-01  .2471E-03 -.1752E-01 -.6974E-04  .2486E-01 -.1372E-03  .2984E-01
 .2281E-03 -.1632E-01  .2471E-03 -.1752E-01 -.6974E-04  .2486E-01  .3227E-04 -.2873E-01 -.1372E-03  .2984E-01
 .2471E-03 -.1752E-01 -.6974E-04  .2486E-01  .3227E-04 -.2873E-01  .2281E-03 -.1632E-01  .2471E-03 -.1752E-01
 .3227E-04 -.2873E-01 -.1372E-03  .2984E-01 -.6972E-04  .2486E-01  .2471E-03 -.1752E-01 -.6974E-04  .2486E-01
```

$Y^{zz}_{-3,-3}$

GP78-0461-32

Figure 6b. Partial output of BOTINV - admittance matrices for m = n = –3 for problem 1a.

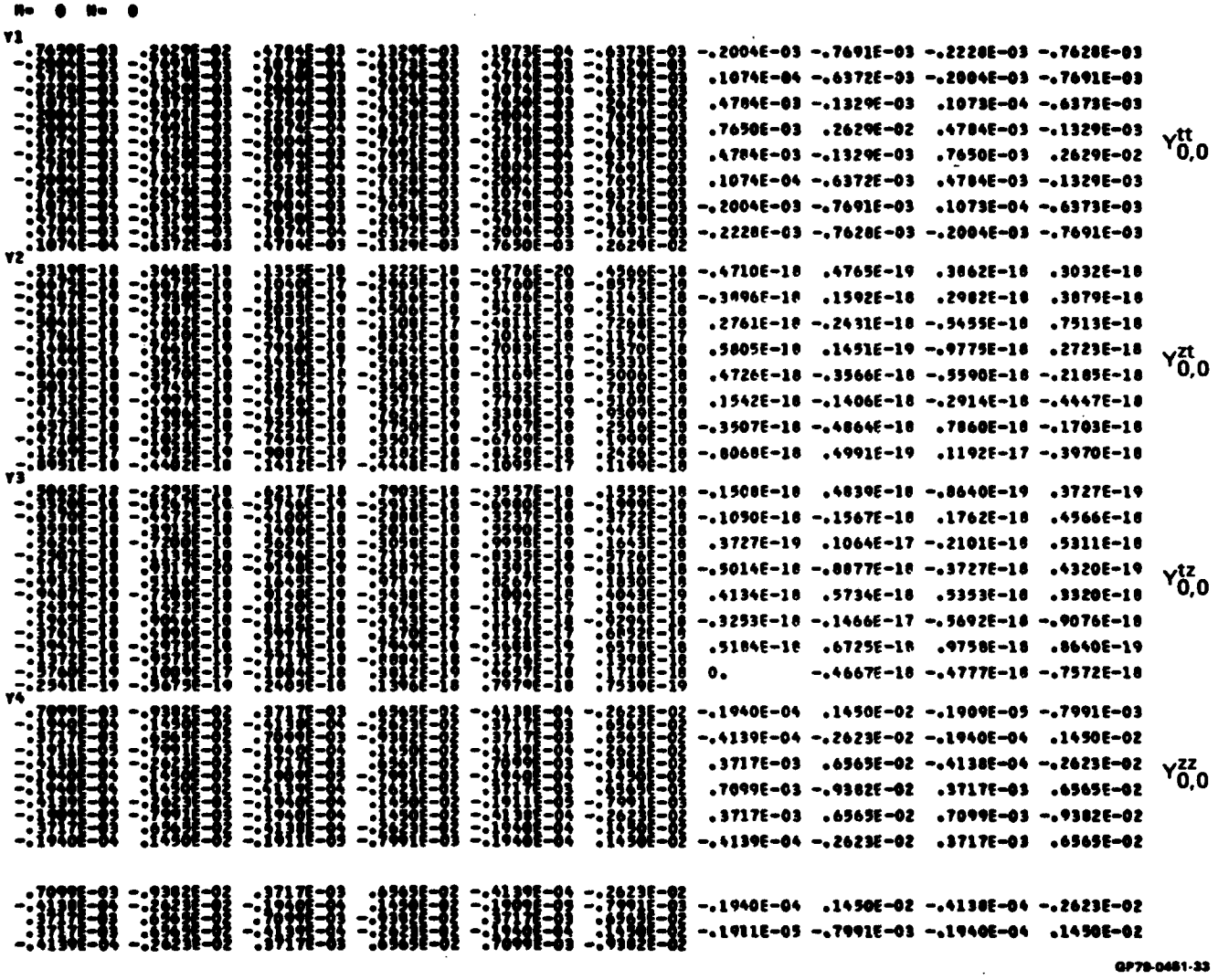

GP79-0481-33

Figure 6c. Partial output of BOTINV - admittance matrices for m = n = 0 for problem 1a.

```
    NPT      NBAND    NMODE     NP       MC      BK
     20        14        4       17       50   .2094397E+00

YH
  0.0000  2.4798  4.5821  5.9867  6.4800  5.9867  4.5821  2.4798  0.0000 -2.4798
 -4.5821 -5.9867 -6.4800 -5.9867 -4.5821 -2.4798  0.0000

XH
  0.0000   .4933  1.8979  4.0002  6.4800  8.9598 11.0621 12.4667 12.9600 12.4667
 11.0621  8.9598  6.4800  4.0002  1.8979   .4933  0.0000

HALF-LENGTH OF BOT =      41.4000

NUMBER OF FIXED ANGLES =  4
NUMBER OF ANGLES PER FIXED ANGLE =  46

F*XED ANGLE     CODE(PHI FIXED = 1, THETA FIXED =2)

   0.0           1
 180.0           1
  90.0           2
 -90.0           2

NUMBER OF SLOT ANTENNAS =  1

ANTENNA NO.    IS     Z0          Z1                 E0              TEXC        ZEXC
       1        4  -31.0500    31.0500     1.0000     0.0000     1.0000      0.0000
```

Figure 7a. Partial output of BOTRA for problem 1a.

```
M= -3  N= -3
V
VM .9070311E-04 -.4701087E-03  .6824476E-04 -.5931252E-03

        T-EXCITATION
          0:      0:      0:      0:      0:      0:      .15     0.      0.      0.
          0.      0.      0.      0.      0.      0.

        Z-EXCITATION
          0:      0:      0:      0:      0:      0:      0.      0.      0.      0.
          0.      0.      0.      0.      0.      0.

VM
        T-EXCITATION
          0:      0:      0:      0:      0:      0:      .15     0.      0.      0.
          0.      0.      0.      0.      0.      0.

        Z-EXCITATION
          0:      0:      0:      0:      0:      0:      0.      0.      0.      0.
          0.      0.      0.      0.      0.      0.

POWER IN CURRENT MODES =    .769E-03   CUMMULATIVE POWER =    .769E-03

M= -2  N= -3
V
VM -.7578504E-04  .1106460E-04 -.5825230E-04  .2733491E-04

        T-EXCITATION
          0:      0:      0:      0:      0:      0:     -.32     0.      0.      0.
          0.      0.      0.      0.      0.      0.

        Z-EXCITATION
          0:      0:      0:      0:      0:      0:      0.      0.      0.      0.
          0.      0.      0.      0.      0.      0.

VM
        T-EXCITATION
          0:      0:      0:      0:      0:      0:      .15     0.      0.      0.
          0.      0.      0.      0.      0.      0.

        Z-EXCITATION
```

V^t_{-3} V^z_{-3} V^t_{-3} V^z_{-3}

Figure 7a. Partial output of BOTRA for problem 1a. (concluded)

GP78-0461-24

Power radiation patterns

Horizontal plane ($\phi = 0^{o}$)

TOTAL POWER(DB) = -2.21

PHI	THETA	POWER(DB) θ	POWER(DB) φ
0.0	0.0	-205.70	-76.39
0.0	4.0	-206.01	-76.04
0.0	8.0	-206.05	-75.48
0.0	12.0	-204.89	-74.83
0.0	16.0	-202.30	-73.36
0.0	20.0	-199.24	-70.34
0.0	24.0	-196.41	-66.47
0.0	28.0	-194.07	-62.73
0.0	32.0	-192.29	-59.47
0.0	36.0	-191.12	-56.79
0.0	40.0	-190.63	-54.74
0.0	44.0	-190.96	-53.39
0.0	48.0	-192.37	-52.89
0.0	52.0	-195.38	-53.60
0.0	56.0	-201.22	-56.56
0.0	60.0	-202.70	-69.55
0.0	64.0	-196.45	-57.89
0.0	68.0	-193.21	-49.37
0.0	72.0	-191.87	-44.68
0.0	76.0	-191.93	-41.58
0.0	80.0	-193.39	-39.49
0.0	84.0	-196.89	-38.19
0.0	88.0	-205.98	-37.55
0.0	92.0	-205.98	-37.55
0.0	96.0	-196.89	-38.19
0.0	100.0	-193.39	-39.49
0.0	104.0	-191.93	-41.58
0.0	108.0	-191.87	-44.68
0.0	112.0	-193.21	-49.37
0.0	116.0	-196.45	-57.89
0.0	120.0	-202.70	-69.55
0.0	124.0	-201.22	-56.56
0.0	128.0	-195.38	-53.60
0.0	132.0	-192.37	-52.89
0.0	136.0	-190.96	-53.39
0.0	140.0	-190.63	-54.74
0.0	144.0	-191.12	-56.79
0.0	148.0	-192.29	-59.47
0.0	152.0	-194.07	-62.73
0.0	156.0	-196.41	-66.47
0.0	160.0	-199.24	-70.34
0.0	164.0	-202.30	-73.36
0.0	168.0	-204.89	-74.83
0.0	172.0	-206.05	-75.48
0.0	176.0	-206.01	-76.04
0.0	180.0	-205.70	-76.39

GP79-0481-36

Figure 7b. Partial output of BOTRA for problem 1a.

PHI	THETA	POWER(DB) Φ	θ
180.0	0.0	-203.64	-76.39
180.0	4.0	-203.44	-75.95
180.0	8.0	-203.24	-74.58
180.0	12.0	-203.01	-72.76
180.0	16.0	-202.73	-70.91
180.0	20.0	-202.42	-69.11
180.0	24.0	-202.13	-67.27
180.0	28.0	-202.00	-65.30
180.0	32.0	-202.17	-63.25
180.0	36.0	-202.83	-61.31
180.0	40.0	-204.08	-59.70
180.0	44.0	-205.60	-58.63
180.0	48.0	-205.85	-58.36
180.0	52.0	-204.27	-59.28
180.0	56.0	-202.80	-62.54
180.0	60.0	-202.71	-74.42
180.0	64.0	-204.79	-62.41
180.0	68.0	-211.41	-54.57
180.0	72.0	-219.13	-50.02
180.0	76.0	-207.31	-46.95
180.0	80.0	-204.81	-44.85
180.0	84.0	-206.36	-43.52
180.0	88.0	-214.59	-42.68
180.0	92.0	-214.59	-42.88
180.0	96.0	-206.36	-43.52
180.0	100.0	-204.81	-44.85
180.0	104.0	-207.31	-46.95
180.0	108.0	-219.13	-50.02
180.0	112.0	-211.41	-54.57
180.0	116.0	-204.79	-62.41
180.0	120.0	-202.71	-74.42
180.0	124.0	-202.80	-62.54
180.0	128.0	-204.27	-59.28
180.0	132.0	-205.85	-58.36
180.0	136.0	-205.60	-58.63
180.0	140.0	-204.08	-59.70
180.0	144.0	-202.83	-61.31
180.0	148.0	-202.17	-63.25
180.0	152.0	-202.00	-65.30
180.0	156.0	-202.13	-67.27
180.0	160.0	-202.42	-69.11
180.0	164.0	-202.73	-70.91
180.0	168.0	-203.01	-72.76
180.0	172.0	-203.24	-74.58
180.0	176.0	-203.44	-75.95
180.0	180.0	-203.64	-76.39

Horizontal plane ($\phi = 180^{o}$)

GP79-0481-106

Figure 7b. Partial output of BOTRA for problem 1a. (continued)

PHI	THETA	POWER(DB)	
		θ	θ
0.0	90.0	-315.69	-37.48
4.0	90.0	-204.13	-37.48
8.0	90.0	-198.12	-37.49
12.0	90.0	-194.62	-37.50
16.0	90.0	-192.15	-37.52
20.0	90.0	-190.25	-37.54
24.0	90.0	-188.71	-37.56
28.0	90.0	-187.43	-37.59
32.0	90.0	-186.34	-37.62
36.0	90.0	-185.40	-37.65
40.0	90.0	-184.58	-37.69
44.0	90.0	-183.86	-37.73
48.0	90.0	-183.22	-37.77
52.0	90.0	-182.66	-37.82
56.0	90.0	-182.17	-37.88
60.0	90.0	-181.74	-37.96
64.0	90.0	-181.37	-38.05
68.0	90.0	-181.05	-38.16
72.0	90.0	-180.78	-38.30
76.0	90.0	-180.56	-38.47
80.0	90.0	-180.38	-38.68
84.0	90.0	-180.25	-38.94
88.0	90.0	-180.15	-39.24
92.0	90.0	-180.11	-39.60
96.0	90.0	-180.10	-40.02
100.0	90.0	-180.14	-40.50
104.0	90.0	-180.22	-41.05
108.0	90.0	-180.35	-41.68
112.0	90.0	-180.52	-42.37
116.0	90.0	-180.75	-43.13
120.0	90.0	-181.03	-43.92
124.0	90.0	-181.36	-44.72
128.0	90.0	-181.76	-45.44
132.0	90.0	-182.23	-46.01
136.0	90.0	-182.78	-46.33
140.0	90.0	-183.42	-46.36
144.0	90.0	-184.17	-46.11
148.0	90.0	-185.04	-45.66
152.0	90.0	-186.07	-45.13
156.0	90.0	-187.29	-44.57
160.0	90.0	-188.78	-44.06
164.0	90.0	-190.63	-43.62
168.0	90.0	-193.07	-43.26
172.0	90.0	-196.55	-43.00
176.0	90.0	-202.54	-42.85
180.0	90.0	-317.80	-42.80

Roll plane ($\theta = 90^{O}$)

GP79-0481-104

Figure 7b. Partial output of BOTRA for problem 1a. (continued)

PHI	THETA	POWER(DB) θ	POWER(DB) ϕ	
0.0	-90.0	-318.94	-42.80	
4.0	-90.0	-202.54	-42.85	
8.0	-90.0	-196.55	-43.00	
12.0	-90.0	-193.07	-43.26	
16.0	-90.0	-190.63	-43.62	
20.0	-90.0	-188.78	-44.06	
24.0	-90.0	-187.29	-44.57	
28.0	-90.0	-186.07	-45.13	
32.0	-90.0	-185.04	-45.66	
36.0	-90.0	-184.17	-46.11	
40.0	-90.0	-183.42	-46.36	
44.0	-90.0	-182.78	-46.33	
48.0	-90.0	-182.23	-46.01	
52.0	-90.0	-181.76	-45.44	
56.0	-90.0	-181.36	-44.72	
60.0	-90.0	-181.03	-43.92	
64.0	-90.0	-180.75	-43.13	
68.0	-90.0	-180.52	-42.37	
72.0	-90.0	-180.35	-41.68	
76.0	-90.0	-180.22	-41.05	Roll plane
80.0	-90.0	-180.14	-40.50	($\theta = -90^{o}$)
84.0	-90.0	-180.10	-40.02	
88.0	-90.0	-180.11	-39.60	
92.0	-90.0	-180.15	-39.24	
96.0	-90.0	-180.25	-38.94	
100.0	-90.0	-180.38	-38.68	
104.0	-90.0	-180.56	-38.47	
108.0	-90.0	-180.78	-38.30	
112.0	-90.0	-181.05	-38.16	
116.0	-90.0	-181.37	-38.05	
120.0	-90.0	-181.74	-37.96	
124.0	-90.0	-182.17	-37.88	
128.0	-90.0	-182.66	-37.82	
132.0	-90.0	-183.22	-37.77	
136.0	-90.0	-183.86	-37.73	
140.0	-90.0	-184.58	-37.69	
144.0	-90.0	-185.40	-37.65	
148.0	-90.0	-186.34	-37.62	
152.0	-90.0	-187.43	-37.59	
156.0	-90.0	-188.71	-37.56	
160.0	-90.0	-190.25	-37.54	
164.0	-90.0	-192.15	-37.52	
168.0	-90.0	-194.62	-37.50	
172.0	-90.0	-198.12	-37.49	
176.0	-90.0	-204.13	-37.48	
180.0	-90.0	-312.13	-37.48	

OP79-0481-103

Figure 7b. Partial output of BOTRA for problem 1a. (concluded)

```
T-DIRECTED CURRENTS FOR MODE -3
 -.3612E-05  -.1004E-03       .4985E-05   .9337E-05       .1209E-04  -.9460E-04       .1361E-04  -.4599E-04
  .1209E-04  -.9460E-04       .4985E-05   .9337E-05      -.3612E-05  -.1004E-03      -.7802E-05   .2665E-04

Z-DIRECTED CURRENTS FOR MODE -3
 -.1689E-03  -.3139E-05       .2569E-03  -.2045E-05      -.4973E-03   .9588E-06      -.2398E-09   .4494E-10
  .4973E-03  -.9590E-06      -.2569E-03   .2045E-05       .1689E-03   .3139E-05      -.4974E-09   .6553E-10

T-DIRECTED CURRENTS FOR MODE -2
  .1543E-04   .1930E-03      -.2221E-04   .8464E-04      -.7340E-04   .1409E-03      -.9823E-04  -.4288E-03
 -.7340E-04   .1409E-03      -.2221E-04   .8464E-04       .1543E-04   .1830E-03       .2812E-04   .1208E-03

Z-DIRECTED CURRENTS FOR MODE -2
  .1187E-03  -.2840E-04      -.2601E-03  -.5997E-04       .6419E-03  -.5793E-04      -.4783E-09   .1196E-09
 -.6419E-03   .5793E-04       .2001E-03   .5997E-04      -.1187E-03   .2840E-04      -.1708E-09   .7716E-10

T-DIRECTED CURRENTS FOR MODE -1
 -.3700E-04  -.3210E-03       .1735E-04  -.2331E-03       .1533E-03  -.9571E-04       .2403E-03   .1038E-02
  .1533E-03  -.9571E-04       .1735E-04  -.2331E-03      -.3700E-04  -.3210E-03      -.3915E-04  -.3108E-03

Z-DIRECTED CURRENTS FOR MODE -1
 -.5907E-04   .3298E-05       .9317E-04   .3730E-04      -.4380E-03   .5668E-04       .2462E-09  -.1012E-09
  .4380E-03  -.5668E-04      -.9317E-04  -.3750E-04       .5907E-04  -.3298E-05       .5011E-10  -.4809E-10

T-DIRECTED CURRENTS FOR MODE  0
 -.1138E-03  -.1169E-02       .3296E-04  -.8792E-03       .5358E-03  -.1240E-03       .8763E-03   .3917E-02
  .5358E-03  -.1240E-03       .3296E-04  -.8792E-03      -.1139E-03  -.1169E-02      -.8524E-04  -.1209E-02

Z-DIRECTED CURRENTS FOR MODE  0
 -.6559E-17   .2622E-17       .7928E-17  -.2633E-18      -.1306E-16   .1962E-17       .1293E-17  -.5542E-18
  .9324E-17   .6268E-18      -.2297E-17  -.4323E-17       .3524E-18   .4388E-17       .3955E-17  -.3801E-17

T-DIRECTED CURRENTS FOR MODE  1
 -.3700E-04  -.3210E-03       .1735E-04  -.2331E-03       .1533E-03  -.9571E-04       .2403E-03   .1038E-02
  .1533E-03  -.9571E-04       .1735E-04  -.2331E-03      -.3700E-04  -.3210E-03      -.3915E-04  -.3108E-03

Z-DIRECTED CURRENTS FOR MODE  1
  .5907E-04  -.3298E-05      -.9317E-04  -.3750E-04       .4380E-03  -.5668E-04      -.2462E-09   .1012E-09
 -.4380E-03   .5568E-04       .9317E-04   .3753E-04      -.5907E-04   .3295E-05      -.5011E-10   .4809E-10

T-DIRECTED CURRENTS FOR MODE  2
  .1543E-04   .1930E-03      -.2221E-04   .8464E-04      -.7340E-04   .1409E-03      -.9823E-04  -.4288E-03
 -.7340E-04   .1409E-03      -.2221E-04   .8464E-04       .1543E-04   .1830E-03       .2812E-04   .1208E-03

Z-DIRECTED CURRENTS FOR MODE  2
 -.1187E-03   .2840E-04       .2001E-03   .5937E-04      -.6419E-03   .5793E-04       .4783E-09  -.1196E-09
  .6419E-03  -.5793E-04      -.2001E-03  -.5997E-04       .1187E-03  -.2840E-04       .1708E-09  -.7716E-10

T-DIRECTED CURRENTS FOR MODE  3
 -.3612E-05  -.1004E-03       .4985E-05   .9337E-05       .1209E-04  -.9460E-04       .1361E-04  -.4599E-04
  .1209E-04  -.9460E-04       .4985E-05   .9337E-05      -.3612E-05  -.1004E-03      -.7802E-05   .2665E-04

Z-DIRECTED CURRENTS FOR MODE  3
  .1689E-03   .3139E-05      -.2569E-03   .2045E-05       .4973E-03  -.9588E-06       .2398E-09  -.4494E-10
 -.4973E-03   .9590E-06       .2569E-03  -.2045E-05      -.1689E-03  -.3139E-05       .4974E-09  -.6553E-10
```

t and z directed current coefficients

GP79-0461-36

Figure 7c. Partial output of BOTRA for problem 1a.

Plot of currents along BOT

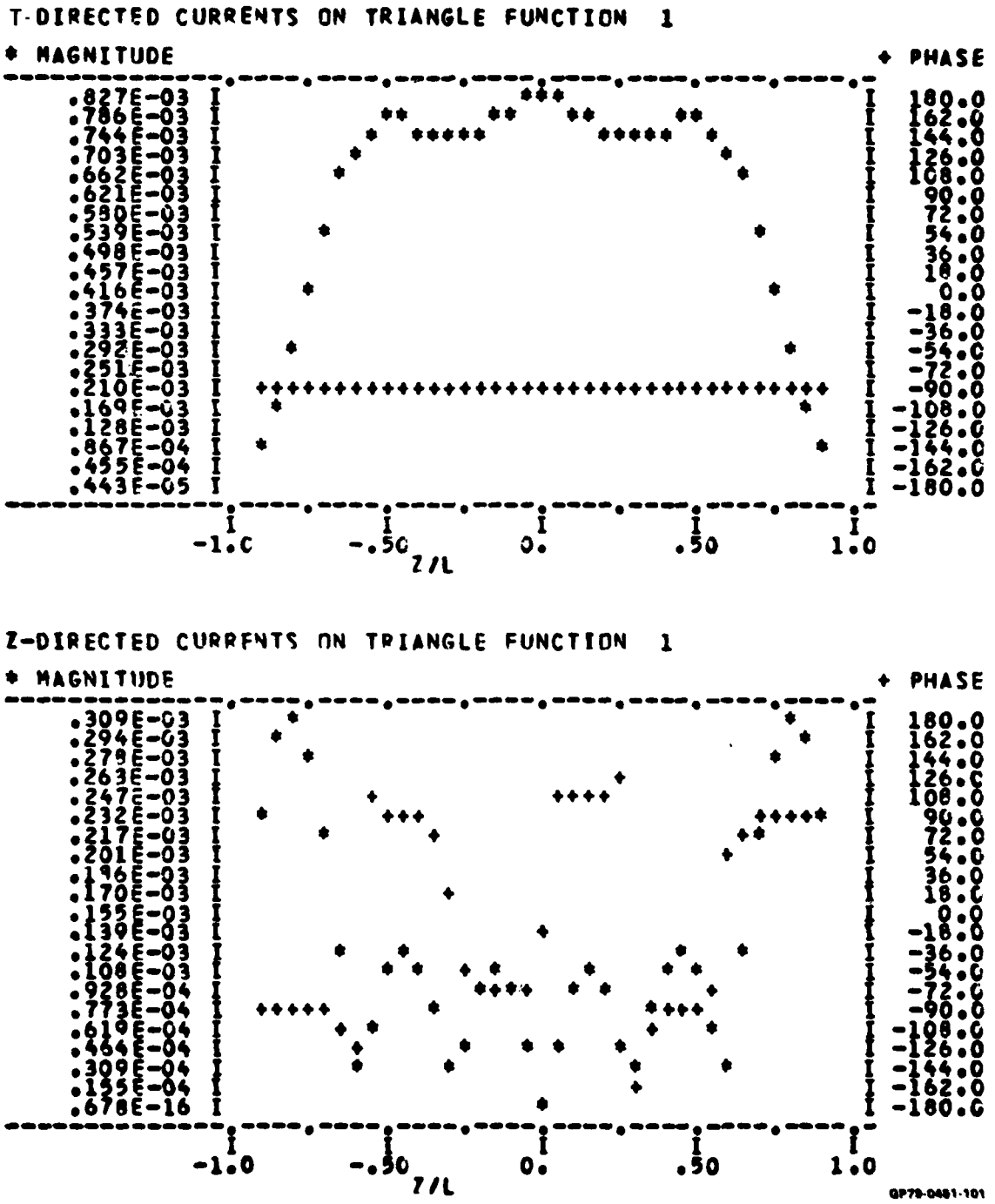

Figure 7c. Partial output of BOTRA for problem 1a. (concluded)

.EAR FIELD ANALYSIS

ZTEST	YTEST	XTEST	E-FIELD FIELD COMPONENTS RADIAL	E-FIELD FIELD COMPONENTS THETA	E-FIELD FIELD COMPONENTS PHI	H-FIELD FIELD COMPONENTS RADIAL	H-FIELD FIELD COMPONENTS THETA	H-FIELD FIELD COMPONENTS PHI
0.0000	0.0000	14.2560	.1033E-06	.3601E-14	.1093E+01	.3992E-16	.1453E-02	.3123E-17
0.0000	0.0000	19.4400	.4552E-07	.1958E-14	.3478E+00	.2440E-16	.8415E-03	.2117E-17
0.0000	0.0000	71.2800	.4246E-08	.5100E-15	.1278E+00	.6287E-17	.3254E-03	.9705E-18
0.0000	0.0000	150.0000	.9580E-09	.1533E-15	.6319E-01	.1604E-17	.1660E-03	.2613E-18
0.0000	0.0000	300.0000	.3313E-09	.3328E-16	.3086E-01	.2145E-18	.8170E-04	.9180E-19

GP79-0661-37

Figure 7d. Partial output of BOTRA - near fields for problem 1a.

2.6.2 Problem 1b

Compute the monostatic (backscatter) cross sections at 10 MHz for the following received and transmitted polarizations $\theta\theta$, $\phi\phi$, $\phi\theta$, and $\theta\phi$ in the horizontal (ϕ = 0) and roll (θ = 90) planes for the cylinder configuration used in problem 1a. For this part of the problem, assume that there is no aperture on the cylinder. Compute the cross sections at 46(NT) equi-spaced angles.

Solution - Since the basic body configuration was not altered, the results from BOTZSS and hence BOTINV in problem 1a are used. The cross sections were obtained from BOTSCM. Figure 8 depicts the input data to execute BOTSCM. Partial listings of the output from BOTSCM including the scattering cross sections are given in Figure 9.

```
 4
20 14
17 30  .2094397E+00
  0.0000   2.4798   4.5821   5.9867   6.4800   5.9867   4.5821   2.4798   -.0000  -2.4798   } Primary
 -4.5821  -5.9867  -6.4800  -5.9867  -4.5821  -2.4798   0.0000                              } BOT
  0.0000    .4933   1.8979   4.0002   6.4803   8.9598  11.0621  12.4667  12.9600  12.4667   } data set
 11.0621   8.9598   6.4800   4.0002   1.8979    .4933   0.0000
41.4
 2 46
    0.0     90.0  } Scattering angles
      1         2
```

GP79-0481-38

Figure 8. Input data for execution of BOTSCM for problem 1b.

```
   NPT      NBAND    NMODE     NP       MC      BK
    20        14        4       17       50  .2094397E+00
YH
  0.0000  2.4798  4.5821  5.9867  6.4800  5.9867  4.5821  2.4798  0.0000 -2.4798
 -4.5821 -5.9867 -6.4800 -5.9867 -4.5821 -2.4798  0.0000
XH
  0.0000  .4933  1.8979  4.0002  6.4800  8.9598 11.0621 12.4667 12.9600 12.4667
 11.0621  8.9598  6.4800  4.0002  1.8979   .4933  0.0000

HALF-LENGTH OF BOT =     41.4000

NUMBER OF FIXED ANGLES =  2
NUMBER OF ANGLES PER FIXED ANGLE =  46

FIXED ANGLE    CODE(PHI FIXED = 1, THETA FIXED =2)
   0.0             1
  90.0             2



M= -3  N= -3
Y
  .9079311F-04 -.4701087E-03  .6824476E-04 -.5931252E-03

M= -2  N= -3
Y
 -.7578504E-04  .1196460E-04 -.5825230E-04  .2733491E-04

M= -1  N= -3
Y
  .8818303E-04  .1279038E-04  .6279109E-04 -.2656702E-04
```

GP78-0451-20

Figure 9a. Partial output of BOTSCM for problem 1b.

Monostatic scattering cross section

Horizontal plane ($\phi = 0^{o}$)

PHI	THETA	MONO-STATIC RCS(DB)			
		VV	HH	VV	HH
0.0	0.0	-3.38	-3.38	-150.38	-150.38
0.0	2.0	-3.55	-3.38	-150.19	-150.15
0.0	4.0	-4.02	-3.38	-150.15	-150.15
0.0	6.0	-4.71	-3.38	-150.26	-150.26
0.0	8.0	-5.38	-3.39	-150.52	-150.52
0.0	10.0	-5.66	-3.41	-150.86	-150.86
0.0	12.0	-5.29	-3.43	-151.04	-151.04
0.0	14.0	-4.45	-3.43	-150.63	-150.63
0.0	16.0	-3.54	-3.40	-149.29	-149.29
0.0	18.0	-2.84	-3.27	-147.24	-147.24
0.0	20.0	-2.54	-3.01	-145.00	-145.00
0.0	22.0	-2.69	-2.57	-142.88	-142.88
0.0	24.0	-3.36	-1.99	-141.04	-141.04
0.0	26.0	-4.56	-1.31	-139.53	-139.53
0.0	28.0	-6.20	-.63	-138.36	-138.36
0.0	30.0	-7.90	-.05	-137.54	-137.54
0.0	32.0	-8.87	.35	-137.10	-137.10
0.0	34.0	-8.90	.53	-137.06	-137.06
0.0	36.0	-8.84	.42	-137.46	-137.46
0.0	38.0	-9.57	-.00	-138.37	-138.37
0.0	40.0	-11.68	-.76	-139.84	-139.84
0.0	42.0	-16.08	-1.86	-141.99	-141.99
0.0	44.0	-23.09	-3.32	-144.94	-144.94
0.0	46.0	-19.29	-5.15	-148.75	-148.75
0.0	48.0	-16.16	-7.42	-152.61	-152.61
0.0	50.0	-16.68	-10.37	-153.51	-153.51
0.0	52.0	-18.59	-14.41	-151.38	-151.38
0.0	54.0	-13.49	-16.99	-148.73	-148.73
0.0	56.0	-8.17	-13.07	-146.35	-146.35
0.0	58.0	-4.9[illegible]	-9.31	-144.58	-144.58
0.0	60.0	-3.33	-7.14	-143.60	-143.60
0.0	62.0	-3.08	-6.32	-143.52	-143.52
0.0	64.0	-4.30	-6.78	-144.42	-144.42
0.0	66.0	-7.66	-8.40	-146.45	-146.45
0.0	68.0	-16.37	-9.85	-149.83	-149.83
0.0	70.0	-16.71	-8.38	-154.57	-154.57
0.0	72.0	-8.58	-5.98	-159.22	-159.22
0.0	74.0	-6.39	-5.00	-162.99	-162.99
0.0	76.0	-7.82	-6.36	-175.97	-175.97
0.0	78.0	-13.28	-13.16	-159.55	-159.55
0.0	80.0	-4.85	-13.13	-153.00	-153.00
0.0	82.0	2.12	-2.09	-150.04	-150.04
0.0	84.0	6.29	2.88	-149.30	-149.30
0.0	86.0	8.87	5.74	-150.72	-150.72
0.0	88.0	10.31	7.28	-155.55	-155.55
0.0	90.0	10.77	7.77	-271.84	-271.84

GP79-0451-40

Figure 9b. Partial output of BOTSCM for problem 1b.

Monostatic scattering cross section
Roll plane ($\theta = 90^{o}$)

PHI	THETA	MONO-STATIC RCS(DB)			
		00	00	00	00
0.0	90.0	10.77	7.77	-271.84	-271.49
4.0	90.0	10.77	7.77	-201.12	-201.12
8.0	90.0	10.78	7.78	-196.54	-196.54
12.0	90.0	10.78	7.78	-195.66	-195.66
16.0	90.0	10.79	7.79	-197.69	-197.69
20.0	90.0	10.79	7.79	-204.98	-204.98
24.0	90.0	10.79	7.79	-209.12	-209.12
28.0	90.0	10.79	7.79	-198.73	-198.73
32.0	90.0	10.78	7.78	-195.84	-195.84
36.0	90.0	10.78	7.78	-196.02	-196.02
40.0	90.0	10.78	7.77	-199.42	-199.42
44.0	90.0	10.77	7.77	-212.71	-212.71
48.0	90.0	10.77	7.77	-203.40	-203.40
52.0	90.0	10.78	7.77	-197.21	-197.21
56.0	90.0	10.78	7.78	-195.58	-195.58
60.0	90.0	10.79	7.79	-196.82	-196.82
64.0	90.0	10.79	7.79	-202.11	-202.11
68.0	90.0	10.79	7.79	-219.06	-219.06
72.0	90.0	10.79	7.79	-200.25	-200.25
76.0	90.0	10.79	7.78	-196.27	-196.27
80.0	90.0	10.78	7.78	-195.74	-195.74
84.0	90.0	10.78	7.77	-198.19	-198.19
88.0	90.0	10.77	7.77	-206.80	-206.80
92.0	90.0	10.77	7.77	-206.80	-206.80
96.0	90.0	10.78	7.77	-198.19	-198.19
100.0	90.0	10.78	7.78	-195.74	-195.74
104.0	90.0	10.79	7.78	-196.27	-196.27
108.0	90.0	10.79	7.79	-200.25	-200.25
112.0	90.0	10.79	7.79	-219.07	-219.07
116.0	90.0	10.79	7.79	-202.11	-202.11
120.0	90.0	10.79	7.79	-196.82	-196.82
124.0	90.0	10.78	7.78	-195.58	-195.58
128.0	90.0	10.78	7.77	-197.21	-197.21
132.0	90.0	10.77	7.77	-203.40	-203.40
136.0	90.0	10.77	7.77	-212.70	-212.70
140.0	90.0	10.78	7.77	-199.42	-199.42
144.0	90.0	10.78	7.78	-196.01	-196.01
148.0	90.0	10.78	7.78	-195.84	-195.84
152.0	90.0	10.79	7.79	-198.73	-198.73
156.0	90.0	10.79	7.79	-209.12	-209.12
160.0	90.0	10.79	7.79	-204.98	-204.98
164.0	90.0	10.79	7.79	-197.69	-197.69
168.0	90.0	10.78	7.78	-195.66	-195.66
172.0	90.0	10.78	7.78	-196.54	-196.54
176.0	90.0	10.77	7.77	-201.12	-201.12
180.0	90.0	10.77	7.77	-268.50	-268.85

GP79-0481-41

Figure 9c. Partial output of BOTSCM for problem 1b.

2.6.3 Problem 1c

Consider the cylinder in problem 1a with a passive aperture subtending an angle of 45° and extending from $-27.9 \leq Z \leq 27.9$ m along the length of the BOT. Let the edges of the aperture parallel to the z-axis be defined by the coordinates YO = 4.5822, XO = 11.062, and Y1 = -0.001, X1 = 12.95. (Let NP = 17 and NMODE = 4.)

a) Calculate the bistatic cross sections when a TM (θ-polarized) wave illuminates the body broadside ($\theta = 90°$). Repeat the analysis for a TE (ϕ-polarized) wave. For this calculation, assume that the body does not have an aperture.

b) Calculate the electric and magnetic fields penetrating the aperture when the body is again illuminated broadside with a 10 MHz TM or TE wave, along a line bisecting the aperture (i.e., the incident angles for the wave are $\theta_i = 90°$, $\phi_i = 22.5°$). Sample the fields at the following points, measured in meters, within the cylinder along a line bisecting the aperture:

ZTEST	YTEST	XTEST
0.0	0.248	7.0787
0.0	0.7439	8.276
0.0	1.2399	9.4734
0.0	1.7359	10.6707
0.0	2.4798	12.4667

and at the following points outside the aperture:

0.0	0.0	14.2560
0.0	0.0	19.44
0.0	0.0	71.28
0.0	0.0	150
0.0	0.0	300

Solution - The solution to the two parts of problem 1c was obtained by running BOTSCB, using BOTINV output from problem 1a as the input. In this analysis, the aperture was intercepted by two triangle functions. (For larger aperture angles, more triangle functions fall within the aperture

opening.) Figures 10 and 11 depict the coordinate file and partial listings of the inputs and outputs of BOTSCB. The bistatic scattering cross section for the apertureless body and the corresponding currents (partial listing) for θ and ϕ-polarized incident waves are given in Figures 11b and 11c, respectively. These outputs constitute the solution of the first part of problem 1c. The solution of the second part of the problem, involving the cylinder with the passive aperture, is summarized in Figure 11d.

```
 4
20 14
17 50   .2094397E+00
  0.0000   2.4798   4.5821   5.9867   6.4800   5.9867   4.5821   2.4798   -.0000 -2.4798
 -4.5821  -5.9867  -6.4800  -5.9867  -4.5821  -2.4798   0.0000                          } Primary BOT data set
  0.0000    .4933   1.8979   4.0002   6.4800   8.9598  11.0621  12.4667  12.9600 12.4667
 11.0621   8.9598   6.4800   4.0002   1.8979    .4933   0.0000
 41.4
  2 46 22.5000 90.0000
    22.5       90.0                                   } Scattering angles and incident field
       1          2
-27.9000 27.9000   4.5822 11.0620   -.0010 12.9590 ·Aperture
 10
    .0000    .2480   7.0787
    .0000    .7439   8.2760
    .0000   1.2399   9.4734
    .0000   1.7359  10.6707
    .0000   2.4798  12.4667
  0.0000   0.0000  14.2560
  0.0000   0.0000  19.4400
  0.0000   0.0000  71.2800
  0.0000   0.0000150.0000
  0.0000   0.0000300.0000
```

Near-field points

GP78-0461-42

Figure 10. Input data for execution of BOTSCB for problem 1c.

```
    NPT      NBAND    NMODE     NP       MC      BK
     20        14        4       17       50   .2094397E+00

YH
  0.0000  2.4798  4.5821  5.9867  6.4800  5.9867  4.5821  2.4798  0.0000 -2.4798
 -4.5821 -5.9867 -6.4800 -5.9867 -4.5821 -2.4798  0.0000

XH
  0.0000  1.4933  3.8979  6.0002  8.4800 10.9598 13.0621 12.4667 12.9600 12.4667
 11.0621  8.9598  6.4800  4.0002  1.8979  .4933  0.0000

HALF-LENGTH OF BOT =     41.4000

NUMBER OF FIXED ANGLES =  2
NUMBER OF ANGLES PER FIXED ANGLE =  46

FIXED ANGLE     CODE(PHI FIXED = 1, THETA FIXED =2)
   22.5            1
   90.0            2




M= -3  N= -3
Y
  .9070311E-04 -.4701087E-03  .6824476E-04 -.5931252E-03

M= -2  N= -3
Y
 -.7578504E-04  .1106460E-04 -.5825230E-04  .2733491E-04

M= -1  N= -3
Y
  .8818333E-04  .1279038E-04  .6279109E-04 -.2656702E-04

M=  0  N= -3
Y
 -.1079845E-03 -.3263554E-04 -.6970442E-04  .2862848E-04
```

GP79-0481-43

Figure 11a. Partial output of BOTSCB for problem 1c.

BI-STATIC RCS(DB). INCIDENT PHI = 22.5 THETA = 90.0

PHI	THETA	00	00	00	00
22.5	0.0	-12.45	-10.85	-127.82	-131.96
22.5	4.00	-10.90	-10.71	-126.78	-131.34
22.5	8.00	-9.73	-10.00	-125.35	-130.87
22.5	12.00	-8.91	-8.86	-123.68	-130.60
22.5	16.00	-8.42	-7.52	-121.97	-130.59
22.5	20.00	-8.29	-6.22	-120.43	-130.95
22.5	24.00	-8.56	-5.19	-119.24	-131.85
22.5	28.00	-9.26	-4.58	-118.60	-133.50
22.5	32.00	-10.49	-4.54	-118.75	-135.97
22.5	36.00	-12.33	-5.23	-120.12	-137.40
22.5	40.00	-16.32	-6.80	-123.74	-134.66
22.5	44.00	-22.54	-8.93	-132.22	-131.23
22.5	48.00	-14.88	-9.44	-125.14	-128.97
22.5	52.00	-8.99	-7.33	-119.24	-128.00
22.5	56.00	-5.36	-5.49	-116.83	-128.47
22.5	60.00	-4.23	-5.24	-116.81	-130.96
22.5	64.00	-5.94	-7.33	-119.68	-137.97
22.5	68.00	-16.55	-11.14	-130.12	-142.66
22.5	72.00	-5.09	-5.09	-124.35	-132.04
22.5	76.00	2.51	.86	-117.76	-128.72
22.5	80.00	6.95	4.51	-116.20	-128.36
22.5	84.00	9.47	6.66	-118.11	-130.84
22.5	88.00	10.65	7.67	-126.48	-139.46
22.5	92.00	10.65	7.67	-126.48	-139.46
22.5	96.00	9.47	6.66	-118.11	-130.84
22.5	100.00	6.95	4.51	-116.20	-128.36
22.5	104.00	2.51	.86	-117.76	-128.72
22.5	108.00	-5.09	-5.09	-124.35	-132.04
22.5	112.00	-16.55	-11.14	-130.12	-142.66
22.5	116.00	-5.94	-7.33	-119.68	-137.97
22.5	120.00	-4.23	-5.24	-116.81	-130.96
22.5	124.00	-5.36	-5.49	-116.83	-128.47
22.5	128.00	-8.99	-7.33	-119.24	-128.00
22.5	132.00	-14.88	-9.44	-125.14	-128.97
22.5	136.00	-22.54	-8.93	-132.22	-131.23
22.5	140.00	-16.32	-6.80	-123.74	-134.66
22.5	144.00	-12.33	-5.23	-120.12	-137.40
22.5	148.00	-10.49	-4.54	-118.75	-135.97
22.5	152.00	-9.26	-4.58	-118.60	-133.50
22.5	156.00	-8.56	-5.19	-119.24	-131.85
22.5	160.00	-8.29	-6.22	-120.43	-130.95
22.5	164.00	-8.42	-7.52	-121.97	-130.59
22.5	168.00	-8.91	-8.86	-123.68	-130.60
22.5	172.00	-9.73	-10.00	-125.35	-130.87
22.5	176.00	-10.90	-10.71	-126.78	-131.34
22.5	180.00	-12.45	-10.85	-127.82	-131.96

(For apertureless body)

Plane at $\phi = 22.5^{o}$

GP79-0451-44

Figure 11b. Partial output of BOTSCB for problem 1c.

```
THETA POLARIZED INCIDENT FIELD

T-DIRECTED CURRENTS FOR MODE -3
 -.2170E-03 -.7005E-04     -.2441E-03  .2333E-04     -.8994E-04  .3678E-04     -.8994E-04 -.3678E-04
 -.2441E-03 -.2333E-04     -.2171E-03  .7005E-04     -.6291E-04  .5041E-04      .6291E-04 -.5041E-04
Z-DIRECTED CURRENTS FOR MODE -3
 -.1768E-03 -.2605E-03     -.1997E-03 -.3300E-03     -.3369E-03 -.6933E-03     -.3370E-03 -.6933E-03
 -.1997E-03 -.3300E-03     -.1768E-03 -.2608E-03     -.2002E-03 -.6384E-04     -.2002E-03 -.6382E-04
T-DIRECTED CURRENTS FOR MODE -2
 -.7999E-04  .2210E-03     -.1269E-03  .1430E-03     -.5633E-04  .3292E-04     -.5633E-04 -.3292E-04
  .1269E-03 -.1430E-03      .7999E-04 -.2210E-03      .9378E-05 -.1110E-03     -.9378E-05  .1110E-03
Z-DIRECTED CURRENTS FOR MODE -2
 -.1880E-03  .2340E-03     -.1386E-03 -.4075E-04      .8691E-05 -.1694E-03      .8688E-05 -.1694E-03
 -.1586E-03 -.4075E-04     -.1880E-03  .2340E-03     -.1286E-03  .3026E-03     -.1286E-03  .3026E-03
T-DIRECTED CURRENTS FOR MODE -1
  .1452E-04 -.1157E-03      .5001E-04 -.7959E-04      .2659E-04 -.3069E-04     -.2659E-04  .3069E-04
 -.5001E-04  .7960E-04     -.1452E-04  .1157E-03      .8895E-05  .5671E-04     -.8895E-05 -.5671E-04
Z-DIRECTED CURRENTS FOR MODE -1
  .1239E-03 -.2136E-03      .1866E-03 -.9609E-05      .6727E-04  .1071E-03      .6728E-04  .1071E-03
  .1866E-03 -.9609E-05      .1239E-03 -.2156E-03     -.1661E-04 -.2114E-03     -.1666E-04 -.2114E-03
T-DIRECTED CURRENTS FOR MODE  0
 -.1887E-09  .3017E-09     -.2786E-09  .1259E-09     -.1126E-09 -.1784E-11      .1126E-09  .1784E-11
  .2786E-09 -.1259E-09      .1887E-09 -.3017E-09      .2722E-10 -.1685E-09     -.2722E-10  .1683E-09
Z-DIRECTED CURRENTS FOR MODE  0
 -.2055E-02  .1278E-02     -.1759E-02  .4115E-02      .3916E-02  .4589E-02      .3916E-02  .4589E-02
 -.1759E-02 -.4115E-02     -.2055E-02  .1278E-02      .6618E-03  .4161E-03      .6618E-03  .4161E-03
T-DIRECTED CURRENTS FOR MODE  1
 -.1452E-04  .1157E-03     -.5001E-04  .7959E-04     -.2659E-04  .3069E-04      .2659E-04 -.3069E-04
  .5001E-04 -.7960E-04      .1452E-04 -.1157E-03     -.8895E-05 -.5671E-04      .8895E-05  .5671E-04
Z-DIRECTED CURRENTS FOR MODE  1
  .1239E-03 -.2136E-03      .1866E-03 -.9609E-05      .6727E-04  .1071E-03      .6728E-04  .1071E-03
  .1866E-03 -.9609E-05      .1239E-03 -.2156E-03     -.1661E-04 -.2114E-03     -.1666E-04 -.2114E-03
T-DIRECTED CURRENTS FOR MODE  2
  .7999E-04 -.2210E-03      .1269E-03 -.1430E-03      .5633E-04 -.3292E-04     -.5633E-04  .3292E-04
 -.1269E-03  .1430E-03     -.7999E-04  .2210E-03     -.9378E-05  .1110E-03      .9378E-05 -.1110E-03
Z-DIRECTED CURRENTS FOR MODE  2
 -.1880E-03  .2340E-03     -.1386E-03 -.4075E-04      .8691E-05 -.1694E-03      .8688E-05 -.1694E-03
 -.1586E-03 -.4075E-04     -.1880E-03  .2340E-03     -.1286E-03  .3026E-03     -.1286E-03  .3026E-03
T-DIRECTED CURRENTS FOR MODE  3
 -.2170E-03  .7005E-04     -.2441E-03 -.2333E-04     -.8994E-04 -.3678E-04      .8994E-04  .3678E-04
  .2441E-03  .2333E-04      .2171E-03 -.7005E-04      .6291E-04 -.5041E-04     -.6291E-04  .5041E-04
Z-DIRECTED CURRENTS FOR MODE  3
 -.1768E-03 -.2605E-03     -.1997E-03 -.3300E-03     -.3369E-03 -.6933E-03     -.3370E-03 -.6933E-03
 -.1997E-03 -.3300E-03     -.1768E-03 -.2608E-03     -.2002E-03 -.6384E-04     -.2002E-03 -.6382E-04
```

t and z directed current coefficients for θ-polarized incident field

GP79-0481-90

Figure 11b. Partial output of BOTSCB for problem 1c. (continued)

BI-STATIC RCS(DB). INCIDENT PHI = 22.5 THETA = 90.0

PHI	THETA	θθ	θθ	θθ	θθ	
						(For apertureless body)
0.0	90.0	10.75	8.32	-152.54	-152.61	
4.0	90.0	10.76	8.16	-154.42	-154.51	
8.0	90.0	10.77	8.02	-156.60	-156.70	
12.0	90.0	10.78	7.91	-159.61	-159.72	
16.0	90.0	10.79	7.84	-163.86	-163.97	
20.0	90.0	10.79	7.80	-172.20	-172.31	
24.0	90.0	10.79	7.79	-176.64	-176.76	
28.0	90.0	10.79	7.82	-165.32	-165.43	
32.0	90.0	10.78	7.89	-160.50	-160.61	
36.0	90.0	10.78	7.99	-157.34	-157.44	
40.0	90.0	10.77	8.12	-155.05	-155.63	
44.0	90.0	10.75	8.27	-152.98	-153.05	
48.0	90.0	10.74	8.45	-151.29	-151.35	
52.0	90.0	10.71	8.64	-149.78	-149.82	
56.0	90.0	10.69	8.85	-148.40	-148.43	
60.0	90.0	10.66	9.06	-147.12	-147.14	
64.0	90.0	10.62	9.27	-145.93	-145.94	
68.0	90.0	10.58	9.47	-144.81	-144.81	
72.0	90.0	10.53	9.66	-143.74	-143.74	
76.0	90.0	10.48	9.84	-142.74	-142.73	
80.0	90.0	10.41	9.99	-141.79	-141.78	Roll plane ($\theta = 90^{o}$)
84.0	90.0	10.34	10.12	-140.89	-140.88	
88.0	90.0	10.27	10.21	-140.05	-140.04	
92.0	90.0	10.19	10.27	-139.26	-139.25	
96.0	90.0	10.10	10.30	-138.53	-138.52	
100.0	90.0	10.03	10.29	-137.85	-137.84	
104.0	90.0	9.97	10.22	-137.22	-137.22	
108.0	90.0	9.92	10.11	-136.66	-136.66	
112.0	90.0	9.92	9.95	-136.15	-136.15	
116.0	90.0	9.95	9.75	-135.70	-135.70	
120.0	90.0	10.05	9.50	-135.31	-135.31	
124.0	90.0	10.21	9.21	-134.99	-134.99	
128.0	90.0	10.43	8.87	-134.72	-134.72	
132.0	90.0	10.73	8.51	-134.52	-134.53	
136.0	90.0	11.09	8.12	-134.38	-134.39	
140.0	90.0	11.51	7.74	-134.33	-134.33	
144.0	90.0	11.96	7.37	-134.35	-134.35	
148.0	90.0	12.43	7.06	-134.44	-134.44	
152.0	90.0	12.92	6.83	-134.62	-134.62	
156.0	90.0	13.40	6.69	-134.89	-134.89	
160.0	90.0	13.86	6.68	-135.27	-135.27	
164.0	90.0	14.31	6.77	-135.76	-135.76	
168.0	90.0	14.72	6.96	-136.38	-136.38	
172.0	90.0	15.09	7.22	-137.15	-137.15	
176.0	90.0	15.43	7.51	-138.11	-138.11	
180.0	90.0	15.72	7.80	-139.31	-139.31	

GP78-0661-90

Figure 11b. Partial output of BOTSCB for problem 1c. (continued)

Plot of currents along BOT for
θ-polarized incident field

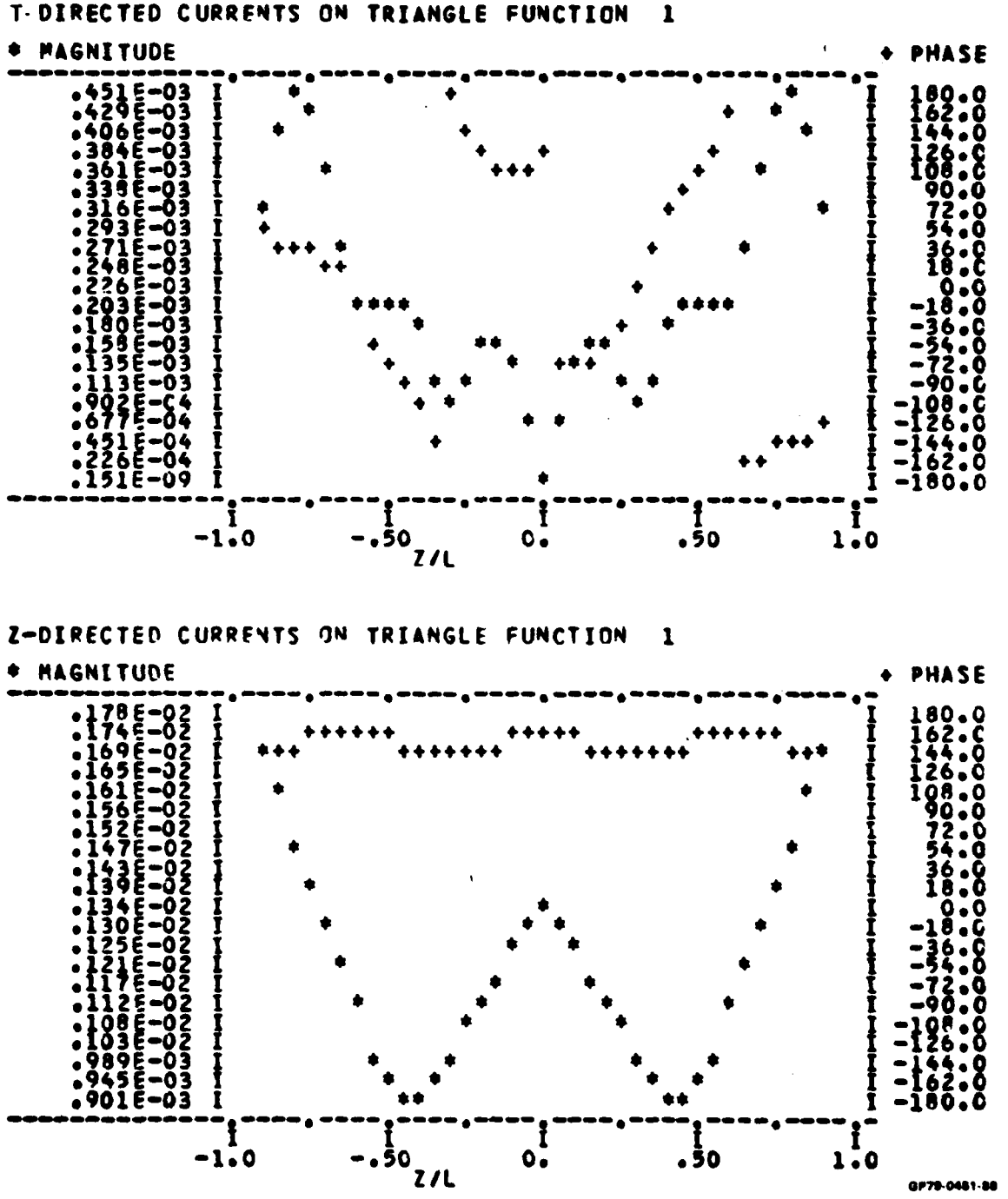

Figure 11b. Partial output of BOTSCB for problem 1c. (concluded)

PHI POLARIZED INCIDENT FIELD

```
T-DIRECTED CURRENTS FOR MODE -3
 .4750E-04  .2758E-04        .1007E-03  .2844E-03       -.8843E-04 -.3291E-03       -.8843E-04 -.3291E-03
 .1007E-03  .2464E-03        .4750E-04  .5754E-04       -.9880E-04 -.2033E-03       -.9880E-04 -.2033E-03

Z-DIRECTED CURRENTS FOR MODE -3
-.9157E-04 -.2700E-03       -.9521E-04 -.2932E-03       -.4483E-04 -.7144E-04       -.4484E-04 -.7143E-04
 .9520E-04  .2002E-03        .9158E-04  .2750E-03       -.4121E-04  .1412E-03       -.4121E-04 -.1412E-03

T-DIRECTED CURRENTS FOR MODE -2
-.2119E-04 -.2303E-03       -.1466E-03 -.3139E-03       -.1899E-03 -.3984E-03       -.1899E-03 -.3984E-03
-.1466E-03 -.3109E-03        .2119E-04  .2356E-05        .1649E-03  .3305E-03        .1649E-03  .3305E-03

Z-DIRECTED CURRENTS FOR MODE -2
-.1641E-03 -.9232E-04       -.1174E-03 -.1320E-03       -.3709E-04 -.9182E-04       -.3708E-04 -.9182E-04
-.1174E-03  .1320E-03        .1641E-03  .9255E-04       -.8466E-04  .2238E-04       -.8469E-04 -.2238E-04

T-DIRECTED CURRENTS FOR MODE -1
-.3861E-03 -.1178E-04       -.1731E-03 -.3243E-03       -.2442E-03 -.4239E-03       -.2442E-03 -.4239E-03
 .1732E-03  .3264E-03        .3459E-05 -.1179E-04       -.2316E-03  .3788E-03       -.2316E-03 -.3788E-03

Z-DIRECTED CURRENTS FOR MODE -1
-.6666E-04 -.4678E-04       -.4114E-04 -.5245E-04       -.1108E-04 -.2403E-04       -.1108E-04 -.2403E-04
 .4114E-04 -.3984E-04        .6666E-04 -.4678E-04        .3660E-04  .1497E-04       -.3660E-04  .1497E-04

T-DIRECTED CURRENTS FOR MODE  0
-.1571E-02 -.2063E-02       -.1428E-02 -.4223E-02       -.3829E-02 -.2293E-02       -.3829E-02 -.2293E-02
 .1424E-02  .4222E-02       -.1571E-02 -.2033E-02        .7459E-03  .2160E-02        .7459E-03  .2160E-02

Z-DIRECTED CURRENTS FOR MODE  0
-.1463E-11 -.2796E-12       -.1241E-12 -.1152E-11       -.4251E-12  .3980E-12        .4251E-12 -.3980E-12
-.1241E-12 -.1146E-11        .1463E-11 -.2834E-12       -.4833E-12  .4605E-12        .8436E-12 -.4605E-12

T-DIRECTED CURRENTS FOR MODE  1
-.3861E-03 -.1178E-04       -.1731E-03 -.3243E-03       -.2442E-03 -.4239E-03       -.2442E-03 -.4239E-03
 .1732E-03  .3264E-03        .3459E-04 -.1179E-04       -.2316E-03  .3788E-03       -.2316E-03 -.3788E-03

Z-DIRECTED CURRENTS FOR MODE  1
-.6666E-04 -.4678E-04       -.4114E-04 -.5245E-04       -.1108E-04 -.2403E-04       -.1108E-04 -.2403E-04
-.4114E-04 -.3984E-04        .6666E-04 -.4678E-04        .3660E-04  .1497E-04       -.3660E-04  .1497E-04

T-DIRECTED CURRENTS FOR MODE  2
-.2119E-04 -.2303E-03       -.1466E-03 -.3139E-03       -.1899E-03 -.3984E-03       -.1899E-03 -.3984E-03
-.1466E-03 -.3109E-03        .2119E-04  .2356E-05        .1649E-03  .3305E-03        .1649E-03  .3305E-03

Z-DIRECTED CURRENTS FOR MODE  2
-.1641E-03 -.9232E-04       -.1174E-03 -.1320E-03       -.3709E-04 -.9182E-04       -.3708E-04 -.9182E-04
-.1174E-03 -.1320E-03        .1641E-03  .9255E-04       -.8466E-04  .2238E-04       -.8469E-04 -.2238E-04

T-DIRECTED CURRENTS FOR MODE  3
 .4750E-04  .2758E-04        .1007E-03  .2844E-03       -.8843E-04 -.3291E-03       -.8843E-04 -.3291E-03
 .1007E-03  .2464E-03        .4750E-04  .5754E-04       -.9880E-04 -.2033E-03       -.9880E-04 -.2033E-03

Z-DIRECTED CURRENTS FOR MODE  3
-.9157E-04 -.2700E-03       -.9521E-04 -.2932E-03       -.4483E-04 -.7144E-04       -.4484E-04 -.7143E-04
-.9520E-04 -.2002E-03        .9158E-04  .2750E-03       -.4121E-04  .1412E-03       -.4121E-04 -.1412E-03
```

t and z directed current coefficients for ϕ-polarized incident field

GP79-0451-45

Figure 11c. Partial output of BOTSCB for problem 1c.

Plot of currents along BOT for
ϕ-polarized incident field

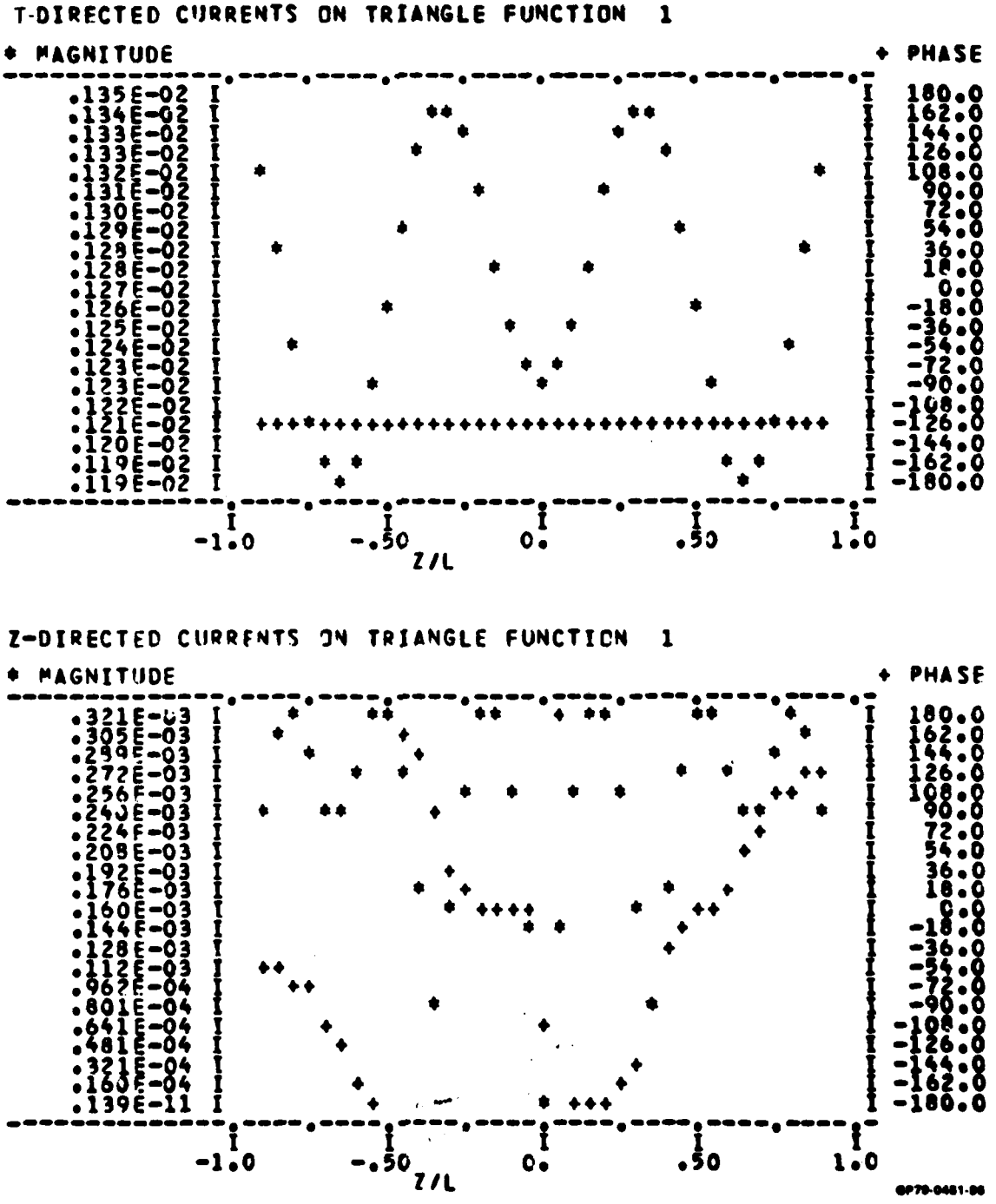

Figure 11c. Partial output of BOTSCB for problem 1c. (concluded)

```
APERTURE ANALYSIS

   Z0        Z1        Y0       X0         Y1       X1
-27.9000  27.9000   4.5822  11.0620    -.0610  12.9590   Aperture coordinates

  LT    VLOW       VHGH       IT

  3      .0001     2.5284     -1
  4     2.5284      .0014      1

 LT  IT                    FPP                                                 FPPZ

  3  -1    .7821E-09   .3751E+00   .1250E+00   .9777E-16   .3750E+00   .1250E+00
  4   1    .1250E+00   .3756E+00   .7821E-07   .1250E+00   .3751E+00   .9777E-08

YA1
 -.5520E-03 -.1961E-02 -.4327E-03 -.6107E-03   Ya^tt  ┐
 -.4331E-03 -.6136E-03 -.5526E-03 -.1963E-02          │
YA2                                                   │
  .1184E-16  .4565E-16 -.6052E-16 -.4866E-16   Ya^zt  │
  .3493E-16  .1223E-16 -.9013E-17 -.1994E-16          │
YA3                                                   ├ Aperture
  .3304E-16  .2660E-18 -.5430E-16  .9374E-18   Ya^tz  │ admittance
  .6985E-16  .1537E-16 -.2456E-16 -.1941E-15          │
YA4                                                   │
 -.4518E-03  .4090E-02 -.3106E-03 -.1628E-02   Ya^zz  │
 -.3107E-03 -.1629E-02 -.4519E-03  .4092E-02          ┘
```

GP79-0451-46

Figure 11d. Partial output of BOTSCB for problem 1c.

NEAR FIELD ANALYSIS (for aperture-coupled fields)

ZTEST	YTEST	XTEST		E-FIELD FIELD COMPONENTS RADIAL	E-FIELD FIELD COMPONENTS THETA	E-FIELD FIELD COMPONENTS PHI	H-FIELD FIELD COMPONENTS RADIAL	H-FIELD FIELD COMPONENTS THETA	H-FIELD FIELD COMPONENTS PHI
0.0000	.2480	7.0787	0 INC POL E-FIELD	.1054E-07	.2108E+00	.3940E-08	.6414E-03	.1243E-15	.1716E-02
			0 INC POL E-FIELD	.3426E+00	.6654E-14	.9167E+00	.3929E-12	.6222E-03	.1469E-12
0.0000	.7439	9.2760	0 INC POL E-FIELD	.1399E-07	.4179E+00	.6373E-08	.6715E-03	.6437E-16	.2148E-02
			0 INC POL E-FIELD	.3233E+00	.1152E-13	.1024E+01	.8620E-12	.1105E-03	.2696E-12
0.0000	1.2399	9.4734	0 INC POL E-FIELD	.1936E-07	.6743E+00	.5203E-08	.6998E-03	.3209E-15	.2604E-02
			0 INC POL E-FIELD	.2894E+00	.1239E-13	.1077E+01	.1713E-11	.9041E-03	.4604E-12
0.0000	1.7359	10.6707	0 INC POL E-FIELD	.2723E-07	.9761E+00	.6416E-08	.6953E-03	.1303E-14	.2951E-02
			0 INC POL E-FIELD	.2449E+00	.7545E-14	.1039E+01	.3184E-11	.1691E-02	.7503E-12
0.0000	2.4798	12.4667	0 INC POL E-FIELD	.1019E-07	.1385E+01	.2029E-08	.4830E-03	.5766E-12	.2628E-02
			0 INC POL E-FIELD	.1416E+00	.4723E-14	.7119E+00	.8512E-11	.1048E-02	.1693E-11
0.0000	0.0000	14.2560	0 INC POL E-FIELD	.7968E-08	.9713E+00	.2304E-07	.2624E-02	.2620E-10	.3129E-02
			0 INC POL E-FIELD	.3015E+00	.4460E-09	.7957E+00	.1101E-11	.1622E-02	.1774E-11
0.0000	0.0000	19.4460	0 INC POL E-FIELD	.2756E-08	.8786E+00	.4504E-03	.9080E-03	.1154E-10	.2256E-02
			0 INC POL E-FIELD	.1043E+00	.2241E-09	.4159E+03	.3812E-12	.1117E-02	.4781E-12
0.0000	0.0000	71.2800	0 INC POL E-FIELD	.1711E-09	.3844E+00	.1114E-08	.6760E-04	.2831E-11	.9067E-03
			0 INC POL E-FIELD	.6475E-02	.6024E-10	.1832E+00	.2837E-13	.4698E-03	.1403E-12
0.0000	0.0000	159.0000	0 INC POL E-FIELD	.3333E-10	.1722E+00	.2257E-09	.1107E-04	.1377E-11	.6432E-03
			0 INC POL E-FIELD	.1261E-02	.2660E-10	.8795E-01	.4646E-14	.2314E-03	.6702E-13
0.0000	0.0000	300.0000	0 INC POL E-FIELD	.1187E-10	.8437E-01	.2544E-09	.2234E-05	.6724E-12	.2229E-03
			0 INC POL E-FIELD	.4491E-03	.1244E-10	.4279E-01	.9376E-15	.1153E-03	.3285E-13

GP79-0451-96

Figure 11d. Partial output of BOTSCB for problem 1c. (concluded)

2.6.4 Problem 2

Consider an asymmetric wing section of 2.76 λ length, depicted subsequently in Figure 17, with coordinates specified in Figure 12. Use NP = 17 points to describe the body and let NMODE = 4. Compute the ϕ-polarized radiation patterns for a t-polarized axial slot antenna of 2.06 λ length and 0.125 λ width, centered about Z = 0, X = 28.796, and Y = 26.085. (The location of this slot corresponds to the eighth triangle function and is denoted as antenna A in Figure 17.) Carry out the analysis at 10 MHz.

Solution - The coordinates for the wing section are input by the user. Then the following sequence of codes are run: BOTZSS, BOTINV, and BOTRA. The input data for execution of these programs are given in Figure 12. The partial outputs from these programs are shown in Figures 13-15. The power radiation patterns are summarized in Figure 16. These results are plotted in Figure 17 for antenna location A, as well as locations B and C. (The latter two patterns are obtained if the aperture coincides with the first and sixth triangle functions in Figure 13, respectively.)

```
  4
 20 14
 17 50   .2013787E-01
 26.0850 31.0710 32.3539 32.9555 33.0593 32.6245 31.8038 30.7098 28.0533 25.7583   } Primary
 24.8511 24.1056 23.6470 23.6347 24.0259 24.7786 26.0850                           } BOT
 28.7960 48.2965 67.7971 87.2976106.7981126.2986145.7992165.2997184.8002165.2997   } data set
145.7992126.2986106.7981 87.2976 67.7971 48.2965 28.7960
430.5716
  2 46
    90.0     -90.0    } Radiation angles
       2        2
  1
-322.924
 322.929
  1.0000    0.0000    } Slot antenna
  1.0000
  0.0000
  0
```

No near-field points

GP79-0461-47

Figure 12. Input data for execution of BOTZSS, BOTINV, and BOTRA for problem 2.

```
    NPT      NBAND    NNODE     NP       MC       BK
     20        14        4       17       50   .2013787E-01

YH
 24.0859 31.0710 32.3539 32.9255 33.0593 32.6265 31.8038 30.7098 28.0530 25.7583
 24.8511 24.1098 23.6470 23.6347 24.0259 24.7786 26.0850

XH
 28.7960 48.2965 67.7971 87.2976106.7981126.2986145.7992165.2997184.8002165.2997
145.7992126.2986106.7981 87.2976 67.7971 48.2965 28.7960

BODY COORDINATES, ♦ INDICATES TRIANGLE PEAK
```

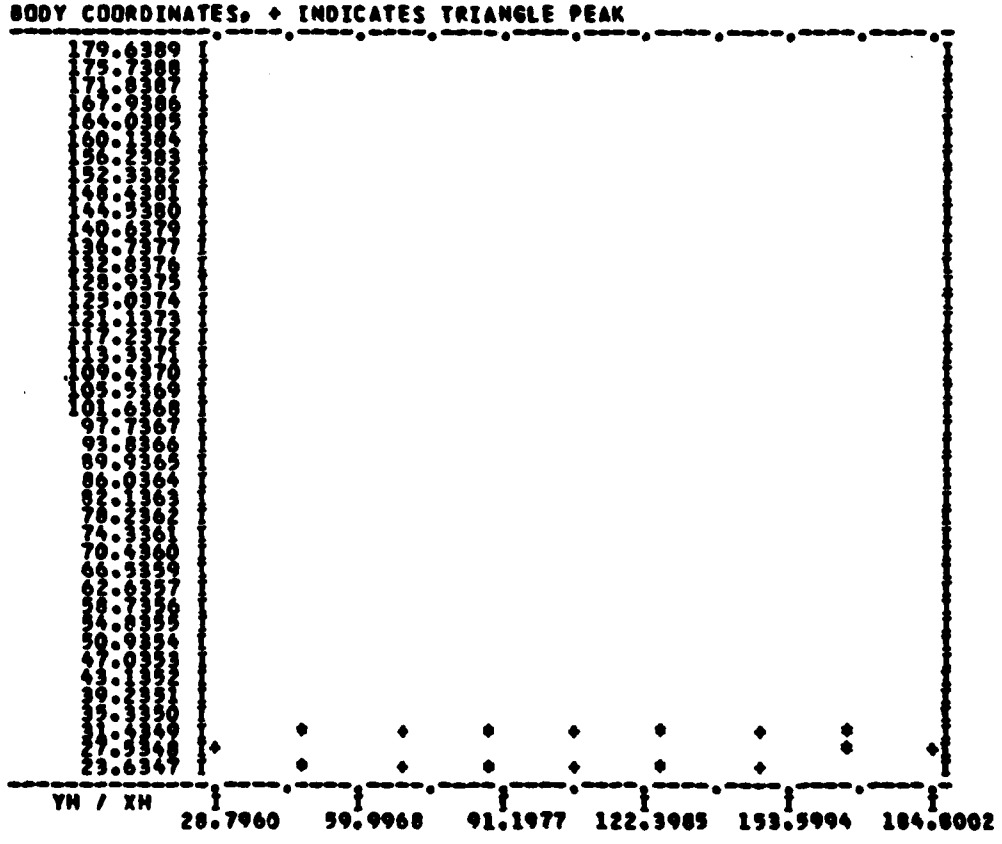


```
HALF-LENGTH OF BOT =     430.5716
```

GP78-0461-48

Figure 13. Partial output of BOTZSS for problem 2.

N= 0 N= 0 NP= 19 MC= 50 BK= .2013787E-01

Z1

72.04	-353.9	66.83	157.3	52.86	55.20
-65.69	-60.31	-71.69	238.9	-.4049	69.73
66.83	157.3	72.45	-353.0	66.93	156.7
-72.04	223.8	-65.82	-60.79	-.5969	6.069
52.86	55.20	66.93	156.7	72.28	-353.5
-65.79	-65.61	-52.02	-47.07	.1533	2.005
.5135	1.206	.3456	4.300	.7823	64.56
.4902	3.781	.4337	.7948	.7466	.9657
-52.02	-47.19	-65.85	-65.87	-71.91	244.0
66.97	156.6	52.81	54.60	.8824	.4309
-65.66	-60.31	-72.04	223.8	-65.79	-65.61
72.44	-353.0	66.98	156.5	1.535	5.516
-71.69	238.9	-65.82	-60.79	-52.02	-47.07
66.98	156.5	72.42	-353.1	2.459	71.40
-.4049	69.73	-.5969	6.069	.1533	2.005
1.535	5.516	2.459	71.40	.8177	-108.9

.5135	1.206	-52.02	-47.19
.3456	4.300	-65.85	-65.87
.7823	64.56	-71.91	244.0
.4033	-98.65	1.012	64.93
1.012	64.93	72.34	-353.4
.4902	3.781	66.97	156.6
.4337	.7948	52.81	54.60
.7466	.9657	.8824	.4309

Impedence matrix $Z^{tt}_{0,0}$

Figure 13. Partial output of BOTZSS for problem 2. (concluded)

```
      NP          NNODE       NBAND
      17            4           14

YN
 26.0850 31.0710 32.3239 32.9555 33.0593 32.6265 31.8038 30.7098 28.0530 25.7583
 24.8511 24.1036 23.6470 23.6347 24.0259 24.7786 26.0850

XN
 28.7960 48.2965 67.7971 87.2976106.7981126.2986145.7992165.2997184.8002165.2997
145.7992126.2986106.7981 87.2976 67.7971 48.2965 28.7960

 THE MINIMUM DIMENSIONS ARE AS FOLLOWS:
       Z          ZI       WORK         NZ          LR
     12544        256         0           0         112

 M= -3  N= -3
Y1
  .3839E-04 -.2566E-02  .3596E-04 -.2612E-02  .2690E-04 -.1300E-02   .1989E-04 -.2793E-02  .4738E-05 -.1214E-02
  [illegible]                                                        .1710E-04 -.1403E-02  .7484E-05 -.2671E-02
                                                                     .3018E-04 -.3069E-02  .1046E-04 -.2259E-02
                                                                     .3874E-04 -.3644E-02  .3039E-04 -.3069E-02
                                                                     .3039E-04 -.3069E-02  .3914E-04 -.2564E-02
                                                                     .1709E-04 -.1404E-02  .3745E-04 -.2656E-02
                                                                     .2033E-04 -.2792E-02  .2843E-04 -.1291E-02
                                                                    -.5768E-07 -.4065E-03  .2121E-04 -.2754E-02
Y2
  [illegible]                                                        .9427E-03  .3532E-04  .1146E-02 -.1010E-04
                                                                    -.1114E-02  .5270E-04 -.2507E-02 -.2665E-05
                                                                     .2366E-02  .9126E-04 -.1631E-02  .5120E-04
                                                                    -.1028E-04 -.3219E-05  .1615E-01  .1323E-03
                                                                    -.2276E-02 -.9984E-04 -.3940E-03 -.1426E-05
                                                                     .1178E-02 -.5866E-04 -.5356E-02 -.1537E-04
                                                                    -.8354E-03 -.4318E-04  .2415E-02 -.4213E-05
                                                                     .6377E-04 -.4012E-05 -.5782E-02 -.6949E-04
```

Admittance matrix

$Y^{tt}_{-3,-3}$

$Y^{zt}_{-3,-3}$

GP79-0461-40

Figure 14. Partial output of BOTINV for problem 2.

```
    NPT      NBAND    NMODE    NP      NC     BK
     20        14       4      17      50   .2013787E-01
YN
 [illegible] 30.7098 28.0530 25.7583
XN
 [illegible]165.2997184.0002165.2997

HALF-LENGTH OF BOT =     430.5716

NUMBER OF FIXED ANGLES =  2
NUMBER OF ANGLES PER FIXED ANGLE =  46


FIXED ANGLE    CODE(PHI FIXED = 1, THETA FIXED =2)
  90.0          2
 -90.0          2

NUMBER OF SLOT ANTENNAS =  1

ANTENNA NO.   IS    ZO        Z1           EO          TEXC       ZEXC
      1        8 -322.9290  322.9290    1.0000     0.0000     1.0000     0.0000


M= -3  N= -3
Y
VR .3838891E-04 -.2565773E-02  .3595749E-04 -.2612063E-02
      T-EXCITATION
         0.      0.      0.      0.      0.      0.      0.      0.      0.      0.  V^t_-3
         0.      0.      0.      0.      .15     0.
      Z-EXCITATION
         0.      0.      0.      0.      0.      0.      0.      0.      0.      0.  V^z_-3
         0.      0.      0.      0.      0.      0.
VN
      T-EXCITATION
         0.      0.      0.      0.      0.      0.      0.      0.      0.      0.  V^t_-3
         0.      0.      0.      0.      .15     0.
      Z-EXCITATION
         0.      0.      0.      0.      0.      0.      0.      0.      0.      0.  V^z_-3
         0.      0.      0.      0.      0.      0.
POWER IN CURRENT MODES =    .329E-03   CUMMULATIVE POWER =    .329E-03
```

GP79-0451-80

Figure 15. Partial output of BOTRA for problem 2.

TOTAL POWER(DB) = -5.17

PHI	THETA	POWER(DB) Φ	POWER(DB) θ
0.0	90.0	-235.48	-75.99
4.0	90.0	-233.28	-76.05
8.0	90.0	-230.15	-76.13
12.0	90.0	-227.52	-76.22
16.0	90.0	-225.40	-76.32
20.0	90.0	-223.65	-76.45
24.0	90.0	-222.18	-76.60
28.0	90.0	-220.91	-76.77
32.0	90.0	-219.81	-76.97
36.0	90.0	-218.83	-77.21
40.0	90.0	-217.96	-77.47
44.0	90.0	-217.18	-77.78
48.0	90.0	-216.49	-78.11
52.0	90.0	-215.87	-78.48
56.0	90.0	-215.33	-78.86
60.0	90.0	-214.84	-79.26
64.0	90.0	-214.43	-79.66
68.0	90.0	-214.07	-80.02
72.0	90.0	-213.78	-80.33
76.0	90.0	-213.54	-80.54
80.0	90.0	-213.36	-80.63
84.0	90.0	-213.24	-80.59
88.0	90.0	-213.18	-80.42
92.0	90.0	-213.18	-80.14
96.0	90.0	-213.23	-79.77
100.0	90.0	-213.35	-79.36
104.0	90.0	-213.52	-78.92
108.0	90.0	-213.75	-78.48
112.0	90.0	-214.04	-78.06
116.0	90.0	-214.40	-77.67
120.0	90.0	-214.82	-77.31
124.0	90.0	-215.30	-76.99
128.0	90.0	-215.85	-76.70
132.0	90.0	-216.48	-76.46
136.0	90.0	-217.18	-76.25
140.0	90.0	-217.97	-76.07
144.0	90.0	-218.86	-75.92
148.0	90.0	-219.87	-75.81
152.0	90.0	-221.01	-75.71
156.0	90.0	-222.33	-75.64
160.0	90.0	-223.89	-75.59
164.0	90.0	-225.75	-75.56
168.0	90.0	-228.09	-75.54
172.0	90.0	-231.21	-75.53
176.0	90.0	-235.65	-75.53
180.0	90.0	-240.20	-75.54

Power radiation patterns

Roll plane ($\theta = 90^{o}$)

GP79-0481-81

Figure 16a. Partial output of BOTRA for problem 2.

PHI	THETA	POWER(DB) φ	POWER(DB) θ
0.0	-90.0	-240.20	-75.54
4.0	-90.0	-236.50	-75.56
8.0	-90.0	-231.82	-75.60
12.0	-90.0	-228.54	-75.64
16.0	-90.0	-226.11	-75.70
20.0	-90.0	-224.18	-75.77
24.0	-90.0	-222.60	-75.86
28.0	-90.0	-221.25	-75.96
32.0	-90.0	-220.09	-76.09
36.0	-90.0	-219.06	-76.24
40.0	-90.0	-218.16	-76.41
44.0	-90.0	-217.35	-76.61
48.0	-90.0	-216.63	-76.83
52.0	-90.0	-215.99	-77.08
56.0	-90.0	-215.42	-77.34
60.0	-90.0	-214.93	-77.61
64.0	-90.0	-214.49	-77.88
68.0	-90.0	-214.12	-78.14
72.0	-90.0	-213.82	-78.37
76.0	-90.0	-213.57	-78.57
80.0	-90.0	-213.38	-78.70
84.0	-90.0	-213.25	-78.77
88.0	-90.0	-213.19	-78.77
92.0	-90.0	-213.18	-78.69
96.0	-90.0	-213.23	-78.55
100.0	-90.0	-213.33	-78.35
104.0	-90.0	-213.50	-78.12
108.0	-90.0	-213.73	-77.87
112.0	-90.0	-214.03	-77.60
116.0	-90.0	-214.38	-77.34
120.0	-90.0	-214.80	-77.10
124.0	-90.0	-215.29	-76.87
128.0	-90.0	-215.84	-76.66
132.0	-90.0	-216.47	-76.48
136.0	-90.0	-217.18	-76.32
140.0	-90.0	-217.97	-76.19
144.0	-90.0	-218.87	-76.08
148.0	-90.0	-219.88	-76.00
152.0	-90.0	-221.03	-75.94
156.0	-90.0	-222.35	-75.91
160.0	-90.0	-223.89	-75.88
164.0	-90.0	-225.73	-75.88
168.0	-90.0	-227.97	-75.89
172.0	-90.0	-230.75	-75.91
176.0	-90.0	-233.92	-75.95
180.0	-90.0	-235.48	-75.99

Roll plane ($\theta = -90^{o}$)

GP79-0451-98

Figure 16a. Partial output of BOTRA for problem 2. (concluded)

```
T-DIRECTED CURRENTS FOR MODE -3
 -.1110E-03  -.4776E-03          .3827E-05  -.2268E-03        -.9445E-05  -.3823E-03        -.1501E-04  -.3019E-04
  .1176E-04  -.3748E-03          .4959E-05  -.2256E-03        -.3351E-06  -.4757E-03        -.7649E-05  -.5944E-03

Z-DIRECTED CURRENTS FOR MODE -3
 -.2096E-02  -.1438E-04          -.7247E-03  -.2629E-05        -.8144E-03  -.1960E-04         .9121E-03  -.1824E-05
 -.8276E-03   .2014E-04           .7319E-03  -.2477E-05        -.2115E-02  -.1458E-04         .7143E-05  -.1538E-05

T-DIRECTED CURRENTS FOR MODE -2
 -.1721E-04   .4190E-03          -.2430E-04   .8420E-03        -.3021E-04   .1340E-02        -.3207E-04  -.1427E-02
 -.3560E-04   .1341E-02          -.3075E-04   .8436E-03        -.2400E-04   .4158E-03        -.8436E-03  -.1063E-02

Z-DIRECTED CURRENTS FOR MODE -2
 -.2714E-02   .2360E-05          -.4233E-03  -.5926E-05        -.8968E-03   .1291E-04        -.7389E-05  -.1043E-03
  .9014E-03  -.1712E-04           .4240E-03  -.1074E-04        -.2743E-02   .1823E-05        -.1734E-04   .7888E-05

T-DIRECTED CURRENTS FOR MODE -1
  .2916E-04  -.1135E-02          .4677E-04  -.1536E-02         .3796E-04  -.3700E-02         .2534E-04  -.4886E-02
  .4266E-04  -.3727E-02          .6361E-04  -.1553E-02         .7343E-04   .1139E-02         .5142E-04  -.4883E-02

Z-DIRECTED CURRENTS FOR MODE -1
 -.2270E-02  -.7661E-05          -.1671E-02  -.9317E-05        -.1030E-02  -.1470E-04         .1301E-04  -.1316E-04
 -.1029E-02   .1871E-04           .1675E-02  -.1827E-04        -.2304E-02  -.4902E-05         .1656E-04  -.8499E-05

T-DIRECTED CURRENTS FOR MODE  0
 -.3791E-03  -.8399E-02          .1698E-03  -.5434E-02        -.7042E-04  -.1688E-01        -.2479E-03  -.2230E-01
 -.7579E-04  -.1702E-01          .2267E-03  -.5594E-02        -.4764E-03  -.8114E-02        -.5059E-03  -.2502E-01

Z-DIRECTED CURRENTS FOR MODE  0
  .3475E-17  -.6412E-17          -.6411E-17  -.1454E-17        -.5527E-17  -.8397E-17        -.1113E-17  -.3206E-17
  .3768E-17  -.2164E-16          -.6742E-17   .1049E-16        -.8344E-17  -.9314E-17         .2688E-17  -.2051E-17

T-DIRECTED CURRENTS FOR MODE  1
  .2916E-04  -.1135E-02          .4677E-04  -.1536E-02         .3796E-04  -.3700E-02         .2534E-04  -.4886E-02
  .4266E-04  -.3727E-02          .6361E-04  -.1553E-02         .7343E-04   .1139E-02         .5142E-04  -.4883E-02

Z-DIRECTED CURRENTS FOR MODE  1
 -.2270E-02  -.7661E-05          -.1671E-02  -.9317E-05        -.1030E-02  -.1470E-04         .1301E-04  -.1316E-04
  .1029E-02  -.1871E-04           .1675E-02  -.1827E-04        -.2304E-02  -.4902E-05         .1656E-04  -.8499E-05

T-DIRECTED CURRENTS FOR MODE  2
 -.1721E-04   .4190E-03          -.2430E-04   .8420E-03        -.3021E-04   .1340E-02        -.3207E-04  -.1427E-02
 -.3560E-04   .1341E-02          -.3075E-04   .8436E-03        -.2400E-04   .4158E-03        -.8436E-03  -.1063E-02

Z-DIRECTED CURRENTS FOR MODE  2
 -.2714E-02   .2360E-05          -.4233E-03  -.5926E-05        -.8968E-03   .1291E-04        -.7389E-05  -.1043E-03
 -.9014E-03   .1712E-04           .4240E-03  -.1074E-04        -.2743E-02   .1823E-05        -.1734E-04   .7888E-05

T-DIRECTED CURRENTS FOR MODE  3
 -.1110E-03  -.4776E-03          .3827E-05  -.2268E-03        -.9445E-05  -.3823E-03        -.1501E-04  -.3019E-04
  .1176E-04  -.3748E-03          .4959E-05  -.2256E-03        -.3351E-06  -.4757E-03        -.7649E-05  -.5944E-03

Z-DIRECTED CURRENTS FOR MODE  3
 -.2096E-02  -.1438E-04          -.7247E-03  -.2629E-05        -.8144E-03  -.1960E-04         .9121E-03  -.1824E-05
  .8276E-03  -.2014E-04           .7319E-03  -.2477E-05        -.2115E-02  -.1458E-04         .7143E-05  -.1538E-05
```

t and z directed current coefficients

GP79-0481-52

Figure 16b. Partial output of BOTRA for problem 2.

Plot of currents along BOT

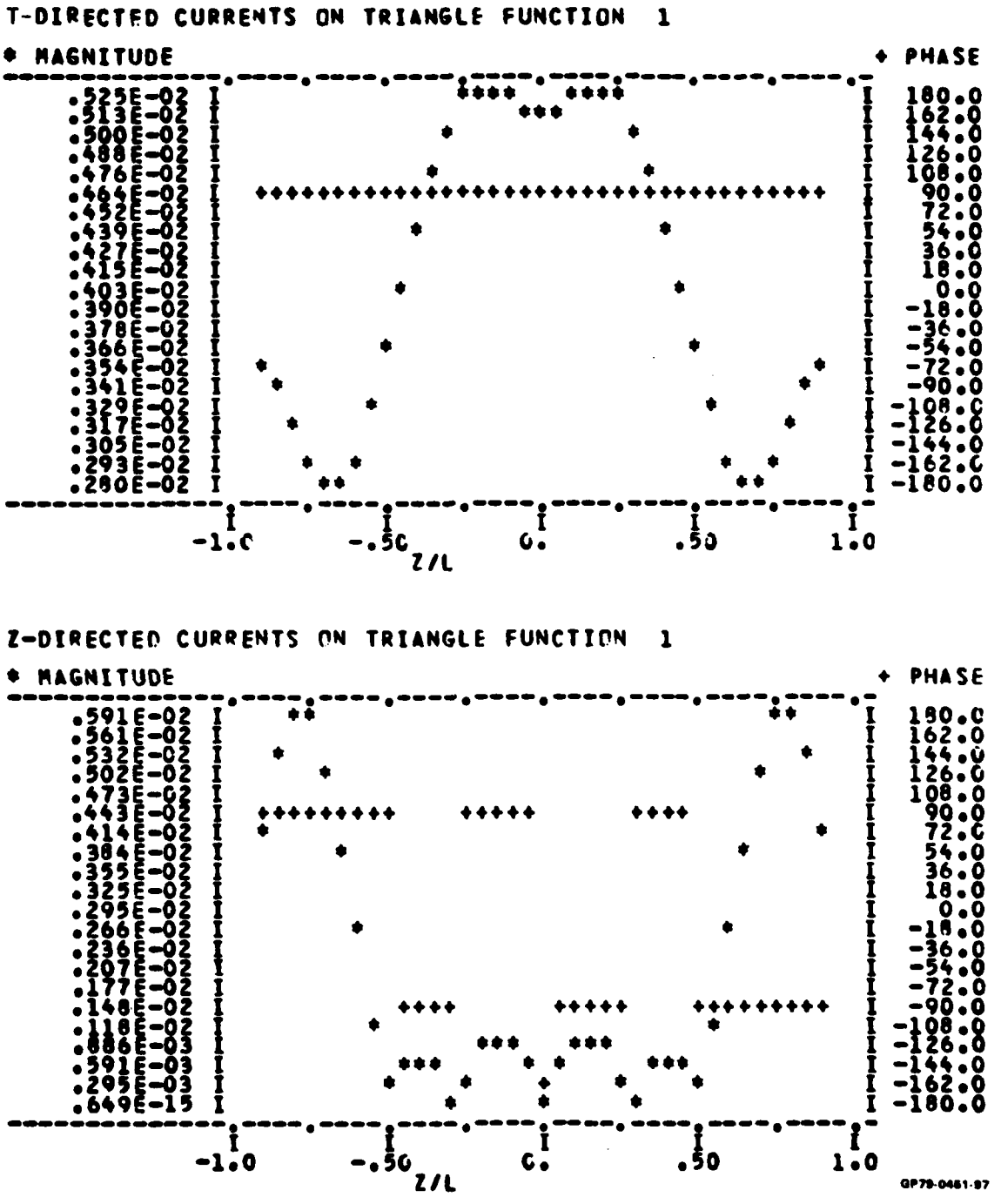

Figure 16b. Partial output of BOTRA for problem 2. (concluded)

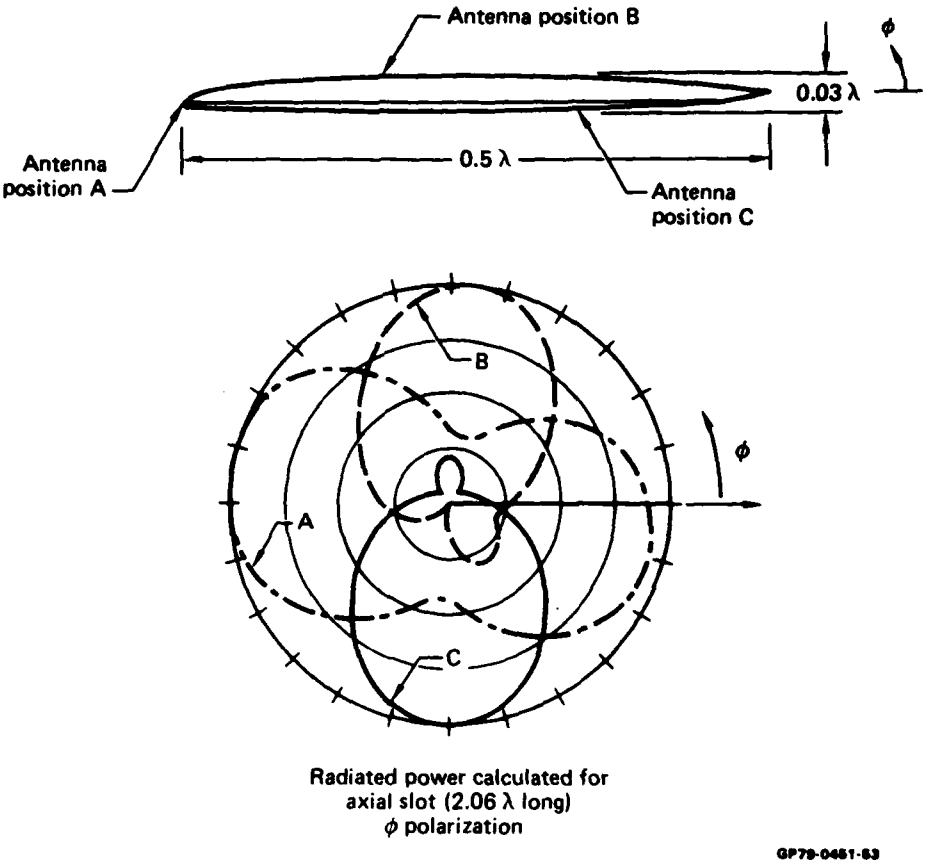

Figure 17. Computed radiation patterns for wing section.

2.6.5 Problem 3

Consider a square cylinder with sides 0.3183 λ and a length of 2.76 λ. Illuminate the cylinder broadside (θ = 90°) with a TM (θ-polarized) wave. Repeat the analysis for a TE (ϕ-polarized) wave.

a) Compute the resulting bistatic cross sections for all polarizations both in the horizontal (ϕ = 0°) plane and the roll (θ = 90°) plane at 46(NT) equi-spaced angles.

b) Compute the magnitude and phase of the currents induced by the TM and TE illumination.

Solution - The calculations were carried out at 10 MHz (λ = 30 m). The body was represented by 17(MP) coordinate points, and 4(NMODE) modes were used. The coordinate points are such that the corners of the cylinder correspond to triangle function peaks. This restriction is necessary to obtain proper accuracy in the calculations. The execution of BOTSEG is shown in Figure 18a in the time-share mode. Input data to execute BOTZSS, BOTINV, and BOTSCB are summarized in Figure 18b. Partial listings of the inputs and outputs for these programs are given in Figures 19-21.

The results for the two parts of this problem are given in Figures 21b and 21c. Comparison of the bistatic scattering results using the present analysis with published data is summarized in Figure 15 of Volume I. The aperture penetration and near-field analysis options were not exercised in this problem.

```
+RNH BOTSEG
?   6   17                          (2I3)
?  0.0            0.0
?  0.0          4.7745
?  9.5490       4.7745
?  9.5490      -4.7745               (4E10.4)
?  0.0         -4.7745
?  0.0            0.0

PERIMETER =   38.1960

NP =  17.

YH
      0.0000    2.3873    4.7745    4.7745    4.7745    4.7745    4.7745    2.3873    0.0000   -2.3873

     -4.7745   -4.7745   -4.7745   -4.7745   -4.7745   -2.3873    0.0000

XH    0.0000    0.0000    0.0000    2.3873    4.7745    7.1618    9.5490    9.5490    9.5490    9.5490

      9.5490    7.1618    4.7745    2.3873     .0000    0.0000    0.0000

BODY COORDINATES + INDICATES TRIANGLE PEAK
```

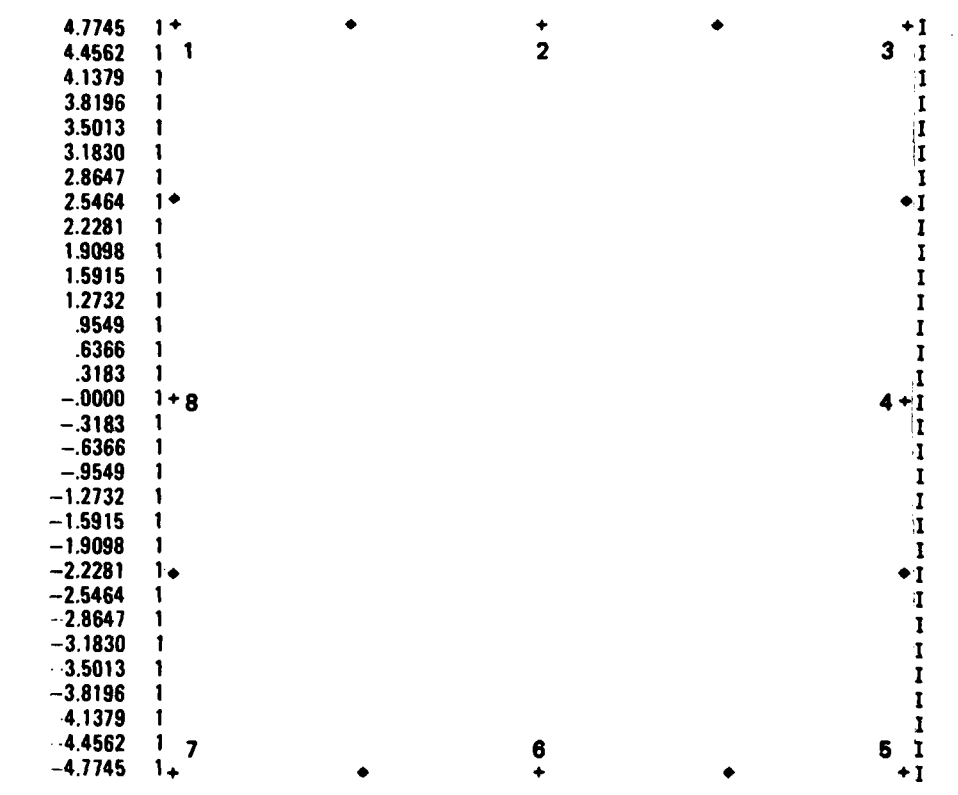


```
YH / XH          1         1         1         1         1         1
                0.0000    1.9098    3.8196    5.7294    7.6392    9.5490
STOP
```

GP79-0451-84

Figure 18a. Execution of BOTSEG for problem 3, with triangle functions numbered on the plot.

```
     4
    20 16
    17 50   .2094397E+00
      0.0000  2.3873  4.7745  4.7745  4.7745  4.7745  4.7745  2.3873  0.0000 -2.3873
     -4.7745 -4.7745 -4.7745 -4.7745 -4.7745 -2.3873  0.0000
      0.0000  0.0000  0.0000  2.3873  4.7745  7.1618  9.5490  9.5490  9.5490  9.5490
      9.5490  7.1618  4.7745  2.3873  0.0000  0.0000  0.0000
    41.4
     2 46    .0000 90.0000
        0.0     90.0
        1        2
```

Primary BOT data set (first block); Scattering angles and incident field (second block)

GP79-0451-56

Figure 18b. Input data for execution of BOTZSS, BOTINV, and BOTSCB for problem 3.

```
   NPT     NBAND   NMODE    NP      NC       BK
    20      14       4      17      50    .2094397E+00

YN
  0.0000  2.3873  4.7745  4.7745  4.7745  4.7745  4.7745  2.3873  0.0000 -2.3873
 -4.7745 -4.7745 -4.7745 -4.7745 -4.7745 -2.3873  0.0000

XN
  0.0000  0.0000  0.0000  2.3873  4.7745  7.1618  9.5490  9.5490  9.5490  9.5490
  9.5490  7.1618  4.7745  2.3873  0.0000  0.0000  0.0000

HALF-LENGTH OF BOT =     41.4000

 M=   9  N=   0  NP= 19  MC= 50  PK=  .2094397E+00

71
  47.42    -202.6    47.56    128.5    26.94    63.74    15.42    64.52    20.99    50.41
  15.42     64.52    26.94     63.74   47.56   128.5     16.47    87.88    16.40    65.59
  47.56    128.5     89.07   -253.6    46.59   127.5     47.56   128.5     26.94    63.74
  8.319     92.83    16.40     65.54   16.47    87.88    89.07  -253.6     46.59   127.5
  26.94     63.74    46.59    127.5    47.43  -202.6     46.59   127.5     47.43  -202.6
  15.42     64.52    20.99     50.41   15.42    64.52    16.47    87.88    47.56   128.5
  15.42     64.52    16.47     87.88   47.56   128.5     16.40    65.54    26.94    63.74
  16.47     87.88    16.40     65.54   8.320    92.83    8.320    92.83    15.42    64.52
  20.99     50.41    16.40     65.54   26.94    63.74
  47.56    128.5     26.94     63.74   15.42    64.52
  15.42     64.52    8.319     92.83   15.42    64.52
  89.07   -253.6     46.59    127.5    16.47    87.88
  26.94     63.74    16.40     65.54   20.99    50.41
  46.59    127.5     47.42   -202.6    47.56   128.5
  47.56    128.5     16.47     87.88   15.42    64.52
  16.47     87.88    47.56    128.5    89.07  -253.6
```

Impedance matrix $Z^{tt}_{0,0}$

GP79-0451-80

Figure 19. Partial output of BOTZSS for problem 3.

```
      NP          NNODE       NBAND
      17            4           14

YM
  0.0000  2.3873  4.7745  4.7745  4.7745  4.7745  4.7745  2.3873  0.0000 -2.3873
 -4.7745 -4.7745 -4.7745 -4.7745 -4.7745 -2.3873  0.0000

XM
  0.0000  0.0000  0.0000  2.3873  4.7745  7.1618  9.5490  9.5490  9.5490  9.5490
  9.5490  7.1618  4.7745  2.3873  0.0000  0.0000  0.0000

THE MINIMUM DIMENSIONS ARE AS FOLLOWS:
      Z          ZI        WORK         NZ         LR
   12544         256          0          0        112

M= -3  N= -3

Y1
 .7190E-04 -.6034E-03  .6005E-04 -.6739E-03  .1674E-04 -.1277E-03 -.1311E-04 -.7519E-03 -.3018E-04  .2914E-03
-.1374E-04 -.7516E-03  .1646E-04 -.1218E-03  .5911E-04 -.6739E-03
 .6005E-04 -.6739E-03  .7856E-04 -.5068E-03  .6025E-04 -.6722E-03  .1768E-04  .3297E-04 -.1370E-04 -.7515E-03
-.3013E-04  .1629E-03 -.1370E-04 -.7512E-03  .1800E-04  .3226E-04
 .1674E-04 -.1277E-03  .6025E-04 -.6722E-03  .7388E-04 -.5908E-03  .5945E-04 -.6749E-03  .1780E-04  .1285E-03
-.1353E-04 -.7503E-03 -.3000E-04  .2894E-03 -.1348E-04 -.7473E-03
-.6311E-04 -.7519E-03  .1768E-04  .3297E-04  .5945E-04 -.6749E-03  .7997E-04 -.5043E-03  .6006E-04 -.6711E-03
 .1885E-04  .3417E-04 -.1337E-04 -.7488E-03 -.3038E-04  .1616E-03
-.3018E-04  .2914E-03 -.1370E-04 -.7515E-03  .1780E-04 -.1285E-03  .6006E-04 -.6711E-03  .7183E-04 -.6007E-03
 .5979E-04 -.6710E-03  .1511E-04  .1183E-03 -.1262E-04 -.7471E-03
-.1374E-04 -.7516E-03 -.3013E-04  .1629E-03 -.1353E-04 -.7503E-03  .1885E-04  .3417E-04  .5979E-04 -.6710E-03
 .6008E-04 -.6739E-03  .6008E-04 -.6674E-03  .1833E-04  .3440E-04
 .1846E-04 -.1218E-03 -.1370E-04 -.7512E-03 -.3000E-04  .2894E-03 -.1337E-04 -.7488E-03  .1511E-04  .1183E-03
 .6008E-04 -.6674E-03  .6919E-04 -.6092E-03  .6027E-04 -.6709E-03
 .5911E-04 -.6739E-03  .1800E-04  .3226E-04 -.1348E-04 -.7473E-03
 .1833E-04  .3440E-04  .6027E-04 -.6709E-03  .7993E-04 -.5028E-03 -.3038E-04  .1616E-03 -.1262E-04 -.7471E-03
Y2
-.1011E-03 -.6317E-05  .4196E-02 -.6507E-04 -.2367E-02  .8122E-04  .1531E-02  .2137E-04 -.6199E-04  .1463E-04
-.1400E-02 -.5351E-04  .2295E-02 -.7154E-04 -.4178E-02 -.5908E-04
-.3168E-02 -.8903E-04 -.2606E-04  .4760E-06  .3252E-02 -.8257E-04 -.1852E-02  .8302E-04  .1213E-02  .4892E-04
-.6789E-04 -.1216E-04 -.1099E-02 -.6467E-04  .1744E-02 -.6604E-04
-.2281E-02 -.7109E-04 -.4143E-02 -.6860E-04 -.3956E-04 -.9301E-05  .4195E-02  .5443E-04 -.2337E-02  .7814E-04
-.1490E-02 -.3031E-04 -.2581E-04  .2317E-05 -.1426E-02 -.4081E-04
-.3088E-02 -.1706E-04 -.1728E-02 -.5686E-04 -.2166E-02 -.9438E-04 -.2188E-04  .4255E-05  .3237E-02  .8533E-04
-.1834E-02  .7639E-04 -.1194E-02 -.5408E-04 -.5610E-04 -.4857E-05
-.6870E-04 -.1034E-04 -.1414E-02 -.4407E-04 -.2302E-02 -.7618E-04 -.4164E-02 -.6280E-04 -.1601E-04 -.1017E-05
 .4187E-02 -.6312E-04 -.2320E-02 -.7510E-04 -.1927E-02 -.3003E-04
 .8217E-02 -.5127E-04 -.6691E-04 -.9813E-05 -.1007E-02 -.6396E-04  .1733E-02 -.6127E-04 -.3169E-02 -.8839E-04
-.3232E-04 -.2479E-05  .3254E-02 -.8601E-04 -.1850E-02 -.7579E-04
-.2380E-02 -.8954E-04 -.1517E-02 -.2917E-04 -.3327E-04 -.1420E-05 -.1433E-02 -.3465E-04  .2304E-02 -.8296E-04
-.4144E-02 -.6216E-04 -.5846E-04 -.8549E-05 -.4234E-02 -.5040E-04
-.3264E-02 -.8630E-04 -.1048E-02 -.7419E-04 -.1208E-02 -.8092E-04 -.6984E-04  .1953E-05 -.1079E-02 -.6051E-04
-.1709E-02 -.5995E-04 -.3124E-02 -.1001E-03 -.6577E-04  .1252E-04
```

Admittance matrix

$Y^{tt}_{-3,-3}$

$Y^{zt}_{-3,-3}$

GP79-0461-67

Figure 20. Partial output of BOTINV for problem 3.

```
    NPT      NBAND    NMODE     NP       MC       BK
     20        14        4       17       50   .2094397E+00

YH
  0.0000  2.3873  4.7745  4.7745  4.7745  4.7745  4.7745  2.3873  0.0000 -2.3873
 -4.7745 -4.7745 -4.7745 -4.7745 -4.7745 -2.3873  0.0000

XH
  0.0000  0.0000  0.0000  2.3873  4.7745  7.1618  9.5490  9.5490  9.5490  9.5490
  9.5490  7.1618  4.7745  2.3873  0.0000  0.0000  0.0000

HALF-LENGTH OF BOT =      41.4000

NUMBER OF FIXED ANGLES =  2
NUMBER OF ANGLES PER FIXED ANGLE =  46

FIXED ANGLE     CODE(PHI FIXED = 1, THETA FIXED =2)
    0.0             1
   90.0             2



M= -3  N= -3

Y
 .7189509E-04 -.6033521E-03  .6005373E-04 -.6739350E-03

M= -2  N= -3

Y
-.6336747E-04  .6889634E-06 -.4920743E-04  .1958407E-04

M= -1  N= -3

Y
 .7044501E-04  .2308832E-04  .4977628E-04 -.1812870E-04

M=  0  N= -3

Y
-.8299667E-04 -.4713423E-04 -.5359391E-04  .1778258E-04
```

OP79-0451-58

Figure 21a. Partial output of BOTSCB for problem 3.

BI-STATIC RCS(DBI). INCIDENT PHI = 0.0 THETA = 90.0

PHI	THETA	**	**	**	**	
0.0	0.0	-14.82	-11.27	-61.35	-76.63	
0.0	4.0	-12.68	-11.02	-60.86	-76.14	
0.0	8.0	-11.06	-10.15	-59.74	-75.54	
0.0	12.0	-9.87	-9.86	-58.25	-74.84	
0.0	16.0	-9.08	-7.40	-56.67	-74.09	
0.0	20.0	-8.71	-6.02	-55.25	-73.30	
0.0	24.0	-8.79	-4.91	-54.18	-72.55	
0.0	28.0	-9.39	-4.23	-53.65	-71.87	
0.0	32.0	-10.70	-4.15	-53.84	-71.35	
0.0	36.0	-13.15	-4.85	-55.10	-71.03	
0.0	40.0	-18.16	-6.62	-58.11	-71.03	
0.0	44.0	-23.62	-9.64	-64.67	-71.42	
0.0	46.0	-13.55	-11.44	-64.55	-72.37	
0.0	52.0	-7.99	-8.45	-57.86	-74.08	
0.0	56.0	-5.01	-5.68	-55.11	-76.86	
0.0	60.0	-4.08	-4.81	-54.91	-80.92	
0.0	64.0	-5.99	-6.23	-57.49	-82.82	
0.0	68.0	-17.37	-10.18	-65.97	-79.65	
0.0	72.0	-5.46	-6.65	-64.38	-77.17	
0.0	76.0	2.81	-.28	-57.20	-76.38	
0.0	80.0	7.19	3.62	-55.50	-77.28	
0.0	84.0	9.70	5.89	-57.37	-80.45	Plane at $\phi = 0^{o}$
0.0	88.0	10.86	6.94	-65.72	-89.38	
0.0	92.0	10.86	6.94	-65.72	-89.38	
0.0	96.0	9.70	5.89	-57.37	-80.45	
0.0	100.0	7.19	3.62	-55.50	-77.28	
0.0	104.0	2.81	-.28	-57.20	-76.38	
0.0	108.0	-5.46	-6.65	-64.38	-77.17	
0.0	112.0	-17.37	-10.18	-65.97	-79.65	
0.0	116.0	-5.99	-6.23	-57.49	-82.82	
0.0	120.0	-4.08	-4.81	-54.91	-80.92	
0.0	124.0	-5.01	-5.68	-55.11	-76.86	
0.0	128.0	-7.99	-8.45	-57.86	-74.08	
0.0	132.0	-13.55	-11.44	-64.55	-72.37	
0.0	136.0	-23.62	-9.64	-64.67	-71.42	
0.0	140.0	-18.16	-6.62	-58.11	-71.03	
0.0	144.0	-13.15	-4.85	-55.10	-71.03	
0.0	148.0	-10.70	-4.15	-53.84	-71.35	
0.0	152.0	-9.39	-4.23	-53.65	-71.87	
0.0	156.0	-8.79	-4.91	-54.18	-72.55	
0.0	160.0	-8.71	-6.02	-55.25	-73.30	
0.0	164.0	-9.08	-7.40	-56.67	-74.09	
0.0	168.0	-9.87	-8.86	-58.25	-74.84	
0.0	172.0	-11.06	-10.15	-59.74	-75.54	
0.0	176.0	-12.68	-11.02	-60.86	-76.14	
0.0	180.0	-14.82	-11.27	-61.35	-76.63	

GP79-0461-59

Figure 21b. Partial output of BOTSCB for problem 3.

```
THETA POLARIZED INCIDENT FIELD

T-DIRECTED CURRENTS FOR MODE -3
 -.1034E-03  -.8724E-04  -.2196E-03  -.1015E-03  -.1483E-03  -.1381E-04  -.1465E-06   .1051E-05
 -.1489E-03   .1239E-04  -.2204E-03   .1043E-03  -.1020E-03   .8284E-04  -.6192E-06   .2269E-05

Z-DIRECTED CURRENTS FOR MODE -3
 -.2425E-03  -.1445E-03  -.3377E-03  -.2174E-03  -.3128E-03  -.2023E-03  -.5558E-03  -.3501E-03
 -.3060E-03  -.2007E-03  -.3486E-03  -.2200E-03  -.2336E-03  -.1418E-03  -.2866E-03   .6184E-05

T-DIRECTED CURRENTS FOR MODE -2
 -.1364E-04  -.1569E-03  -.5308E-04   .1962E-03  -.6202E-04   .1008E-03  -.2640E-06  -.3370E-06
  .6129E-04  -.1019E-03   .5288E-04  -.1961E-03   .1436E-04  -.1560E-03  -.8906E-07  -.1985E-06

Z-DIRECTED CURRENTS FOR MODE -2
  .1016E-03   .3054E-03  -.2528E-03   .1318E-03   .1982E-04  -.8506E-04  -.1211E-03  -.1145E-03
  .1813E-04  -.8813E-04  -.2486E-03   .1365E-03   .9909E-04   .3046E-03  -.1909E-03   .2544E-03

T-DIRECTED CURRENTS FOR MODE -1
 -.1177E-04  -.7831E-04  -.1732E-05  -.9108E-04   .1877E-04  -.5103E-04   .7204E-07  -.1875E-06
 -.1819E-04   .5129E-04  -.1714E-05   .9094E-04   .1128E-04   .7813E-04   .4399E-07   .1055E-06

Z-DIRECTED CURRENTS FOR MODE -1
 -.1539E-03  -.1944E-03   .1968E-03  -.1479E-03   .3078E-04   .4301E-04   .1553E-03   .5905E-04
  .3266E-04   .4460E-04   .1929E-03  -.1495E-03  -.1515E-03  -.1944E-03   .3112E-04  -.1862E-03

T-DIRECTED CURRENTS FOR MODE  0
 -.4856E-10   .2609E-09  -.1469E-09   .2629E-09  -.1614E-09   .1032E-09  -.1024E-11  -.1424E-12
  .1606E-09  -.1037E-09   .1472E-09  -.2647E-09   .4973E-10  -.2588E-09   .4217E-12  -.6360E-13

Z-DIRECTED CURRENTS FOR MODE  0
 -.1901E-03   .1253E-02  -.2815E-02   .3630E-03  -.7758E-03  -.6353E-02   .2372E-02  -.3865E-02
 -.7619E-03  -.6425E-02  -.2810E-02   .4493E-03  -.2048E-03   .1221E-02   .8348E-03  -.1152E-03

T-DIRECTED CURRENTS FOR MODE  1
  .1177E-04  -.7831E-04  -.1732E-05   .9108E-04  -.1877E-04  -.5103E-04  -.7204E-07   .1875E-06
  .1819E-04  -.5129E-04  -.1714E-05  -.9094E-04  -.1128E-04  -.7813E-04  -.4399E-07  -.1055E-06

Z-DIRECTED CURRENTS FOR MODE  1
 -.1539E-03  -.1944E-03   .1968E-03  -.1479E-03   .3078E-04   .4301E-04   .1553E-03   .5905E-04
  .3266E-04   .4460E-04   .1929E-03  -.1495E-03  -.1515E-03  -.1944E-03   .3112E-04  -.1862E-03

T-DIRECTED CURRENTS FOR MODE  2
  .1364E-04  -.1569E-03  -.5308E-04   .1962E-03  -.6202E-04   .1008E-03  -.2640E-06  -.3370E-06
 -.6129E-04  -.1019E-03   .5288E-04  -.1961E-03   .1436E-04  -.1560E-03  -.8906E-07  -.1985E-06

Z-DIRECTED CURRENTS FOR MODE  2
  .1016E-03   .3054E-03  -.2528E-03   .1318E-03   .1982E-04  -.8506E-04  -.1211E-03  -.1145E-03
  .1813E-04  -.8813E-04  -.2486E-03   .1365E-03   .9909E-04   .3046E-03  -.1909E-03   .2544E-03

T-DIRECTED CURRENTS FOR MODE  3
 -.1034E-03   .8724E-04  -.2196E-03  -.1015E-03  -.1483E-03  -.1381E-04  -.1465E-06   .1051E-05
  .1489E-03  -.1239E-04  -.2204E-03   .1043E-03  -.1020E-03   .8284E-04  -.6192E-06   .2269E-05

Z-DIRECTED CURRENTS FOR MODE  3
 -.2425E-03  -.1445E-03  -.3377E-03  -.2174E-03  -.3128E-03  -.2023E-03  -.5558E-03  -.3501E-03
 -.3060E-03  -.2007E-03  -.3486E-03  -.2200E-03  -.2336E-03  -.1418E-03  -.2866E-03   .6184E-05
```

t and z directed current coefficents for θ-polarized incident field

Figure 21b. Partial output of BOTSCB for problem 3. (continued)

BI-STATIC RCS(DB). INCIDENT PHI = 0.0 THETA = 90.0

PHI	THETA	ΦΦ	ΘΘ	ΦΘ	ΘΦ
0.0	90.0	11.01	7.07	-184.29	-184.29
4.0	90.0	11.00	7.11	-168.23	-159.82
8.0	90.0	10.97	7.21	-162.71	-153.80
12.0	90.0	10.93	7.37	-159.27	-150.31
16.0	90.0	10.86	7.58	-156.69	-147.87
20.0	90.0	10.78	7.83	-154.58	-146.01
24.0	90.0	10.68	8.12	-152.74	-144.52
28.0	90.0	10.57	8.42	-151.07	-143.20
32.0	90.0	10.45	8.72	-149.53	-142.26
36.0	90.0	10.32	9.02	-148.09	-141.38
40.0	90.0	10.19	9.30	-146.72	-140.61
44.0	90.0	10.05	9.56	-145.43	-139.94
48.0	90.0	9.90	9.79	-144.22	-139.36
52.0	90.0	9.77	9.98	-143.07	-138.83
56.0	90.0	9.64	10.12	-142.00	-138.37
60.0	90.0	9.52	10.21	-141.01	-137.95
64.0	90.0	9.42	10.26	-140.09	-137.57
68.0	90.0	9.33	10.24	-139.24	-137.23
72.0	90.0	9.28	10.17	-138.47	-136.92
76.0	90.0	9.25	10.04	-137.77	-136.64
80.0	90.0	9.26	9.84	-137.14	-136.39
84.0	90.0	9.31	9.58	-136.58	-136.16
88.0	90.0	9.40	9.26	-136.09	-135.96
92.0	90.0	9.55	8.87	-135.66	-135.78
96.0	90.0	9.74	8.41	-135.31	-135.64
100.0	90.0	9.98	7.90	-135.02	-135.53
104.0	90.0	10.27	7.35	-134.80	-135.45
108.0	90.0	10.59	6.76	-134.64	-135.41
112.0	90.0	10.95	6.17	-134.56	-135.41
116.0	90.0	11.33	5.61	-134.55	-135.47
120.0	90.0	11.73	5.16	-134.61	-135.57
124.0	90.0	12.14	4.85	-134.75	-135.74
128.0	90.0	12.55	4.73	-134.97	-135.97
132.0	90.0	12.95	4.83	-135.27	-136.28
136.0	90.0	13.33	5.10	-135.67	-136.68
140.0	90.0	13.70	5.50	-136.18	-137.17
144.0	90.0	14.05	5.98	-136.81	-137.78
148.0	90.0	14.36	6.48	-137.58	-138.53
152.0	90.0	14.65	6.97	-138.51	-139.45
156.0	90.0	14.90	7.41	-139.66	-140.57
160.0	90.0	15.11	7.80	-141.09	-141.98
164.0	90.0	15.29	8.12	-142.88	-143.77
168.0	90.0	15.43	8.38	-145.28	-146.15
172.0	90.0	15.53	8.56	-148.72	-149.59
176.0	90.0	15.59	8.67	-154.66	-155.57
180.0	90.0	15.61	8.71	-192.62	-191.56

Roll plane ($\theta = 90^{\circ}$)

GP79-0481-87

Figure 21b. Partial output of BOTSCB for problem 3. (continued)

Plots of current along BOT for
θ-polarized incident field.

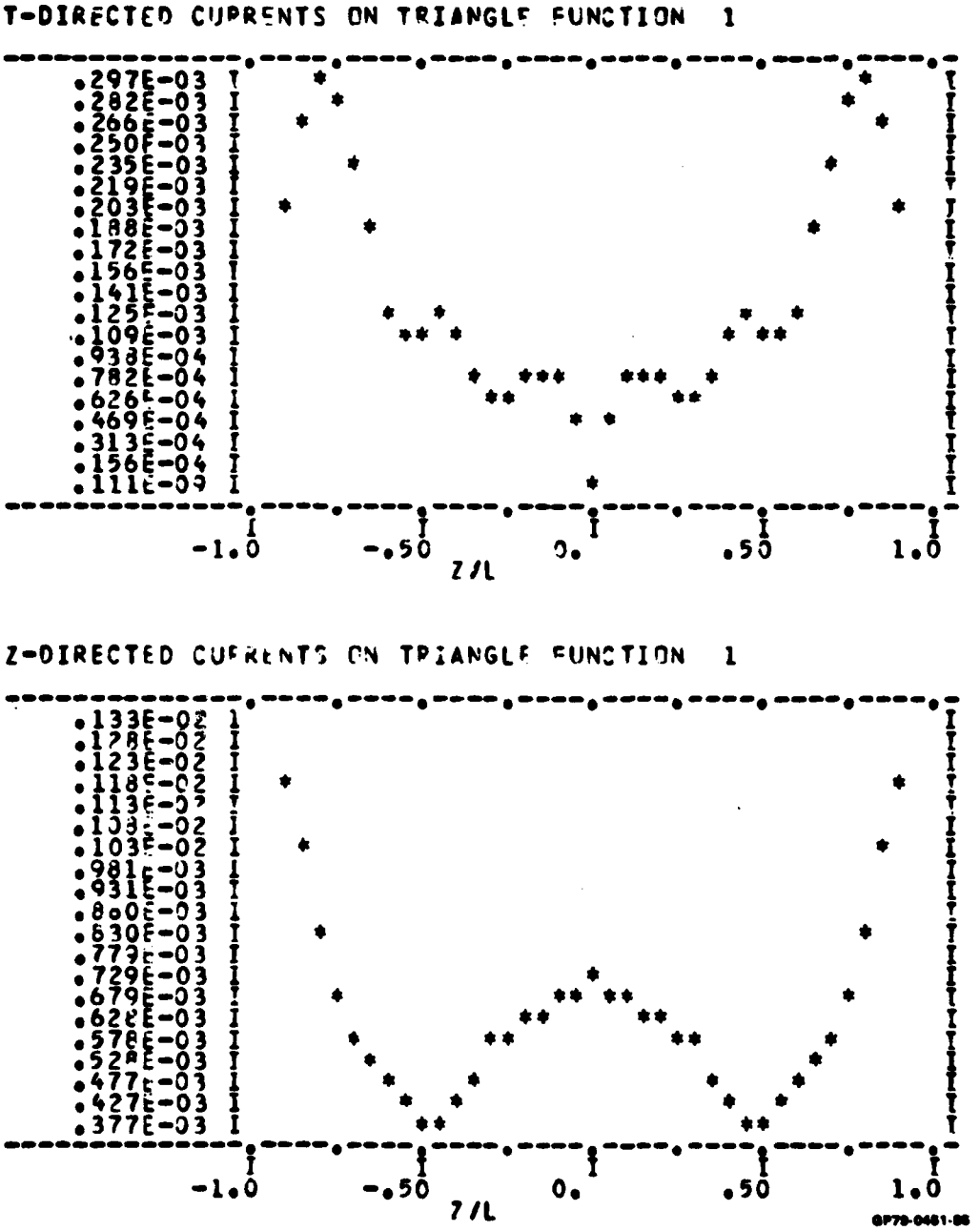

Figure 21b. Partial output of BOTSCB for problem 3. (concluded)

PHI POLARIZED INCIDENT FIELD

T-DIRECTED CURRENTS FOR MODE -3
-.1721E-04 -.1033E-03 .1282E-03 .1472E-03 -.1348E-03 -.2815E-03 -.1343E-03 .3156E-03
.1350E-03 .2796E-03 .1303E-03 .1466E-03 -.1625E-04 -.1040E-03 -.1442E-03 -.2498E-03

Z-DIRECTED CURRENTS FOR MODE -3
-.5576E-04 -.3008E-03 -.1421E-03 -.1671E-03 -.4754E-04 -.1999E-03 -.3224E-05 .3703E-05
.5004E-04 .1942E-03 .1408E-03 .1721E-03 .5542E-04 .2952E-03 .2727E-05 .2286E-05

T-DIRECTED CURRENTS FOR MODE -2
.7333E-04 .2024E-03 -.1285E-03 -.1329E-03 -.2062E-03 -.3382E-03 -.2149E-03 -.3711E-03
-.2068E-03 -.3364E-03 -.1315E-03 -.1314E-03 .7086E-04 .2032E-03 .1940E-03 .3672E-03

Z-DIRECTED CURRENTS FOR MODE -2
.1376E-03 -.3625E-04 .1588E-03 -.1351E-03 .7153E-04 -.9006E-04 -.3725E-06 -.4287E-06
-.7109E-04 .8895E-04 -.1613E-03 .1358E-03 -.1342E-03 .3307E-04 -.4211E-06 .4020E-05

T-DIRECTED CURRENTS FOR MODE -1
-.1238E-03 -.2211E-03 .1272E-03 .1378E-03 .2509E-03 .3482E-03 .2623E-03 .3629E-03
.2514E-03 .3466E-03 .1305E-03 .1355E-03 -.1209E-03 -.2229E-03 -.2515E-03 -.3674E-03

Z-DIRECTED CURRENTS FOR MODE -1
-.5039E-04 .2175E-04 -.5717E-04 .6312E-04 -.1315E-04 .3562E-04 .4856E-07 .2278E-06
.1309E-04 -.3526E-04 .5841E-04 -.6353E-04 .4924E-04 -.2034E-04 -.2690E-06 -.1555E-05

T-DIRECTED CURRENTS FOR MODE 0
-.1495E-02 .7439E-03 -.1706E-02 -.3735E-02 .1569E-02 -.4251E-02 .3552E-02 -.3574E-02
.1524E-02 -.4238E-02 -.1714E-02 -.3743E-02 -.1501E-02 .7189E-03 -.1747E-03 .3299E-02

Z-DIRECTED CURRENTS FOR MODE 0
.1568E-11 -.5271E-12 .1003E-11 .5973E-12 .4158E-13 .1073E-11 -.7230E-14 -.1346E-14
-.2753E-13 -.1079E-11 -.1013E-11 -.5898E-12 -.1555E-11 .5209E-12 -.8987E-14 -.2484E-14

T-DIRECTED CURRENTS FOR MODE 1
-.1238E-03 -.2211E-03 .1272E-03 .1378E-03 .2509E-03 .3482E-03 .2623E-03 .3629E-03
.2514E-03 .3466E-03 .1305E-03 .1355E-03 -.1209E-03 -.2229E-03 -.2515E-03 -.3674E-03

Z-DIRECTED CURRENTS FOR MODE 1
.5039E-04 -.2175E-04 .5717E-04 -.6312E-04 .1315E-04 -.3562E-04 -.4856E-07 -.2278E-06
-.1309E-04 .3526E-04 -.5841E-04 .6353E-04 -.4924E-04 .2034E-04 .2690E-06 .1555E-05

T-DIRECTED CURRENTS FOR MODE 2
.7333E-04 .2024E-03 -.1285E-03 -.1329E-03 -.2062E-03 -.3382E-03 -.2149E-03 -.3711E-03
-.2068E-03 -.3364E-03 -.1315E-03 -.1314E-03 .7086E-04 .2032E-03 .1940E-03 .3672E-03

Z-DIRECTED CURRENTS FOR MODE 2
-.1376E-03 .3625E-04 -.1588E-03 .1351E-03 -.7153E-04 .9006E-04 .3725E-06 .4287E-06
.7109E-04 -.8895E-04 .1613E-03 -.1358E-03 .1342E-03 -.3307E-04 -.4211E-06 -.4020E-05

T-DIRECTED CURRENTS FOR MODE 3
-.1721E-04 -.1033E-03 .1282E-03 .1472E-03 -.1348E-03 -.2815E-03 -.1343E-03 .3156E-03
.1350E-03 .2796E-03 .1303E-03 .1466E-03 -.1625E-04 -.1040E-03 -.1442E-03 -.2498E-03

Z-DIRECTED CURRENTS FOR MODE 3
.5576E-04 .3008E-03 .1421E-03 -.1671E-03 -.4754E-04 -.1999E-03 -.3224E-05 -.3703E-05
-.5004E-04 -.1942E-03 -.1408E-03 -.1721E-03 -.5542E-04 -.2952E-03 -.2727E-05 -.2286E-05

t and z directed current coefficients for ϕ-polarized incident field

Figure 21c. Partial output of BOTSCB for problem 3.

GP79-0461-100

Plots of currents along BOT for
ϕ-polarized incident field

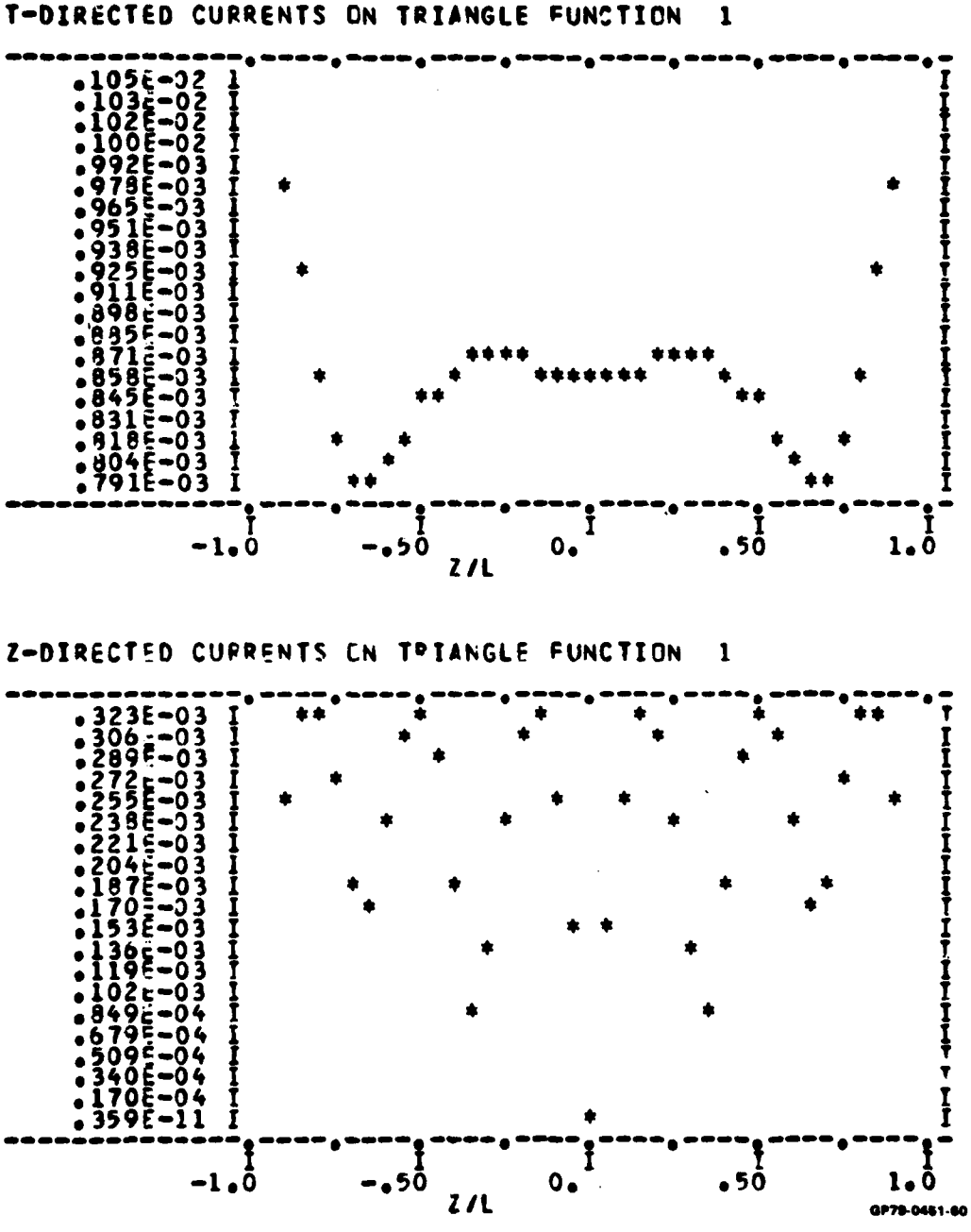

Figure 21c. Partial output of BOTSCB for problem 3. (concluded)

2.6.6 Problem 4

Determine the field penetration into a fuselage equipment compartment represented by a BOT, depicted in Figure 22. Assume that the aperture, centered about Z = 0, is 1.656 λ in axial length and 0.63 λ in width. Let the illumination of the body be broadside (θ = 90°) at 75 MHz in either θ or ϕ polarization. Compute the fields at the following points:

Sample Point	ZTEST	YTEST	XTEST
1	0.0	3.8242	-5.0
2	0.0	3.8242	-3.0
3	0.0	3.8242	-1.0
4	0.0	3.8242	+1.0
5	0.0	3.8242	+3.0
6	0.0	3.8242	+5.0

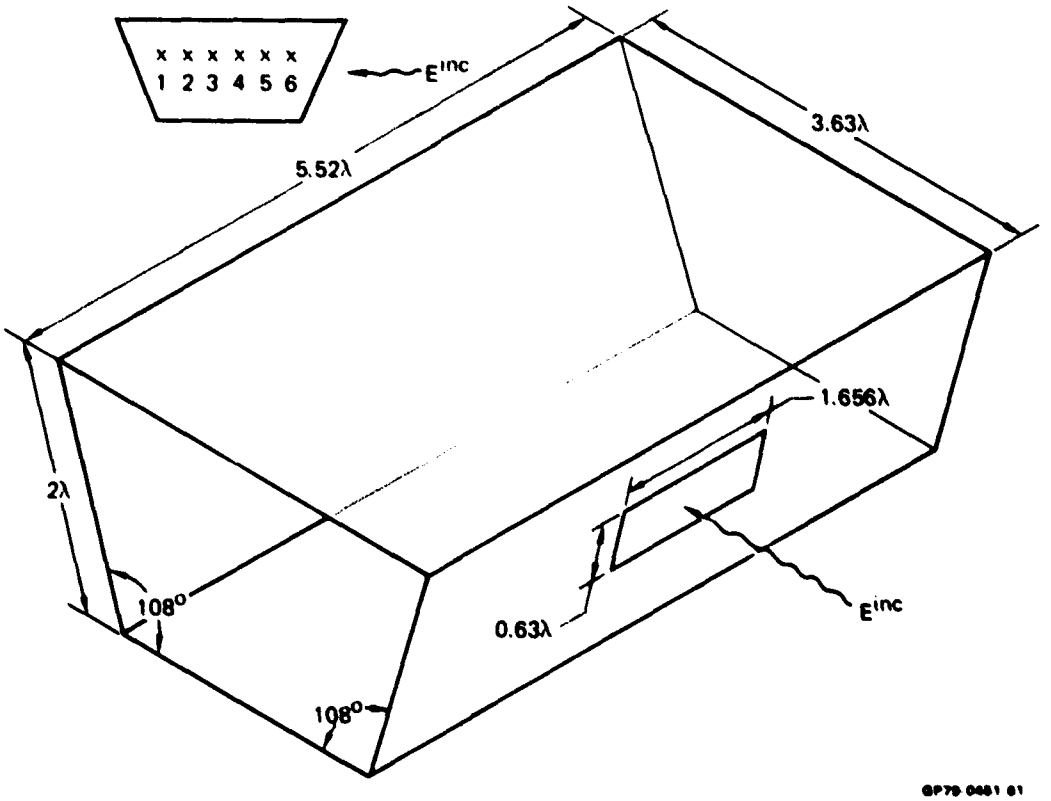

Figure 22. Equipment compartment with aperture.

Solution - The solution was implemented by running BOTZSS, BOTINV, and BOTSCB in sequence. The parameters NP and NMODE were 33 and 4, respectively. The necessary input data to execute the above programs are given in Figure 23, with the partial outputs from BOTZSS, BOTINV, and BOTSCB shown in Figures 24, 25, and 26, respectively. The bistatic scattering cross sections and the currents on the body with the aperture sealed are shown for θ and ϕ illumination in Figures 26b and 26c, respectively. The electric and magnetic field components inside the body at the various sampling points are summarized in Figure 26d.

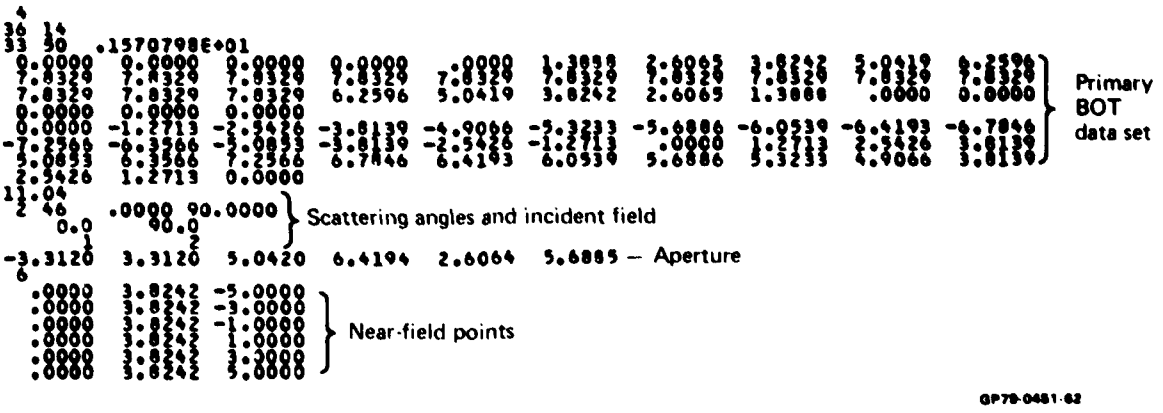

GP79-0451-62

Figure 23. Input data for execution of BOTZSS, BOTINV, and BOTSCB for problem 4.

```
    NPT      NBAND    NMODE     NP       MC       BK
     36        14        4       33       50   .1570798E+01

YH
 0.0000  0.0000  0.0000  0.0000  0.0000  1.3888  2.6765  3.8242  5.0419  6.2596
 7.8329  7.8329  7.8329  7.8329  7.8329  7.8329  7.8329  7.8329  7.8329  7.8329
 7.8329  7.8329  7.8329  6.2596  5.0419  3.8242  2.6765  1.3888  0.0000  0.0000
 0.0000  0.0000  0.0000

XH
 0.0000 -1.2713 -2.5426 -3.8139 -4.9066 -5.3233 -5.6886 -6.0539 -6.4193 -6.7846
-7.2566 -6.3566 -5.0853 -3.8139 -2.5426 -1.2713  0.0000  1.2713  2.5426  3.8139
 6.0853  6.3566  7.2566  6.7846  6.4193  6.0539  5.6886  5.3233  4.9066  3.8139
 2.5426  1.2713  0.0000
```

BODY COORDINATES, + INDICATES TRIANGLE PEAK

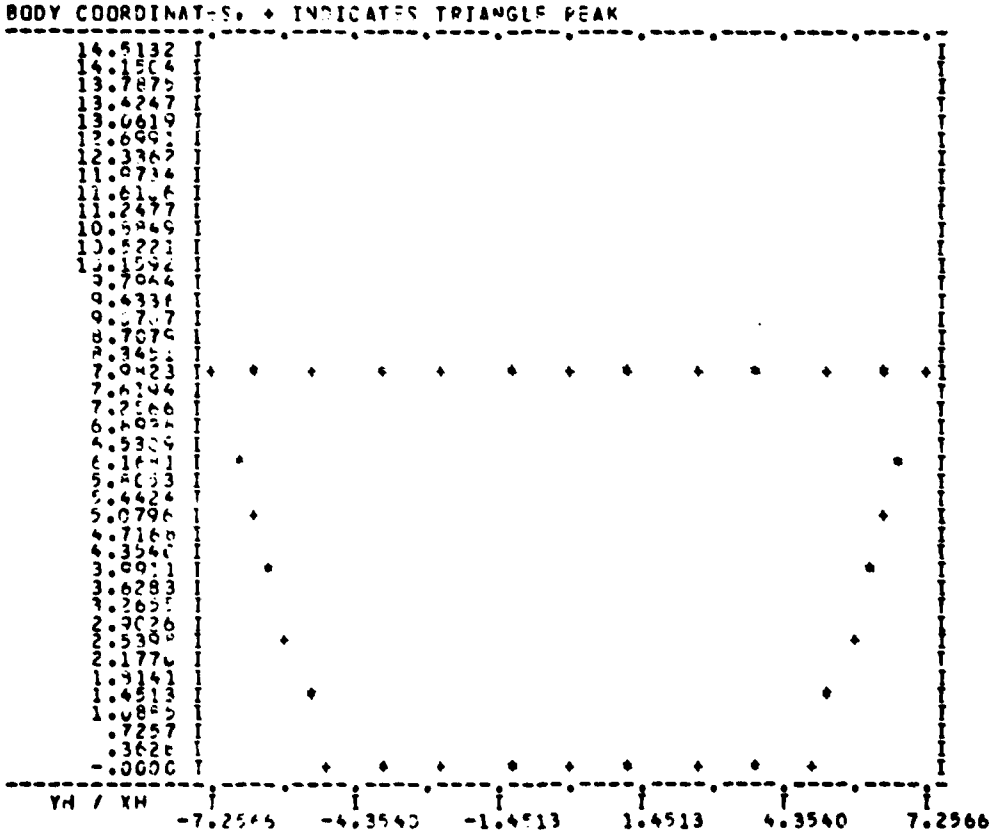

HALF-LENGTH OF BOT = 11.0400

GP79-0461-03

Figure 24. Partial output of BOTZSS for problem 4.

[illegible] 0 [illegible] 0 NP= 35 NC= 50 BK= .1570798E+01

[illegible]	-19.34	117.4	4.545	-16.92	-10.20	12.34	-1.270	-56.21	21.28
[illegible]	-38.83	-101.5	-107.2	-101.9	-39.90	-28.99	38.35	14.49	3.351
[illegible]	-19.88	11.99	2.715	-12.08	1.915	4.930	-7.539	-8.815	2.711
[illegible]	3.279								
[illegible]	4.545	208.0	43.12	101.0	6.109	-5.544	6.028	-29.27	-29.38
[illegible]	-66.94	-58.74	-76.73	-65.59	26.73	33.23	18.86	-14.86	-13.39
[illegible]	43.19	-32.61	-17.36	38.49	-32.13	30.51	13.35	4.905	-7.258
[illegible]	2.161								
[illegible]	-16.20	101.0	6.109	210.8	-7.845	99.83	-2.311	-11.02	4.119
-10.02	20.53	36.98	14.87	-17.32	-30.15	9.648	22.08	-9.995	-13.95
[illegible]	55.96	-76.32	-11.76	8.180	-94.10	38.62	-32.16	-12.16	1.609
14.42	5.177								
12.34	-1.270	-5.544	6.028	99.83	-2.311	215.2	-3.598	98.06	19.99
14.97	-49.33	-32.31	21.06	15.14	-11.37	-4.560	8.662	-1.033	-5.213
-3.184	56.17	-67.66	57.54	-76.25	-11.40	-32.80	-17.24	11.96	2.803
-12.35	-3.724								
-56.21	21.25	-29.27	-29.38	-11.02	4.119	98.06	19.99	184.8	97.56
129.2	28.34	-9.049	-9.377	5.442	-.2032	-2.114	2.041	1.639	-2.625
16.48	17.69	-2.817	56.32	-16.35	56.08	-10.81	43.20	-9.303	-19.87
26.76	24.94								
-98.76	-38.83	-38.95	-66.84	-10.02	20.53	14.97	-49.33	129.2	28.34
192.1	-19.38	103.9	4.960	-8.692	2.639	2.146	-7.691	3.528	7.256
1.471	-2.806	-1.170	-5.195	-10.24	-13.71	-14.74	-13.21	14.49	3.351
-29.00	38.32								
-101.5	-107.2	-58.74	-76.73	36.98	14.87	-32.31	21.06	-9.049	-9.377
103.9	4.960	205.9	-11.63	102.6	1.751	-6.214	3.151	2.146	-7.691
-2.119	2.378	.289	8.782	10.01	21.91	33.12	18.71	-28.99	38.35
-102.5	-39.27								
-101.9	-39.90	-65.59	26.73	-17.32	-30.15	15.14	-11.37	5.442	-.2032
-8.692	2.639	102.6	1.751	205.9	-11.64	102.6	1.751	-8.692	2.639
5.873	-.5848	14.63	-11.76	-17.61	-29.86	-65.52	26.75	-101.9	-39.90
-103.7	-108.4								
-28.99	38.35	33.23	18.86	9.648	22.06	-4.560	8.662	-2.114	2.041
2.146	-7.691	-6.214	3.151	102.6	1.751	205.9	-11.63	103.9	4.960
-10.15	-9.358	-31.42	21.68	37.00	15.15	-58.45	-76.82	-101.5	-107.2
-102.5	-39.27								
14.49	3.351	-14.86	-13.39	-9.995	-13.95	-1.033	-5.213	1.639	-2.625
3.528	7.256	2.146	-7.691	-8.692	2.639	103.9	4.960	192.1	-19.38
130.1	26.81	15.55	-49.29	-11.00	20.41	-38.55	-66.42	-98.76	-38.83
-29.00	38.32								
-9.313	-19.88	-11.08	43.18	-16.93	55.96	-3.184	56.17	16.48	17.89
1.471	-2.808	-2.119	2.378	5.873	-.5848	-10.15	-9.358	130.1	26.81
162.1	93.42	97.03	20.37	-10.57	3.287	-28.97	-28.92	-55.95	21.28
26.76	24.94								
11.99	2.715	-32.61	-17.36	-76.32	-11.76	-67.66	57.54	-2.817	56.32
-1.170	-5.195	-4.289	8.782	14.63	-11.78	-31.42	21.68	15.55	-49.29
97.03	20.37	215.2	-3.598	99.83	-2.311	-5.728	6.252	12.29	-1.663
-12.35	-3.724								
-12.08	1.915	38.49	-32.13	8.180	-94.10	-76.25	-11.40	-16.35	56.08
-10.24	-13.71	10.01	21.91	-17.61	-29.86	37.00	15.15	-11.00	20.41
-10.57	3.287	99.83	-2.311	210.8	-7.945	101.2	6.561	-16.83	-10.35
14.42	5.177								
4.930	-7.539	30.51	13.35	38.62	-32.16	-32.80	-17.24	-10.81	43.20
-14.74	-13.21	33.12	18.71	-65.52	26.75	-58.45	-76.82	-38.55	-66.42
-28.97	-28.92	-5.728	6.252	101.2	6.561	206.6	41.50	117.1	4.068
-10.90	2.181								
-8.815	2.711	4.905	-7.258	-12.16	1.609	11.96	2.803	-9.303	-19.87
14.49	3.351	-28.99	38.35	-101.9	-39.90	-101.5	-107.2	-98.76	-38.83
-55.95	21.28	12.29	-1.663	-16.83	-10.35	117.1	4.068	200.0	-15.34
103.3	3.279								
103.3	3.279	-16.90	2.181	14.42	5.177	-12.35	-3.724	26.76	24.94
-29.00	38.32	-102.5	-39.27	-103.7	-108.4	-102.5	-39.27	-29.00	38.32
26.76	24.94	-12.35	-3.724	14.42	5.177	-10.90	2.181	103.3	3.279
205.9	-11.64								

Impedance matrix $Z^{tt}_{0,0}$ (partial)

Figure 24. Partial output of BOTZSS for problem 4. (concluded)

```
        NP          NMODE       NRAND
        33            4           14

YH
  0.0000   0.0000   0.0000   0.0000   0.0000   1.3818   2.6065   3.8242   5.0419   6.2596
  7.8329   7.8329   7.8329   7.8329   7.8329   7.8329   7.8329   7.8329   7.8329   7.8329
  7.8329   7.8329   7.8329   6.2596   5.0419   3.8242   2.6065   1.3818   0.0000   0.0000
  0.0000   0.0000   0.0000

XH
  0.0000  -1.2713  -2.5426  -3.8139  -4.9066  -5.3233  -5.6886  -6.0539  -6.4193  -6.7846
 -7.2566  -6.3566  -5.0853  -3.8139  -2.5426  -1.2713   0.0000   1.2713   2.5426   3.8139
  5.0853   6.3566   7.2566   6.7846   6.4193   6.0539   5.6886   5.3233   4.9066   3.8139
  2.5426   1.2713   0.0000

 THE MINIMUM DIMENSIONS ARE AS FOLLOWS:

        Y          ZI         WORK          NZ          LR

    50174        1024           0           0         224
```

Figure 25. Partial output of BOTINV for problem 4.

```
M= -3  N= -3
V1
 .2[illegible]E-02  .6235E-02 -.1321E-02 -.4817E-02  .3765E-03 -.5187E-02 -.1247E-02 -.5559E-02  .2470E-02  .3356E-02
-.1572E-02  .1244E-02  .7840E-03 -.1299E-02  .6205E-03 -.1936E-02 -.9461E-03  .3853E-02  .8370E-03 -.5401E-03
-.1623E-02 -.9835E-03  .2024[illegible]-02  .1717E-02 -.2454E-02  .3658E-03  .3976E-02 -.1194E-02 -.3152E-02 -.1345E-02
 .4329E-03 -.4219E-03
-.1391E-02 -.4317E-02
 .1643E-02 -.3236E-02 -.3023E-03  .3877E-02 -.7341E-03  .1774E-02 -.6777E-03 -.2733E-02  .3560E-03 -.2679E-02
 .2768E-02  .1976E-02 -.3950E-02  .3544E-03  .4195E-02 -.3157E-02 -.4295E-02  .5460E-02  .3937E-02 -.1164E-02
-.5411E-03  .1224E-02
 .3765E-03  .2147E-02 -.1001E-02 -.2214E-02  .1545E-02  .9931E-03 -.6358E-03 -.9987E-03  .1864E-02 -.1434E-02
-.2834E-02  .3017E-02  .1600E-02 -.5044E-02  .3920E-03  .1001E-02  .6885E-03  .2796E-02 -.1381E-02  .2508E-03
-.2577E-02 -.1414E-02  .4552E-02  .2056E-02 -.4170E-02 -.9852E-03  .4156E-02 -.3178E-02 -.2431E-02  .4214E-03
-.4412E-03 -.2837E-02
-.1247E-02 -.5539E-02  .1013E-02  .2253E-02 -.6358E-03 -.9987E-03  .3363E-02 -.7364E-03 -.3515E-02 -.8305E-04
 .3303E-03 -.5043E-03 -.1812E-02  .4234E-04  .7420E-03 -.2289E-02 -.2657E-02 -.1225E-02  .3659E-02 -.2153E-02
 .1468E-03  .4101E-03 -.6493E-02 -.2805E-02  .4507E-02  .2106E-02 -.3993E-02  .1860E-02  .1890E-02  .1665E-02
 .1101E-03  .2848E-03
 .2477E-03  .3356E-02
-.1911E-02 -.3170E-02 -.1426E-02  .9256E-03  .1789E-02 -.7483E-03 -.1976E-02  .4474E-02  .2801E-02 -.3192E-02
-.3682E-02  .7553E-03  .4794E-02  .3673E-02 -.2561E-02 -.1485E-02  .2853E-02  .1974E-02 -.1921E-02 -.1050E-02
-.3924E-03 -.3743E-02
-.1572E-02  .1244E-02 -.1463E-02 -.3294E-02 -.2438E-02  .3017E-02 -.3393E-02 -.5063E-03 -.1911E-02 -.3170E-02
 .3620E-03  .7447E-02  .3036E-02 -.6306E-02 -.2281E-02  .3472E-02  .4706E-02 -.6863E-02 -.7310E-02 -.6765E-02
-.3135E-02 -.3253E-02  .3411E-02 -.2254E-02 -.1414E-02  .3601E-03  .2772E-03 -.2705E-02  .9744E-03 -.3913E-03
-.1355E-02  .2229E-02
 .7842E-03 -.2237E-02 -.2.24E-03  .3877E-02  .1490E-02 -.5044E-02 -.1812E-02  .4234E-02 -.1426E-02 -.8256E-03
 .3035E-02 -.6830E-03 -.1696E-02  .5625E-02  .8993E-03 -.4287E-02 -.2131E-02  .3738E-02  .4910E-02 -.4851E-02
-.2243E-03  .4403E-02 -.2692E-03 -.1256E-02  .5944E-03  .2777E-02 -.5623E-03 -.2731E-02 -.1115E-02  .3709E-02
-.9155E-03  .4633E-02
 .4223E-03 -.4335E-02 -.7341E-03 -.1774E-02  .3320E-03  .1001E-02  .7420E-03 -.2289E-02 -.1789E-02 -.7483E-03
-.2284E-02  .3477E-02  .2433E-03 -.4287E-03  .2194E-02  .2782E-02  .7682E-03 -.4407E-02 -.2299E-02  .3624E-02
 .1946E-03 -.9142E-03  .4445E-03 -.2209E-02  .4304E-03  .1024E-02 -.8119E-03  .1812E-02  .7770E-03 -.1915E-02
-.1436E-02  .3768E-02
-.9441E-03  .3884E-03 -.4777E-03 -.2733E-02  .5495E-03  .2796E-02 -.2657E-02 -.1225E-02 -.1970E-02  .4474E-02
 .4786E-03 -.4653E-02 -.2131E-03  .3739E-02 -.7922E-03 -.4407E-02 -.9306E-03  .5931E-02  .3059E-02 -.6695E-02
-.1538E-03  .1.26E-02 -.1557E-02  .4415E-02 -.1627E-02 -.5105E-02 -.2888E-03  .3840E-02  .6460E-03 -.1246E-02
-.4154E-03 -.1624E-02
 .2335E-03 -.5611E-03  .3564E-03 -.2473E-02 -.1331E-02  .2598E-03  .3669E-02 -.2153E-02 -.2801E-02 -.3192E-02
-.7334E-03  .4795E-02  .4910E-02 -.4851E-02 -.2700E-02  .3628E-02  .3059E-02 -.6695E-02  .1296E-03  .4242E-02
-.1445E-02 -.3493E-02  .3217E-02 -.7447E-03 -.2347E-02  .3117E-02 -.1065E-02 -.3350E-02 -.1468E-02  .1309E-02
-.1397E-02  .2324E-02
-.1223E-03 -.2835E-03  .2962E-02  .1976E-02 -.2577E-02 -.1419E-02  .1658E-02  .4019E-02 -.3696E-02 -.7563E-03
 .3035E-02 -.3243E-02 -.2743E-02  .4600E-02 -.1344E-02 -.9132E-03 -.1589E-02  .1996E-02 -.1660E-02 -.3433E-02
-.1638E-02 -.1178E-02  .2179E-02  .2171E-03  .1975E-02 -.1545E-02 -.1459E-02  .1023E-02  .2381E-02  .3350E-02
-.2691E-03 -.3567E-02
 .2647E-03 -.1717E-02 -.3411E-02  .3544E-03  .4552E-02 -.2054E-02 -.5423E-02 -.2625E-02  .1996E-02 -.3973E-02
 .3411E-02 -.9254E-03 -.2490E-02 -.1754E-03  .3445E-03 -.2299E-02 -.1562E-02 -.4415E-02 -.3219E-02 -.7440E-03
-.2573E-02  .2171E-03  .2622E-02  .3561E-03 -.7311E-03 -.1942E-02  .1049E-02  .2269E-02 -.1289E-02 -.9601E-02
-.1063E-02  .2934E-02
-.2453E-02  .3684E-03  .4193E-02 -.3157E-02 -.4170E-02 -.9852E-03  .4507E-02 -.2108E-02 -.2561E-02 -.1485E-02
-.1414E-02  .3611E-03 -.6949E-03  .2777E-02  .4304E-03  .1028E-02 -.1627E-02 -.2947E-02 -.3117E-02
 .1975E-03 -.1564E-03 -.7311E-03 -.1042E-02  .1517E-02  .9709E-03 -.9531E-03 -.2219E-02  .3735E-03  .5149E-02
-.4639E-03 -.2734E-02
 .3974E-03 -.1134E-03 -.4295E-02 -.5463E-02 -.4159E-02 -.3177E-02 -.3993E-02 -.2860E-03 -.2863E-02 -.1976E-02
 .2772E-03 -.2715E-02 -.5923E-03 -.2731E-02 -.8119E-03 -.1812E-02 -.2888E-03 -.3840E-02 -.1065E-02 -.3350E-02
-.1469E-02  .1623E-02  .1038E-02 -.2265E-02 -.3501E-03 -.2219E-02 -.3956E-02 -.2472E-02 -.1315E-02 -.4030E-02
-.2965E-03 -.1537E-02
-.3142E-02 -.1365E-02  .3937E-02 -.1164E-02 -.2431E-02 -.4218E-03 -.1890E-02 -.1665E-02 -.1921E-02 -.1050E-02
 .9744E-03 -.3013E-03 -.1115E-02 -.3709E-02 -.7770E-03 -.1915E-02 -.6460E-03 -.1246E-02 -.1468E-02 -.1308E-02
 .2381E-02 -.3357E-02 -.1282E-02 -.5601E-02 -.3735E-03 -.5189E-02 -.1315E-02 -.1920E-02 -.4185E-02 -.1289E-02
 .8986E-03 -.3371E-03
 .9373E-03 -.4210E-03 -.5411E-03 -.1224E-02 -.5412E-03 -.2827E-02 -.1131E-02 -.2829E-02 -.3026E-03 -.3782E-02
-.1356E-02  .2229E-02  .9106E-03 -.1453E-02 -.1436E-02  .3749E-02  .9101E-03 -.1604E-02 -.1369E-02  .2325E-02
                                                                                                    0979-0451-04
```

Admittance matrix $Y^{tt}_{-3,-3}$ (partial)

Figure 25. Partial output of BOTINV for problem 4. (concluded)

```
    NPT     NRAND    NMODE     NP       MC      RK
     36       14        4       33       50  .1570798E+01

YH
  0.0000  0.0000  0.0000  0.0000  0.0000  1.3088  2.6065  3.8242  5.0419  6.2596
  7.8329  7.8329  7.8329  7.8329  7.8329  7.8329  7.8329  7.8329  7.8329  7.8329
  7.8329  7.8329  7.8329  6.2596  5.0419  3.8242  2.6065  1.3088  0.0000  0.0000
  0.0000  0.0000  0.0000

XH
  0.0000 -1.2713 -2.5426 -3.8139 -4.9566 -5.3233 -5.6899 -6.0539 -6.4193 -6.7846
 -7.2566 -6.8899 -6.5233 -5.8139 -5.0853 -4.9426 -3.8139 -2.5426 -1.2713  0.0000
  1.2713  2.5426  3.8139  4.9566  5.3233  5.6899  6.0539  6.4193  6.7846  7.2566
  6.8899  6.5233  5.8139  5.0853  4.9426  3.8139  2.5426  1.2713  0.0000

HALF-LENGTH OF BOT =     11.0400

NUMBER OF FIXED ANGLES =  2
NUMBER OF ANGLES PER FIXED ANGLE =  46

FIXED ANGLE     CODE(PHI FIXED = 1, THETA FIXED =2)
    0.0              1
   90.0              2


M= -3  N= -3
Y
 .2007121E-02  .4294567E-02 -.1391407E-02 -.4817125E-02

M= -2  N= -3
Y
 .1234457E-02 -.1739611E-02 -.1461CF3F-02  .1694495E-02

M= -1  N= -3
Y
-.7548029E-03  .1365623E-02  .F61CC96E-03 -.1764666E-03

M=  0  N= -3
Y
 .2974443E-03 -.1563840F-03 -.3636430E-03  .2699968E-03
```

GP78-0481-06

Figure 26a. Partial output of BOTSCB for problem 4.

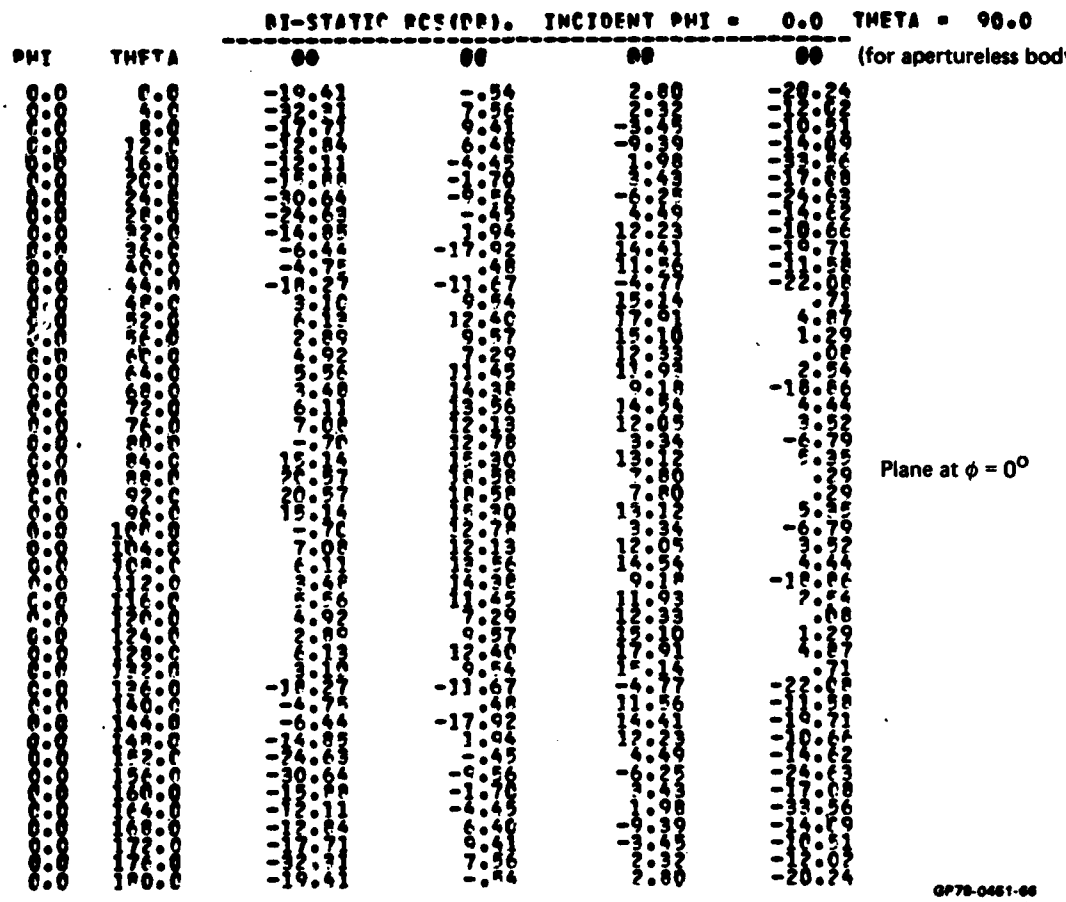

Figure 26b. Partial output of BOTSCB for problem 4.

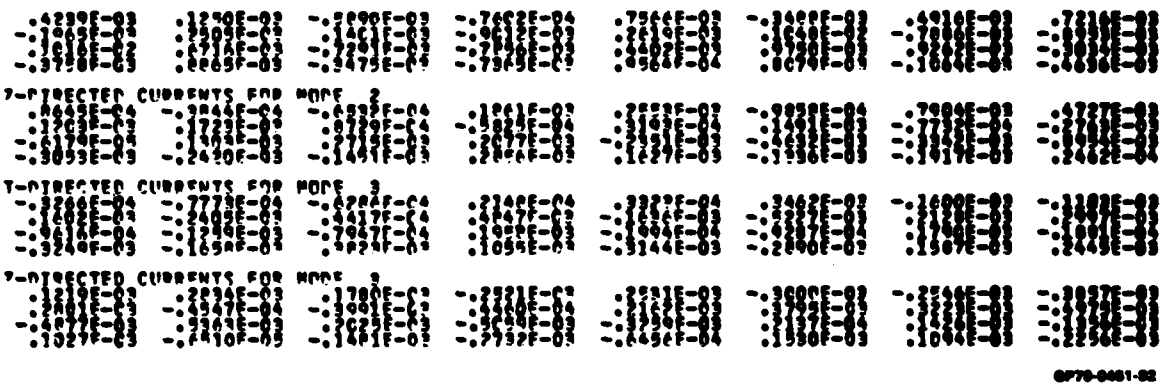

Figure 26b. Partial output of BOTSCB for problem 4. (continued)

```
THETA POLARIZED INCIDENT FIELD

T-DIRECTED CURRENTS FOR MODE -3
  .3266E-04   .7773E-04   .6286E-04  -.2148E-04  -.3323E-04  -.3462E-03   .1600E-03   .1103E-03
 -.1602E-03   .2405E-03  -.4417E-04  -.4847E-03   .1636E-03   .5227E-03  -.2128E-03  -.2997E-03
  .9616E-04   .1259E-03   .7547E-04  -.1958E-03   .1994E-04   .9287E-04  -.1790E-03   .1881E-04
  .3249E-03   .1658E-03  -.3823E-03  -.1055E-03   .3144E-03   .2890E-03  -.1587E-03  -.2445E-03

Z-DIRECTED CURRENTS FOR MODE -3
  .1219E-03   .2834E-03   .1780E-03  -.2521E-03   .2531E-03  -.3000E-03  -.2546E-03  -.3857E-03
  .2801E-03  -.4547E-04  -.3991E-03   .4460E-04   .2162E-03   .3795E-03   .3223E-03  -.4975E-03
 -.4877E-03   .5363E-03   .2625E-03  -.5059E-03  -.3259E-03   .2137E-04   .1426E-03  -.1336E-03
  .1027E-03  -.6510E-05  -.1481E-03  -.2732E-03  -.6456E-04   .1530E-03   .1694E-03  -.2256E-03

T-DIRECTED CURRENTS FOR MODE -2
 -.4239E-03  -.1250E-03   .5890E-03   .7602E-04  -.7566E-03   .3488E-03  -.4916E-03  -.7216E-03
  .1965E-03  -.2505E-03  -.1401E-03   .9012E-03  -.2619E-03  -.1048E-02   .7886E-03   .8953E-03
 -.1016E-02  -.6716E-03   .7291E-03   .7856E-03  -.4402E-03  -.9750E-03  -.9262E-03   .3034E-03
  .4788E-03  -.8885E-03   .2475E-03   .7365E-03  -.9564E-04  -.8079E-03   .1064E-03   .4636E-03

Z-DIRECTED CURRENTS FOR MODE -2
  .8645E-04  -.3844E-04  -.6532E-04   .1861E-03   .2563E-03  -.9858E-04   .7904E-03   .4727E-03
  .1203E-03   .1727E-03   .8729E-04  -.5825E-04   .3193E-04   .1491E-03  -.7732E-04  -.2763E-03
 -.6179E-05   .1263E-03   .2715E-03   .2077E-03  -.2351E-03  -.4632E-03  -.3342E-03  -.8954E-03
 -.3053E-03  -.2620E-03  -.1451E-03   .2856E-03   .1627E-03  -.1236E-03  -.1917E-03   .2462E-04

T-DIRECTED CURRENTS FOR MODE -1
  .8689E-04   .7478E-04  -.1078E-03  -.7249E-04   .9987E-04   .7732E-04   .2502E-03  -.1812E-04
 -.7809E-04   .9725E-04   .8161E-04  -.1824E-03   .1692E-04   .2647E-03  -.6667E-04  -.3271E-03
  .5293E-04   .3341E-03   .1918E-04  -.3237E-03  -.8818E-04   .2161E-03   .2503E-03  -.3462E-04
  .1409E-03  -.6602E-04  -.7361E-04  -.1551E-04   .2391E-04   .1183E-04  -.3692E-04  -.4415E-04

Z-DIRECTED CURRENTS FOR MODE -1
 -.1639E-03   .2679E-03   .3755E-03  -.9501E-03  -.1425E-03  -.1051E-02  -.4559E-03   .1370E-02
  .1200E-03   .4928E-03  -.9220E-04   .4241E-03   .1998E-03  -.1067E-02  -.2535E-03   .1285E-02
  .2476E-03  -.1053E-02  -.1832E-03   .3720E-03  -.3401E-03   .1524E-03  -.1116E-03   .8713E-03
  .5903E-03  -.9644E-03   .2037E-03  -.8673E-03   .1575E-03   .2108E-03  -.6029E-04   .7090E-04

T-DIRECTED CURRENTS FOR MODE  0
  .5872E-11  -.2147E-10  -.1931E-09   .9619E-10  -.2201E-09  -.3208E-10   .1741E-09   .1728E-09
 -.5659E-09  -.2819E-10   .4416E-09   .1956E-09  -.2559E-09  -.2046E-09   .8928E-10   .2732E-09
  .8611E-10  -.3152E-09  -.2101E-09   .2651E-09   .9774E-10  -.1130E-09  -.1069E-09   .3617E-11
 -.4085E-10   .2323E-09   .2540E-09  -.7571E-10  -.2921E-09   .8584E-10   .1368E-09  -.2317E-10

Z-DIRECTED CURRENTS FOR MODE  0
  .3014E-03  -.1795E-02  -.2682E-03   .7756E-03   .1426E-02  -.3373E-02  -.1116E-02  -.5001E-03
  .2307E-04  -.9531E-03   .2885E-04   .3090E-02   .9648E-03  -.2426E-02  -.1358E-02   .2073E-02
  .1392E-02  -.3339E-02  -.1216E-02  -.1469E-02   .9583E-03   .4240E-02  -.5283E-02   .6732E-02
  .5510E-02  -.4607E-02  -.1603E-02  -.5209E-02   .1803E-02   .1901E-02  -.1130E-02   .3687E-03

T-DIRECTED CURRENTS FOR MODE  1
 -.8689E-04  -.7478E-04   .1078E-03   .7249E-04  -.9987E-04  -.7732E-04  -.2502E-03   .1812E-04
  .7809E-04  -.9725E-04  -.8161E-04   .1824E-03  -.1692E-04  -.2647E-03   .6666E-04   .3271E-03
 -.5293E-04  -.3341E-03  -.1018E-04   .3237E-03   .8818E-04  -.2161E-03  -.2503E-03   .3462E-04
 -.1409E-03   .6602E-04   .7361E-04   .1551E-04  -.2391E-04  -.1183E-04   .3692E-04   .4415E-04

Z-DIRECTED CURRENTS FOR MODE  1
 -.1639E-03   .2679E-03   .3755E-03  -.9501E-03  -.1425E-03  -.1051E-02  -.4559E-03   .1370E-02
  .1200E-03   .4928E-03  -.9220E-04   .4241E-03   .1998E-03  -.1067E-02  -.2535E-03   .1285E-02
  .2476E-03  -.1053E-02  -.1832E-03   .3720E-03  -.3401E-03   .1524E-03  -.1116E-03   .8713E-03
  .5903E-03  -.9646E-03   .2037E-03  -.8673E-03   .1575E-03   .2108E-03  -.6029E-04   .7090E-04

T-DIRECTED CURRENTS FOR MODE  2
```

t and z directed current coefficients for θ-polarized incident field

Figure 26b. Partial output of BOTSCB for problem 4. (continued)

GP79-0461-93

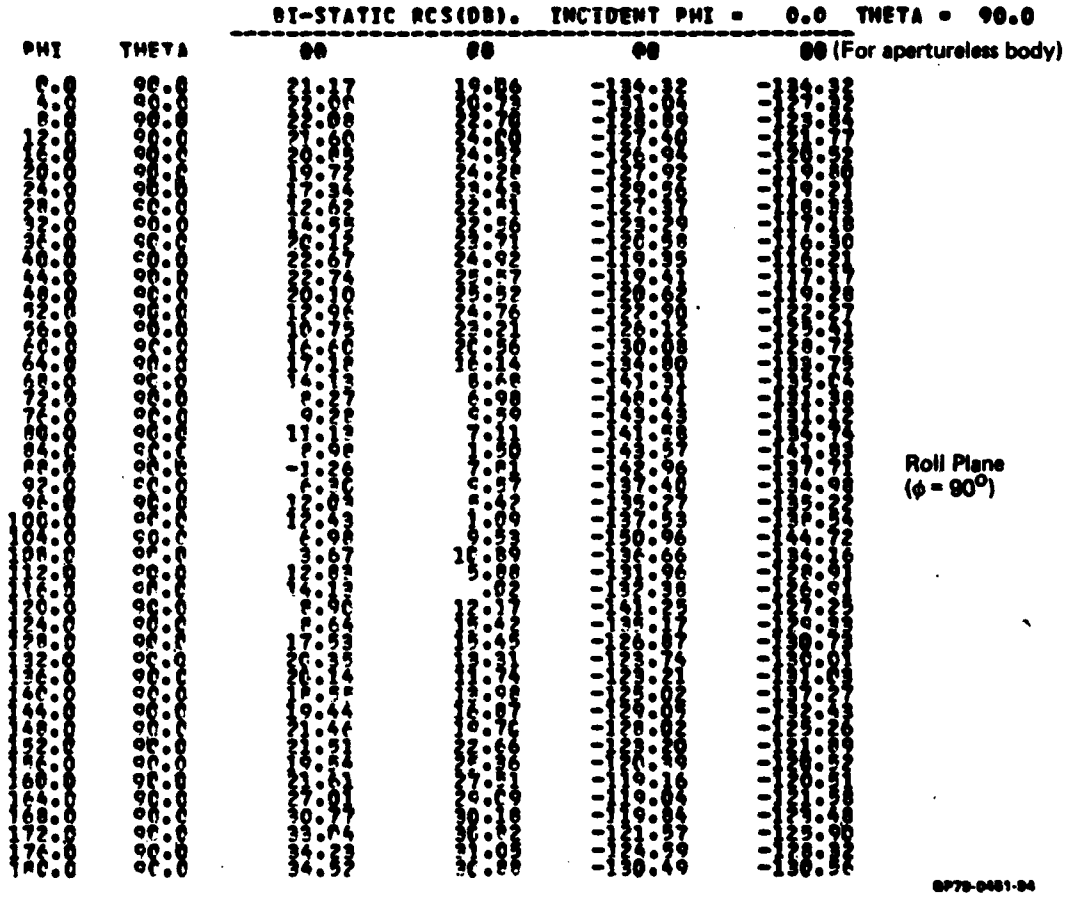

Figure 26b. Partial output of BOTSCB for problem 4. (continued)

Plot of currents along BOT for
θ-polarized incident field

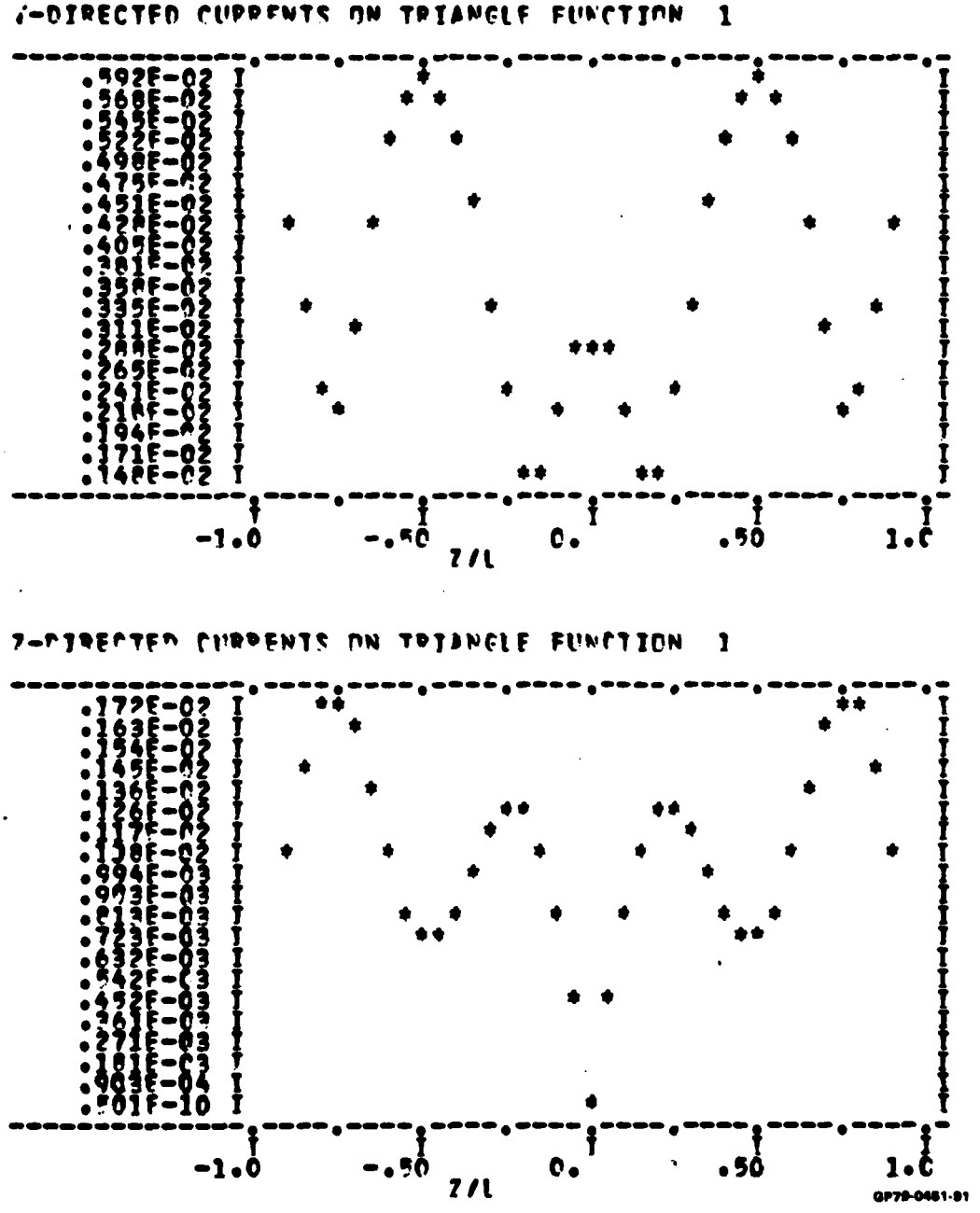

Figure 26b. Partial output of BOTSCB for problem 4. (concluded)

```
PHI POLARIZED INCIDENT FIELD

T-DIRECTED CURRENTS FOR MODE -3
  .1283E-02  -.3668E-03  -.1263E-02   .9474E-03   .2009E-02  -.8271E-04  -.3172E-03   .6037E-04
  .1320E-02  -.3687E-03  -.1683E-02  -.5994E-03   .2185E-02   .3336E-03  -.2091E-02  -.1014E-03
  .3230E-02   .9611E-03  -.3168E-02  -.2302E-02   .1871E-02   .1964E-02   .9498E-03  -.6820E-03
 -.7251E-03  -.2180E-03  -.1801E-03  -.9387E-04   .3833E-03   .7013E-03  -.7818E-03  -.6826E-03
Z-DIRECTED CURRENTS FOR MODE -3
 -.3408E-03  -.5111E-03   .3441E-04  -.6331E-03   .1485E-04   .1026E-03  -.3364E-03  -.2627E-03
  .1621E-04  -.6886E-03   .9991E-04   .5385E-04  -.3451E-03  -.9696E-03  -.6767E-04   .6688E-03
  .6121E-03   .5469E-03  -.5775E-03  -.1156E-02  -.7547E-04   .1035E-02   .3590E-03  -.5291E-03
  .9187E-04   .5407E-03  -.7987E-04   .2783E-03   .4665E-04   .1225E-03   .2522E-03   .6089E-03
T-DIRECTED CURRENTS FOR MODE -2
 -.2149E-02  -.4552E-02   .3578E-02   .4277E-02  -.9123E-03  -.7142E-02  -.6029E-03   .3202E-02
 -.4702E-02  -.2118E-02   .3867E-02   .1059E-02  -.4709E-02  -.1385E-02   .4467E-02   .4475E-02
 -.2248E-02  -.6804E-02  -.1107E-02   .6301E-02  -.4122E-02  -.3181E-02  -.5681E-02  -.3626E-02
 -.5161E-03   .4449E-02  -.5934E-04   .2149E-03   .1103E-02   .1612E-04  -.3035E-03   .2052E-02
Z-DIRECTED CURRENTS FOR MODE -2
 -.1027E-02   .1019E-02  -.4724E-03   .2191E-03   .1011E-02  -.7051E-03   .1094E-03   .2861E-02
  .1159E-02   .1487E-02  -.1588E-02   .2230E-03  -.6534E-03   .8174E-04   .1536E-02  -.9894E-04
 -.9831E-03  -.9061E-03  -.4961E-03   .1470E-02   .7730E-03  -.1387E-02  -.1375E-02  -.2002E-02
 -.9920E-03   .1968E-04   .3518E-03   .2659E-03  -.1122E-02   .9815E-03   .1759E-02  -.1590E-02
T-DIRECTED CURRENTS FOR MODE -1
 -.1018E-02   .1533E-02   .4347E-03  -.1500E-02  -.1127E-02   .1382E-02   .1923E-02   .6265E-03
 -.7702E-03   .2221E-02   .6611E-03  -.2591E-02  -.1512E-03   .3448E-02   .7324E-03  -.4048E-02
 -.1072E-02   .3647E-02   .2752E-02  -.2486E-02  -.2125E-02   .4967E-03   .7556E-03   .2470E-02
  .1078E-02   .4695E-03  -.1622E-03  -.1051E-02  -.3225E-03   .4157E-03   .9604E-03  -.6948E-03
Z-DIRECTED CURRENTS FOR MODE -1
  .2148E-03  -.8169E-04   .3447E-03   .3175E-03   .4154E-04  -.2020E-03  -.4974E-03  -.5956E-03
 -.1554E-05  -.1924E-03  -.2683E-03   .2509E-03   .5775E-03   .1373E-03  -.5497E-03  -.3490E-03
  .9006E-03   .3709E-03   .1241E-03  -.1730E-03  -.3776E-03  -.1278E-03  -.1229E-03   .5718E-03
  .7586E-03   .4022E-02   .2042E-03  -.1372E-03   .1465E-03   .2485E-03  -.3872E-03  -.1964E-03
T-DIRECTED CURRENTS FOR MODE  0
  .1119E-02   .1416E-02  -.6734E-03  -.1224E-02   .1337E-02   .3323E-03   .1050E-02  -.2274E-02
  .2829E-02   .6673E-03  -.2782E-02   .5371E-03   .4041E-02  -.1465E-02  -.4851E-02   .3727E-02
  .4778E-02   .1947E-02  -.5087E-02  -.4882E-02   .1130E-02   .5198E-02   .8248E-02   .2247E-02
  .3979E-02  -.7464E-02  -.3607E-02  -.3728E-04   .1340E-02   .6487E-03  -.1143E-02  -.1480E-02
Z-DIRECTED CURRENTS FOR MODE  0
 -.1707E-10   .5419E-11   .1877E-10   .4244E-11   .1903E-10  -.2876E-12  -.8056E-12  -.1238E-10
  .3636E-11  -.4344E-11   .6916E-11  -.5617E-11   .3767E-11   .1538E-11  -.1167E-10   .6492E-12
  .9695E-11  -.2339E-11  -.1604E-11   .1154E-11   .1496E-10   .2788E-11  -.1757E-10   .1006E-10
 -.4228E-11   .8343E-11   .1477E-10   .4776E-11  -.1248E-10   .5912E-11   .6291E-11  -.7889E-11
T-DIRECTED CURRENTS FOR MODE  1
 -.1018E-02   .1533E-02   .4347E-03  -.1500E-02  -.1127E-02   .1382E-02   .1923E-02   .6265E-03
 -.7702E-03   .2221E-02   .6611E-03  -.2591E-02  -.1512E-03   .3448E-02   .7324E-03  -.4048E-02
 -.1072E-02   .3647E-02   .2752E-02  -.2486E-02  -.2125E-02   .4967E-03   .7556E-03   .2470E-02
  .1078E-02   .4695E-03  -.1622E-03  -.1051E-02  -.3225E-03   .4157E-03   .9604E-03  -.6948E-03
Z-DIRECTED CURRENTS FOR MODE  1
 -.2148E-03   .8169E-04  -.3447E-03  -.3175E-03  -.4154E-04   .2020E-03   .4974E-03   .5956E-03
  .1554E-05   .1924E-03   .2683E-03  -.2509E-03  -.5775E-03  -.1373E-03   .5497E-03   .3490E-03
 -.9006E-03  -.3709E-03  -.1241E-03   .1730E-03   .3776E-03   .1278E-03   .1229E-03  -.5718E-03
 -.7586E-03  -.4022E-03  -.2042E-03   .1372E-03  -.1465E-03  -.2485E-03   .3872E-03   .1964E-03
T-DIRECTED CURRENTS FOR MODE  2
```

t and z directed current coefficients for ϕ-polarized incident field

Figure 26c. Partial output of BOTSCB for problem 4.

GP79-0481-67

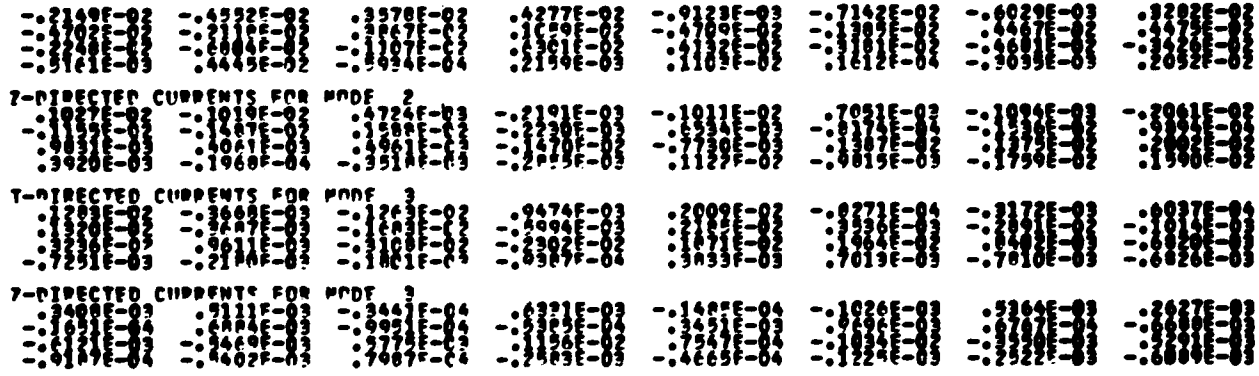

Figure 26c. Partial output of BOTSCB for problem 4. (continued)

Plots of current along BOT for
ϕ-polarized incident field

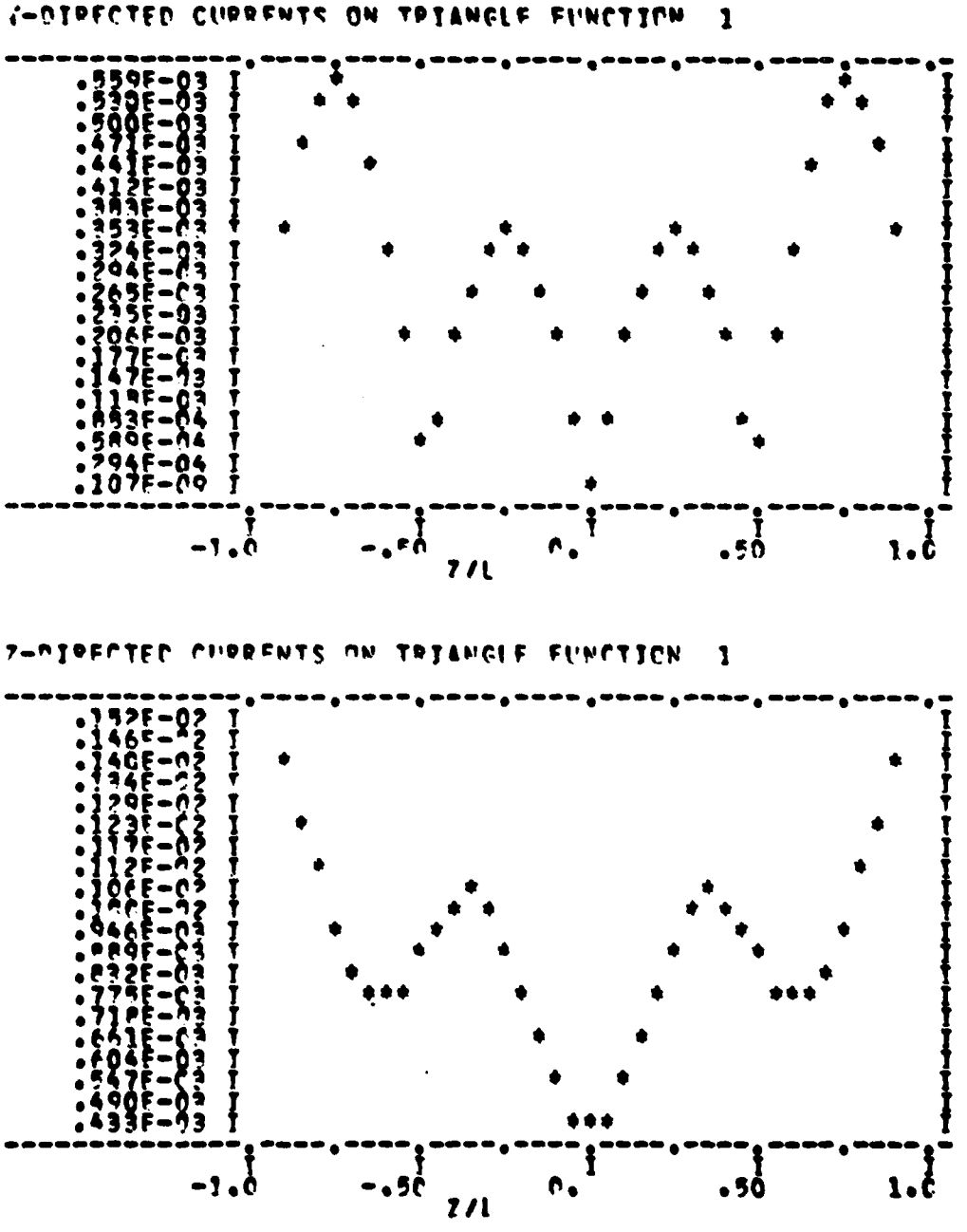

GP79-0481-102

Figure 26c. Partial output of BOTSCB for problem 4. (concluded)

```
APERTURE ANALYSIS

   Z0        Z1        Y0        X0        Y1        Y1
-3.3120    3.3120    9.0420    6.4194    2.6064    9.6885     Aperture coordinates

 LT    VLOW       VHGH      IT

 12      .0001    1.2713    -1
 13    1.2713      .0001     1

LT   IT                FPP                                        FPPZ

12   -1   .2256E-08   .3496E+00   .1250E+00   .2944E-08   .3495E+00   .1250E+00
13    1   .1250E+00   .3624E+00   .2761E-08   .1250E+00   .3623E+00   .3576E-08

YA1
 .1028E-02  -.1781E-02  -.5613E-03  -.1816E-02      Y_a^tt
 .1879E-02  -.2370E-02  -.4241E-02   .7760E-02
YA2
-.2593E-15  -.1816E-15  -.6208E-17  -.1536E-16      Y_a^zt     Aperture
-.5168E-15  -.2366E-15  -.2331E-16  -.3551E-15                 admittance
YA3
 .2819E-15  -.1174E-15  -.1426E-16   .8628E-15      Y_a^tz
 .8000E-16  -.1744E-15  -.6171E-16   .6755E-18
YA4
-.3386E-02  -.3023E-03  -.4161E-03  -.6540E-03      Y_a^zz
-.5002E-03  -.8708E-03  -.3097E-02   .1649E-02
```

```
NEAR FIELD ANALYSIS (for aperture coupled fields)

                                                         E-FIELD                                          H-FIELD
                                          ------------------------------------------     ------------------------------------------
                                                     FIELD COMPONENTS                               FIELD COMPONENTS
ZTEST    YTEST    XTEST                        RADIAL        THETA         PHI              RADIAL        THETA         PHI

0.0000   3.8242  -9.0000
                          0 INC POL E-FIELD   .1516E-07    .1568E+01    .3293E-07        .3962E-02    .2020E-10    .1112E-02
                          0 INC POL F-FIELD   .1780E+01    .1030E-07    .2461E+01        .7112E-11    .4179E-03    .1124E-10
0.0000   3.8242  -3.0000
                          0 INC POL E-FIELD   .4482E-08    .1516E+01    .3256E-07        .1238E-02    .2004E-10    .1633E-02
                          0 INC POL F-FIELD   .9886E+00    .8240E-08    .2112E+01        .5487E-11    .1840E-02    .3263E-11
0.0000   3.8242  -1.0000
                          0 INC POL E-FIELD   .1263E-07    .1371E+01    .1118E-07        .3247E-02    .2248E-10    .9923E-03
                          0 INC POL F-FIELD   .1275E+01    .7129E-08    .7336E+00        .3794E-11    .2533E-02    .7572E-11
0.0000   3.8242   1.0000
                          0 INC POL E-FIELD   .1376E-07    .1451E+01    .1616E-07        .2289E-02    .8278E-10    .1836E-02
                          0 INC POL F-FIELD   .1169E+01    .7429E-08    .8027E+00        .6022E-11    .4826E-02    .7442E-11
0.0000   3.8242   3.0000
                          0 INC POL E-FIELD   .2692E-07    .1136E+01    .2394E-07        .2282E-02    .1816E-02    .2292E-02
                          0 INC POL F-FIELD   .1787E+01    .1676E-07    .1340E+01        .6024E-11    .7838E-02    .4248E-11
0.0000   3.8242   5.0000
                          0 INC POL E-FIELD   .4424E-07    .1495E+01    .3163E-07        .3088E-02    .7296E-10    .2281E-02
                          0 INC POL F-FIELD   .2931E+01    .1096E-07    .1967E+01        .1594E-10    .7838E-02    .1827E-10
                                                                                                                   GP79-0461-06
```

Figure 26d. Partial output of BOTSCB for problem 4.

3. SYSTEMS SECTION: DETAILED PROGRAM DESCRIPTIONS

A detailed description of each main-line MM/BOT program (Figure 1) will be given, including a description of the flow diagram, subroutine input/output arguments, and the special matrix properties used. A description of the common variables used in the program, along with storage methods used in certain arrays, is given in Appendix A. A summary of subroutine calling programs is contained in Appendix B.

3.1 BOTZSS Program

BOTZSS generates the impedance submatrices Z_{mn} for modes m,n where m = 0 to NMODE - 1, n = -m to +m, and $|m - n| <$ NBAND. The impedance matrices are generated in the lower triangular portion of Z_{BOT}. Symmetry conditions are then applied in BOTINV in order to fill the entire Z_{BOT} matrix. The structure of the Z_{BOT} matrix is as follows:

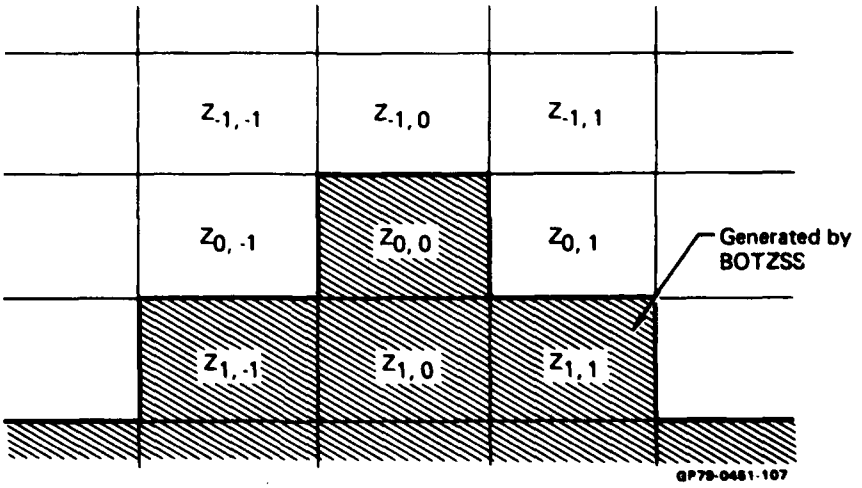

where each of the $Z_{m,n}$ matrices is comprised of four submatrices as follows:

$Z^{tt}_{m,n}$	$Z^{tz}_{m,n}$
$Z^{zt}_{m,n}$	$Z^{zz}_{m,n}$

AD-A087 403 MCDONNELL DOUGLAS RESEARCH LABS ST LOUIS MO F/G 20/14
RADIATION AND SCATTERING FROM BODIES OF TRANSLATION, VOLUME II.--ETC(U)
APR 80 L N MEDGYESI-MITSCHANG, J M PUTNAM F30602-77-C-0233
UNCLASSIFIED RADC-TR-80-142-VOL-2 NL

2 2

END
DATE FILMED
9 80
DTIC

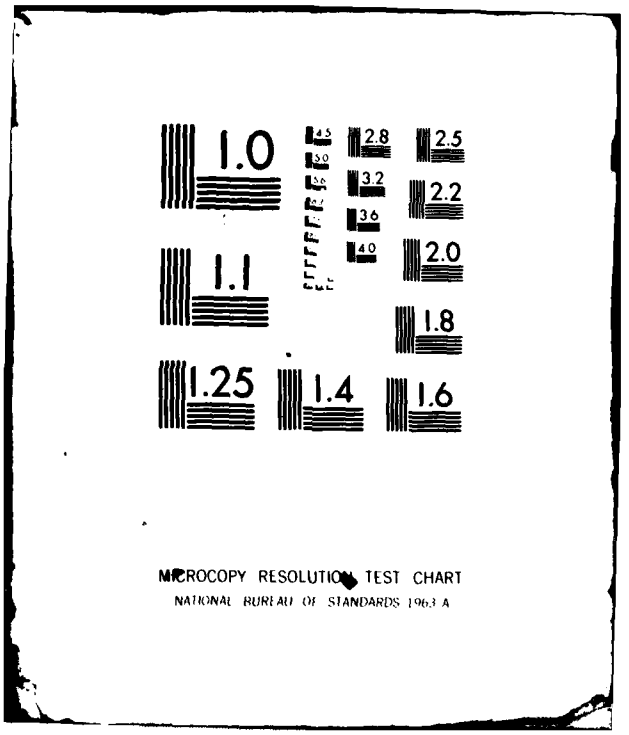
1.0
1.1
1.25
1.4
1.6
1.8
2.0
2.2
2.5
2.8
3.2
3.6
4.0
MICROCOPY RESOLUTION TEST CHART
NATIONAL BUREAU OF STANDARDS 1963 A

Figure 27 shows the flow diagram for BOTZSS. The equation numbers refer to the theoretical expressions in Volume I.

The computation of the Green's function kernel takes advantage of the fact that $G_{m,n}$ is symmetric (i.e., $G_{m,n} = {}_tG_{m,n}$), where t indicates the transpose operation. Only the upper triangular portion is stored as indicated in the appendix; hence, $(G_{m,n})_{i,j}$ is stored in location

$$G(i + (j-1)j/2) \text{ when } i \leq j$$

and

$$G(j + (i-1)i/2) \text{ when } i > j.$$

The section that computes the impedance matrix $Z_{m,n}$ uses the following symmetries:

$$Z^{tt}_{m,n} = {}_t(Z^{tt}_{m,n}),$$

$$m\ {}_t(Z^{tz}_{m,n}) = -\ n\ Z^{zt}_{m,n},$$

and

$$Z^{zz}_{m,n} = {}_t(Z^{zz}_{m,n}).$$

Thus, only the upper triangular portion of each of the $Z^{tt}_{m,n}$, $Z^{zt}_{m,n}$, $Z^{tz}_{m,n}$, and $Z^{zz}_{m,n}$ needs to be computed. The remaining portion is filled using the symmetry conditions above.

In Figure 27, (X_p, Y_p) define a point on the BOT, with ν_p being the angle subtended by the x-axis and the BOT generating curve. The parameter $\delta = \Gamma/L$, where L is the half-length of the BOT measured along the z-axis and Γ is the distance between adjacent (X_p, Y_p) points on the BOT generating curve. Note a triangle function subtends 2 Γ.

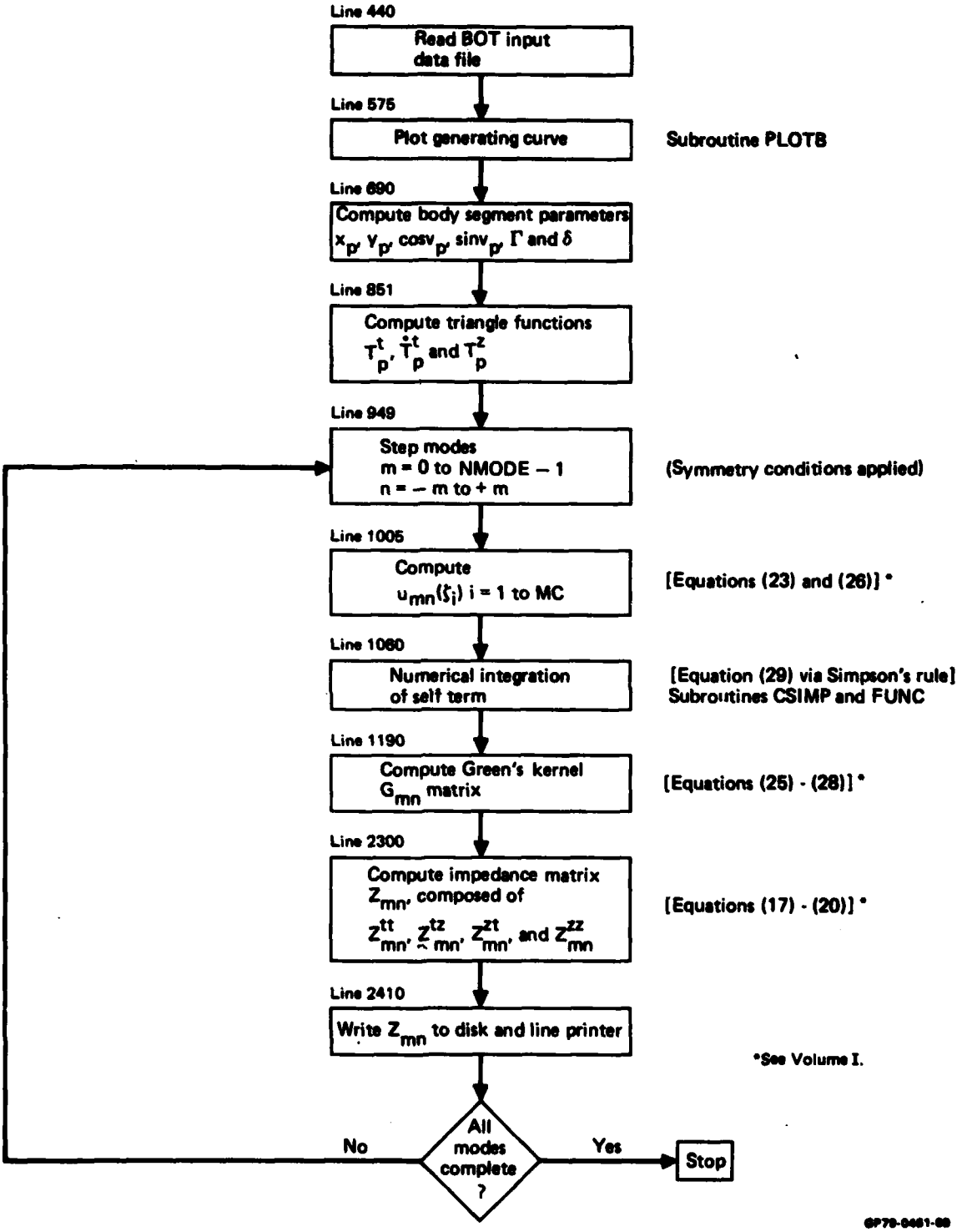

Figure 27. BOTZSS flow diagram.

3.2 BOTZSS Subroutines

3.2.1 Subroutine CSIMP

Subroutine CSIMP is a Simpson integration routine with a calling statement

CALL CSIMP(F,A,B,DEL,IMAX,SI1,S,N,IER).

This routine computes $S = \int_A^B F(x)dx$ using the method of successive bisections of the interval until either a relative error of DEL is achieved or IMAX bisections have been performed. F must be declared external in the calling program. The following are returned by CSIMP:

S - Approximate value of the integral.

SI1 - Previous approximation to the integral. Convergence has occurred if

$$\left|\frac{S - SI1}{S}\right| < DEL.$$

N - Number of intervals used in computing S.

IER - Error return. IER = 0 indicates that convergence has occurred.

3.2.2 Subroutine PLOTB

Subroutine PLOTB plots the points on the generating curve of the BOT. Points on the BOT corresponding to triangle function peaks are indicated with a plus sign. The calling statement is

CALL PLOTB(X,Y,N,NR),

where

X - Array of x coordinates to be plotted

Y - Array of y coordinates to be plotted

N - Number of points to be plotted

NR - Number of line printer rows to use for the y-axis.

The routine uses 51 columns for the x-axis, with the dynamic range on both the x and y axes equal. Hence, depending upon the type of line printer used, NR may have to be adjusted in order to obtain a plot that is not distorted (i.e., the x and y axes have approximately the same physical length on the line printer output).

3.3 BOTINV Program

BOTINV fills the Z_{BOT} matrix using the output file from BOTZSS and inverts this matrix according to the user's specifications. The following symmetries are used to fill Z_{BOT} from the partial Z_{BOT} matrix generated by BOTZSS (see Figure 28 for NMODE = 4):

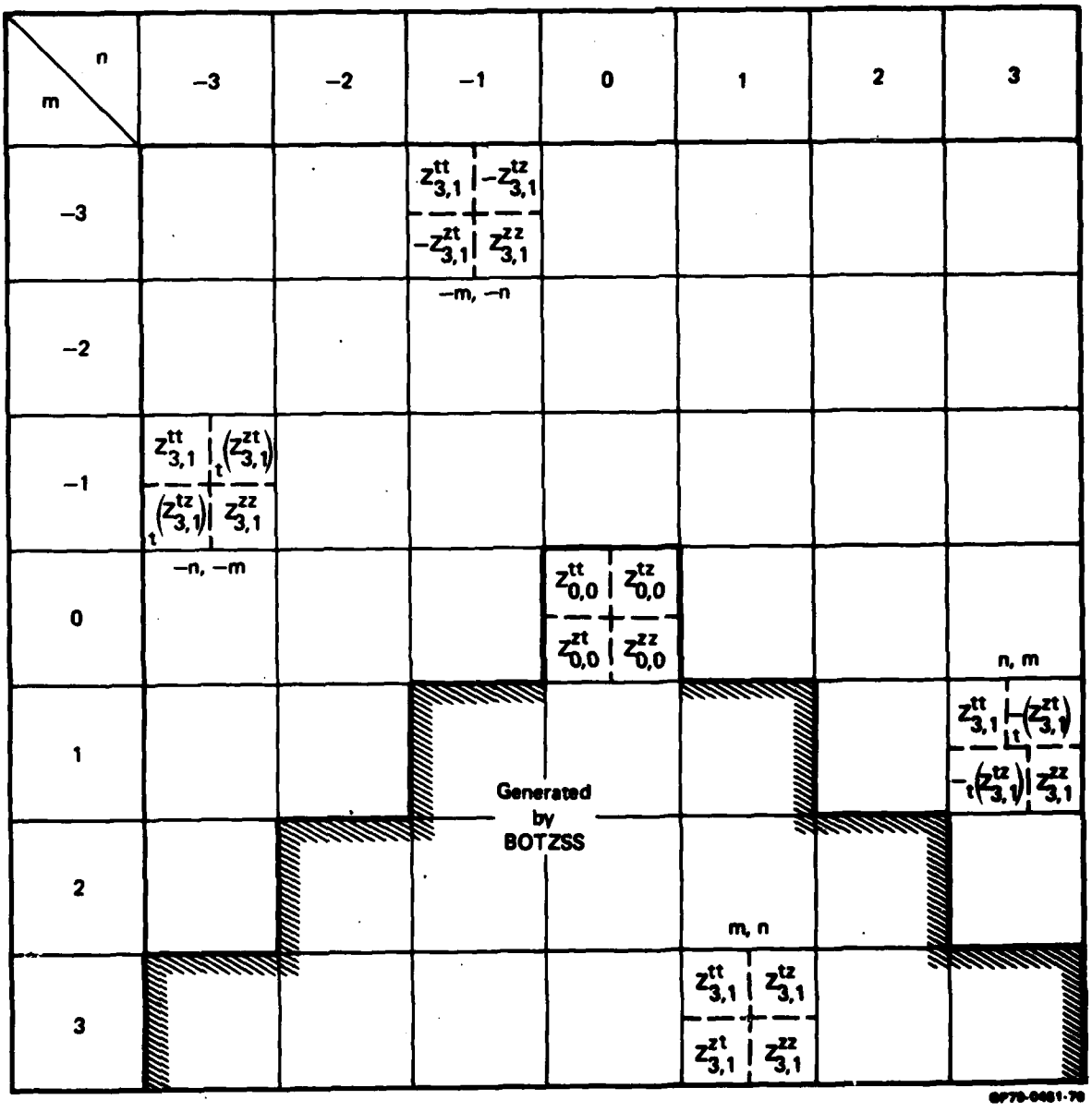

Figure 28. Z_{BOT} matrix symmetries.

Main diagonal symmetry (Compute $Z_{n,m}$ from $Z_{m,n}$)

$$Z_{n,m} = \begin{array}{|c|c|}\hline Z^{tt}_{n,m} & Z^{tz}_{n,m} \\ \hline Z^{zt}_{n,m} & Z^{zz}_{n,m} \\ \hline \end{array} = \begin{array}{|c|c|}\hline Z^{tt}_{m,n} & -t(Z^{zt}_{m,n}) \\ \hline -t(Z^{tz}_{m,n}) & Z^{zz}_{m,n} \\ \hline \end{array}$$

Skew symmetry (Compute $Z_{-n,-m}$ from $Z_{m,n}$)

$$Z_{-n,-m} = \begin{array}{|c|c|}\hline Z^{tt}_{-n,-m} & Z^{tz}_{-n,-m} \\ \hline Z^{zt}_{-n,-m} & Z^{zz}_{-n,-m} \\ \hline \end{array} = \begin{array}{|c|c|}\hline Z^{tt}_{m,n} & t(Z^{zt}_{m,n}) \\ \hline t(Z^{tz}_{m,n}) & Z^{zz}_{m,n} \\ \hline \end{array}$$

Figure 29 shows the flow diagram for BOTINV. Three types of matrix inversions are allowed in BOTINV: total inversion, main diagonal inversion, and partial inversion. Each of these options is described next.

Total Inversion - Total inversion is performed when NBAND $\geq$ 2*NMODE-1. In this case, the Z_{BOT} matrix is stored by columns as follows:

$$(Z^{tt}_{m,n})_{i,j} \quad Z((n + NMODE-1)*LS^2*(2*NMODE-1) + (j-1)*(2*NMODE-1)*LS + (m + NMODE-1)*LS + i)$$

$(Z^{zt}_{m,n})_{i,j}$ is stored at $(Z^{tt}_{m,n})_{i,j}$ + NM

$(Z^{tz}_{m,n})_{i,j}$ is stored at $(Z^{tt}_{m,n})_{i,j}$ + NM*LS*(2*NMODE-1)

$(Z^{zz}_{m,n})_{i,j}$ is stored at $(Z^{tz}_{m,n})_{i,j}$ + NM

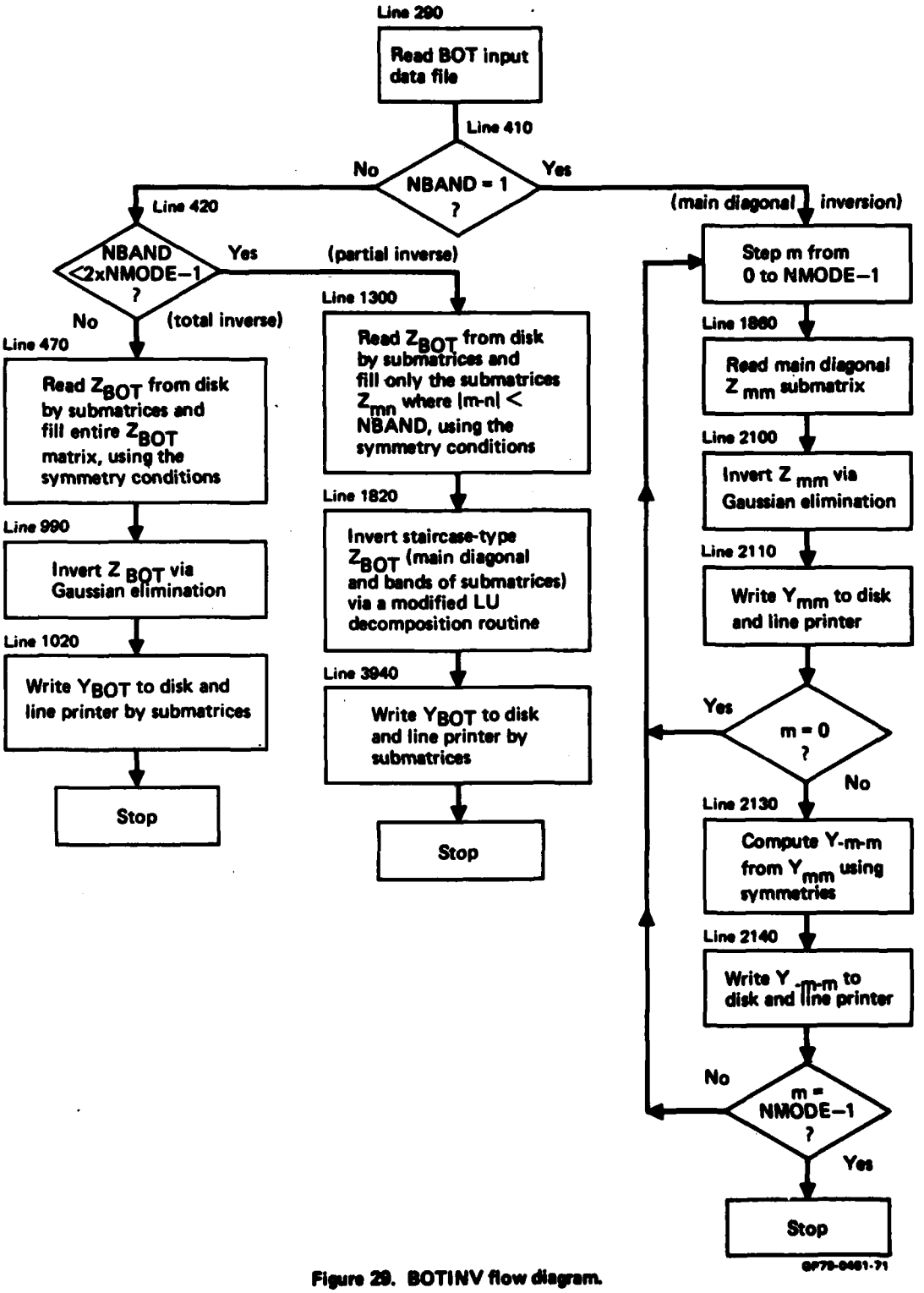

Figure 29. BOTINV flow diagram.

Once the Z_{BOT} matrix is filled, it is inverted using Gaussian elimination with partial pivoting, and written to disk file by submatrices.

Main Diagonal Inversion - Main diagonal inversion is performed when NBAND = 1. In this case, the individual diagonal submatrices are inverted separately using Gaussian elimination. For $m \neq 0$, the following symmetry is used:

$$Z_{-m,-m} = \begin{array}{|c|c|} \hline Z^{tt}_{-m,-m} & Z^{tz}_{-m,-m} \\ \hline Z^{zt}_{-m,-m} & Z^{zz}_{-m,-m} \\ \hline \end{array} = \begin{array}{|c|c|} \hline Z^{tt}_{m,m} & -Z^{tz}_{m,m} \\ \hline -Z^{zt}_{m,m} & Z^{zz}_{m,m} \\ \hline \end{array}$$

which implies that

$$(Z_{-m,-m})^{-1} = Y_{-m,-m}$$

has the same symmetries. Thus, at a given time, only $Z_{m,n}$ where m = 0 to NMODE-1 is inverted. The symmetries are used, and the resulting (2*NMODE-1) submatrices are written to disk file.

Partial Inversion - Partial inversion is performed when NBAND<2*NMODE-1, and NBAND≠1. In this case, the Z_{BOT} matrix is filled only with the $Z_{m,n}$ submatrice for which $|m-n| < NBAND$. The resulting Z_{BOT} matrix has a staircase-type structure. The rest of the matrix is sparse. If each of the $Z_{m,n}$ submatrices are thought of as individual elements, Z_{BOT} can be considered as a banded matrix. A modified LU decomposition can then be used with all arithmetic operations replaced by the corresponding matrix operations. The result is an L and U matrix which are also of a staircase-type, but are lower and upper triangular, respectively, when the submatrices are considered as individual elements. The inverse of Z_{BOT} can then be computed using forward and backward substitution, again replacing arithmetic operations with matrix operations. The result is a full inverted Z_{BOT} matrix which is written to disk file by submatrices.

The Z_{BOT} matrix is stored by columns, if the individual submatrices $Z_{m,n}$ are considered as elements. Only the banded portion is stored. When NMODE = 4 and NBAND = 2 (refer to Figure 28), Z_{BOT} is stored in the following order:

$$Z_{-3,-3},\ Z_{-2,-3},\ Z_{-3,-2},\ Z_{-2,-2},\ Z_{-1,-2},\ Z_{-2,-1}\ \cdots$$

Each submatrix is stored in LS^2 successive locations by columns. For the example above, $Z_{-2,-3}$ would start at index $LS^2 + 1$.

3.4 BOTINV Subroutines

3.4.1 Subroutine LINEQ

Subroutine LINEQ is a standard matrix inversion routine using Gaussian elimination with partial pivoting, with the following calling statement and arguments:

```
CALL LINEQ(LL,C,LR),
```

where

LL - Order of matrix to be inverted.

C - Array containing the matrix to be inverted, stored by columns. On output, C contains the inverted matrix.

LR - Array of length LL used as a work space during the pivoting process.

3.4.2 Subroutine LIST

Subroutine LIST prints individual $Y_{m,n}$ submatrices on the line printer and writes them to a disk file. The calling statement and arguments follow:

```
CALL LIST(M,N,Z),
```

where

M - Index m.

N - Index n

Z - Array containing the $Y_{m,n}$ submatrix, stored by columns.

3.4.3 Subroutine INVBAN

Subroutine INVBAN is a modification of a standard banded matrix inversion routine using LU decomposition without pivoting, where only the banded portion is stored by columns. Arithmetic operations were replaced by their corresponding matrix operations, and indices were multiplied by LS^2 since the elements were replaced by matrices. The calling statement and arguments follow:

```
CALL INVBAN(LS,NMODE,NBAND,NZ,A,Z,WORK),
```

where LS, NMODE, and NBAND are described in Appendix A.

INPUT: NZ - Array used for indexing. In a normal banded matrix A, NZ(I) = NZ(I-1) + (the number of zeroes below the band in column I-1) + (the number of zeroes above the band in column I), where NZ(1) = 0. If A has order n, with only the banded portion stored by columns, then A_{ij} will be stored in location n(j-1) + i - NZ(j).

A - Array containing the staircase-type matrix to be inverted, with storage details described above.

Z - Array of length LS^2 used as work area.

WORK - Array of length LS used as work area.

In addition, three variables are passed in common as follows:

```
COMMON NM,JK(4),LR
```

where

NM - Number of triangle functions

JK - Work array of length 4

LR - Work array of length LS.

3.4.4 Additional Subroutines

The subroutines MULTS, MULT, REPLACE, and ZERO perform matrix operations which are documented in the listings.

3.5 BOTRA Program

BOTRA computes the radiated far and near fields produced by one or more slot antennas on the BOT (see Section 5 of Volume I). Figure 30 shows the flow diagram for BOTRA with equation numbers referenced to Volume I. The parameters (ρ_p, ϕ_p) define (X_p, Y_p) in cylindrical coordinates.

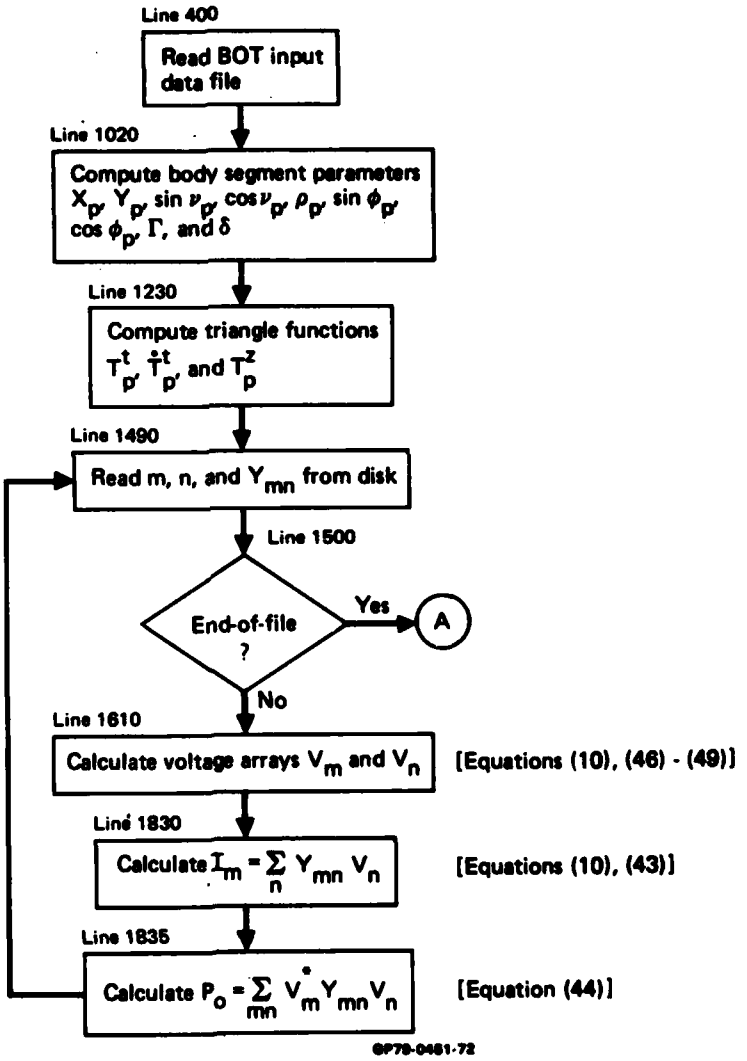

Figure 30. BOTRA flow diagram.

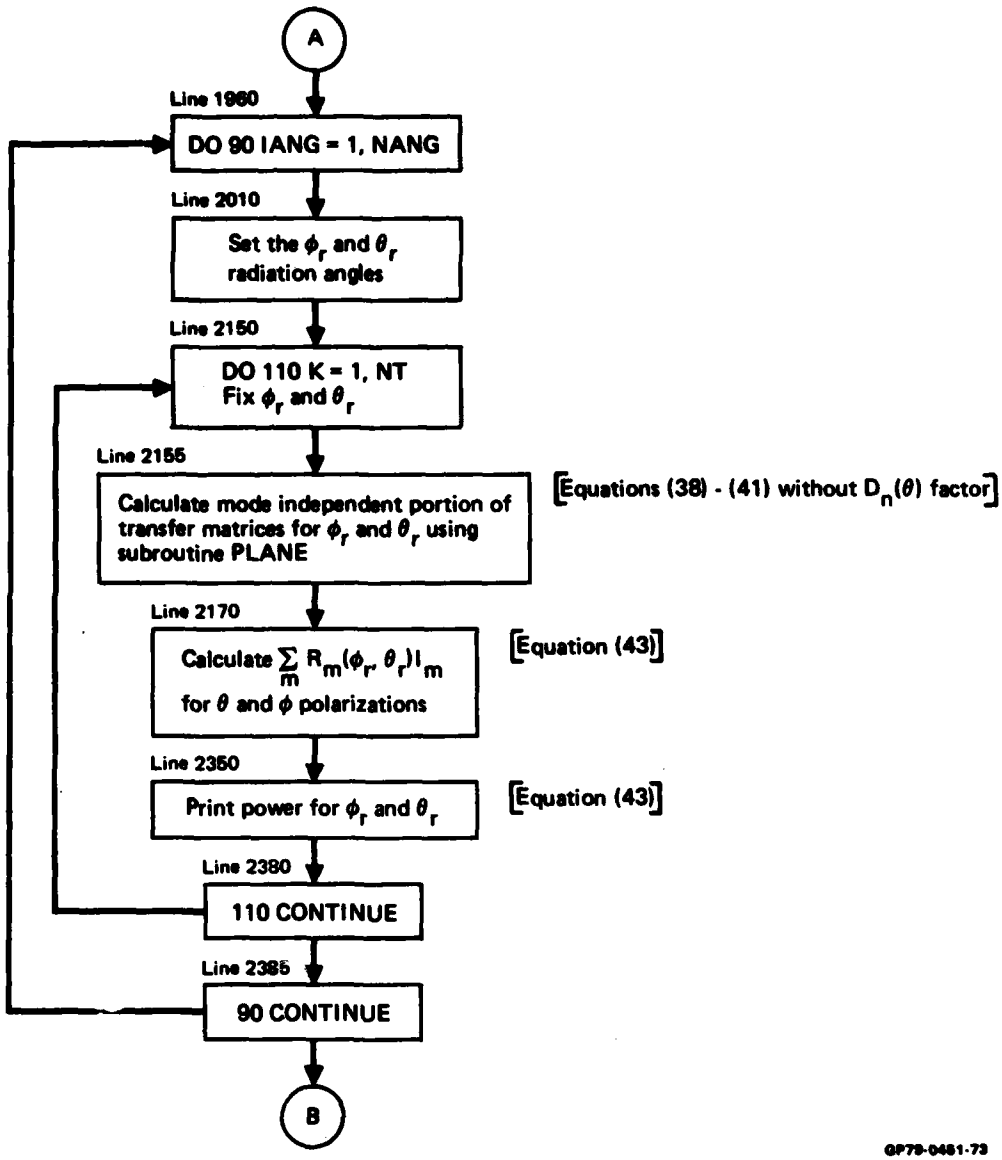

Figure 30. BOTRA flow diagram. (continued)

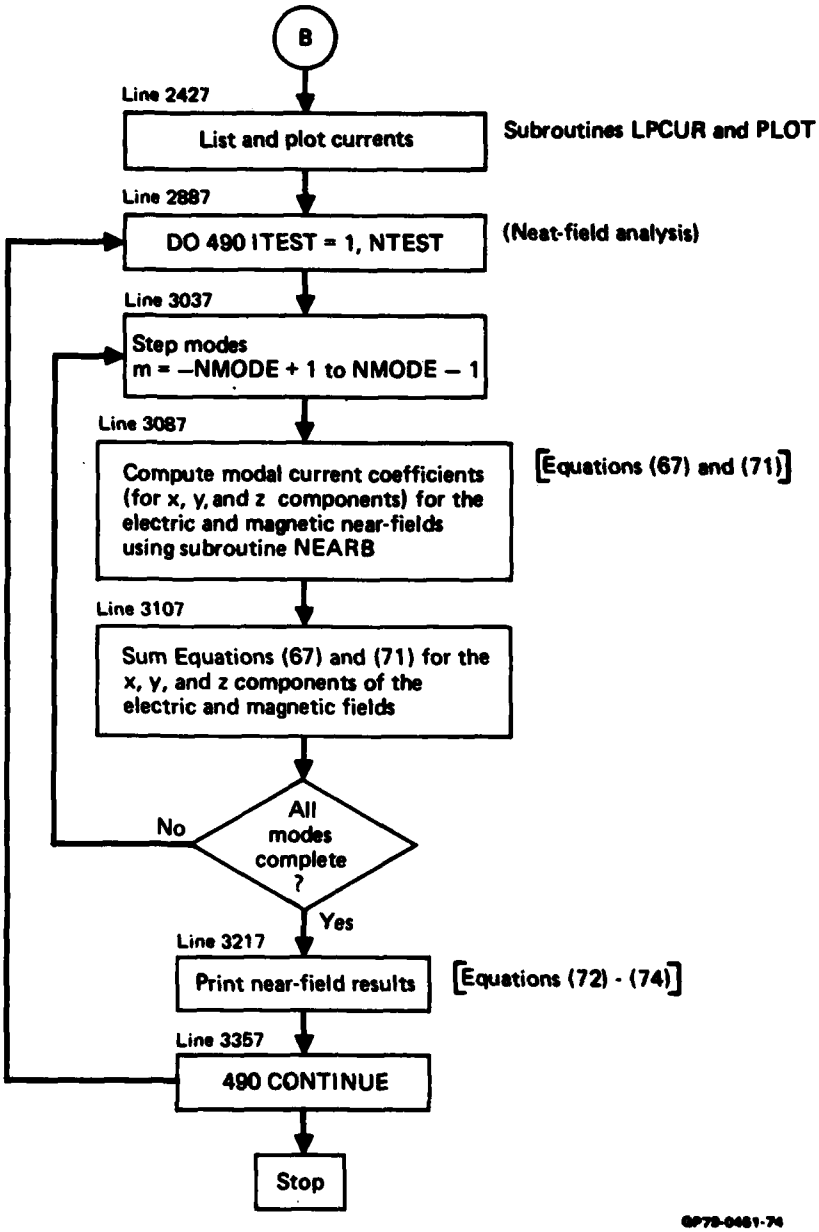

Figure 30. BOTRA flow diagram. (concluded)

3.6 BOTRA Subroutines

3.6.1 Subroutine PLANE

Subroutine PLANE computes the mode independent part of the transfer matrices given in Equations (34-37) of Volume I. The calling statement and argument list is given below:

```
CALL PLANE(RT,RP,TH,NT,PHI),
```

where

RT - Array containing the mode independent part of the θ polarized transfer matrices, for NT different angles. See variable RT in Appendix A for storage details.

RP - Array containing the mode independent part of the ϕ polarized transfer matrices, for NT different angles. See variable RP in Appendix A for storage details.

INPUT: TH - Array containing the NT θ angles.

NT - Number of transfer matrices to be calculated, corresponding to the angles in arrays TH and PHI.

PHI - Array containing the NT ϕ angles.

In addition, the body parameters are passed to subroutine PLANE in the common block BODY. The parameters in BODY are described in Appendix A.

3.6.2 Subroutine NEARB

Subroutine NEARB calculates the electric and magnetic modal current coefficients for the near-field calculations (see Section 6 of Volume I). The flow diagram for NEARB is shown in Figure 31. The calling statement and argument list is described below:

```
CALL NEARB(XTEST,YTEST,ZTEST,ZM),
```

where

INPUT: XTEST - x coordinate of test point.

YTEST - y coordinate of test point.

ZTEST - z coordinate of test point.

OUTPUT: ZM - Array of modal current coefficients for mode M. Storage details are given in the appendix.

In addition, other variables are passed to NEARB in common blocks BODY, TEST, and INT. These variables are described in Appendix A.

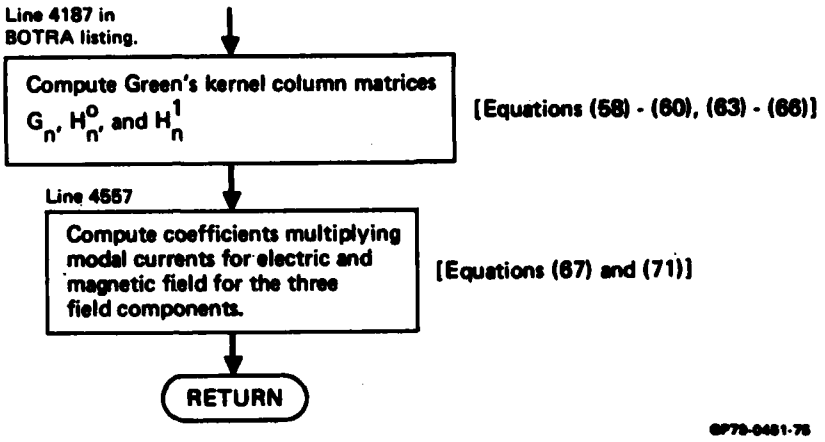

Figure 31. Subroutine NEARB flow diagram.

3.6.3 Subroutine LPCUR

Subroutine LPCUR lists and plots the BOT currents. The entire array of t and z directed modal currents is first printed, followed by plots of the t and z directed currents (magnitude and phase as a function of the normalized z coordinate) for each triangle function on the body. The calling statement and argument list follows:

```
CALL LPCUR(NMODE,NM,CUR),
```

where all of the input variables are described in Appendix A.

3.6.4 Subroutine PLOT

Subroutine PLOT plots the magnitude and phase of the currents on a given triangle function. The calling statement is as follows:

```
CALL PLOT(Y1,Y2),
```

where

INPUT: Y1 - Array containing the current magnitude at 41 equally spaced z coordinates.

Y2 - Array containing the current phase at 41 equally spaced z coordinates.

3.7 BOTSCM Program

BOTSCM computes scattered far fields in the monostatic mode (see Section 5.2 of Volume I). Figure 32 shows the flow diagram for BOTSCM with equation numbers referenced to Volume I. All of the subroutines called by BOTSCM are described in the BOTRA subroutine section. In the flow diagram, all transfer matrices are computed in one call to PLANE, while in BOTRA and BOTSCM, one transfer matrix is calculated at a time.

3.8 BOTSCB Program

BOTSCB computes scattered far fields in the bistatic mode, after which scattered near fields can be calculated with or without an aperture present. Figure 33 shows the flow diagram for BOTSCB with equation numbers referenced to Volume I.

3.9 BOTSCB Subroutines

Subroutines PLANE, NEARB, LPCUR, and PLOT are described in the BOTRA subroutine section. Subroutine LINEQ is described in the BOTINV subroutine section.

3.9.1 Subroutine APPAR

Subroutine APPAR calculates the aperture parameters LT, VLOW, VHGH, IT, and NAM which are described in Appendix A. These variables are returned in common block S. The calling statement and input parameter list is as follows:

```
CALL APPAR(XO,YO,X1,Y1,XH,YH,DH,NP,IEDGE),
```

where

XO, YO, X1, Y1 - Described in the user input section (Section 2).

XH, YH, DH, NP, IEDGE - Described in Appendix A.

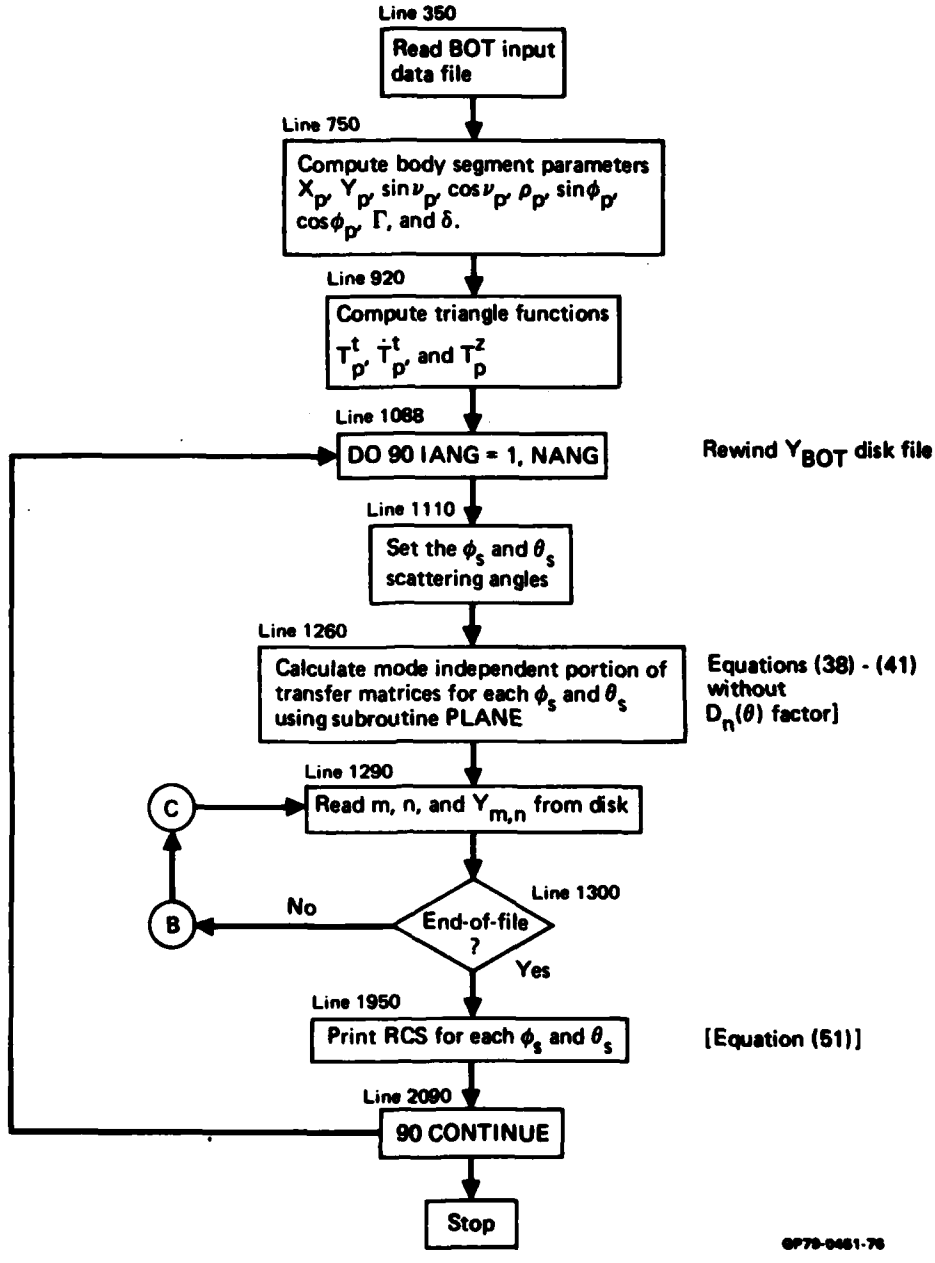

Figure 32. BOTSCM flow diagram.

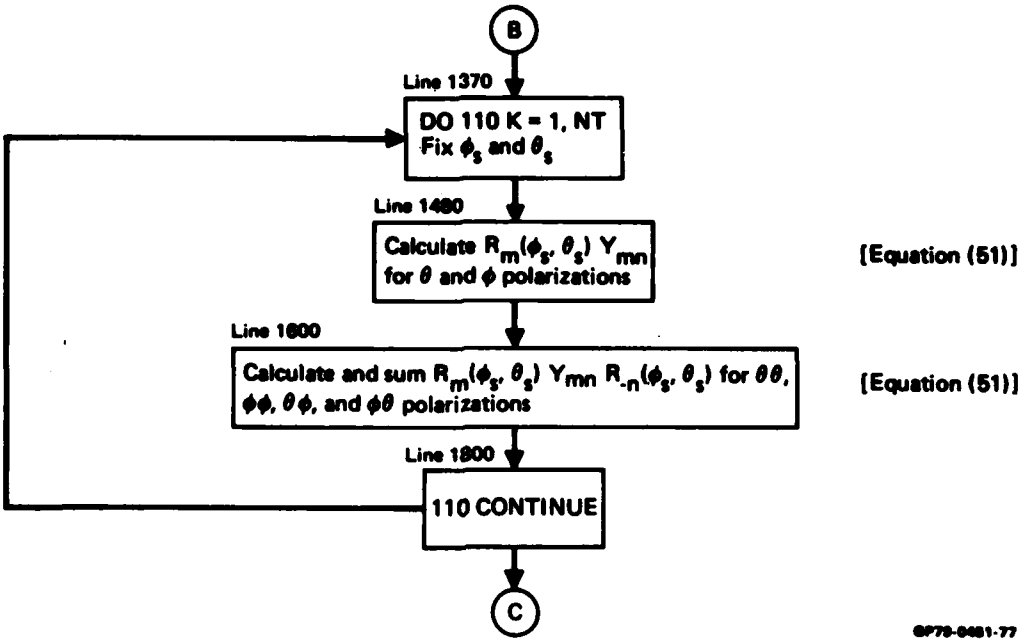

Figure 32. BOTSCM flow diagram. (concluded)

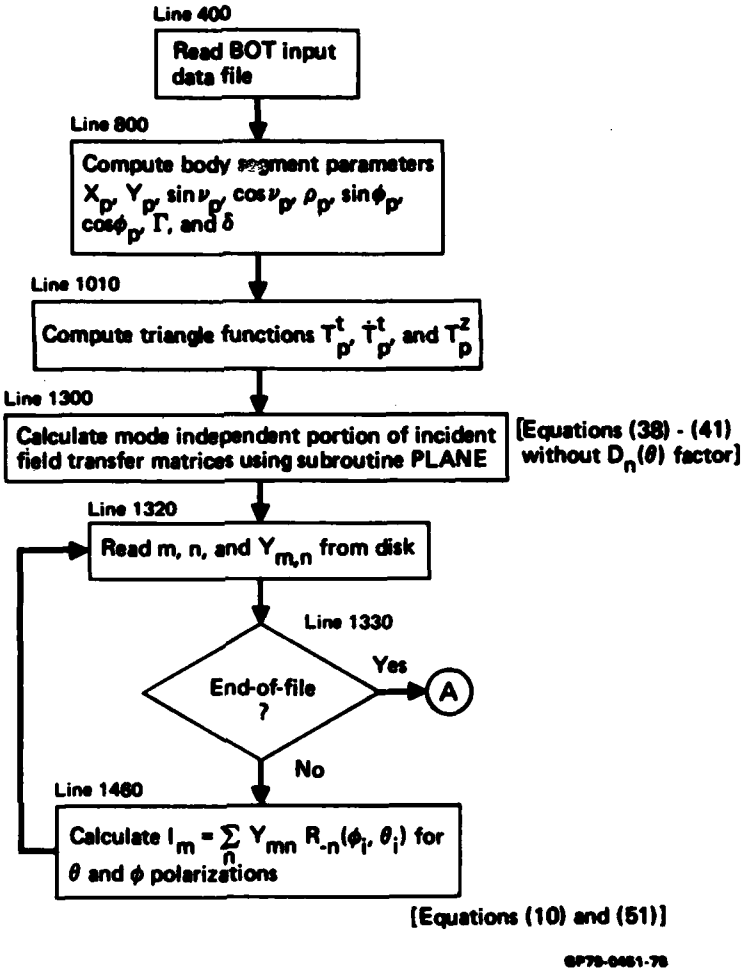

Figure 33. BOTSCB flow diagram.

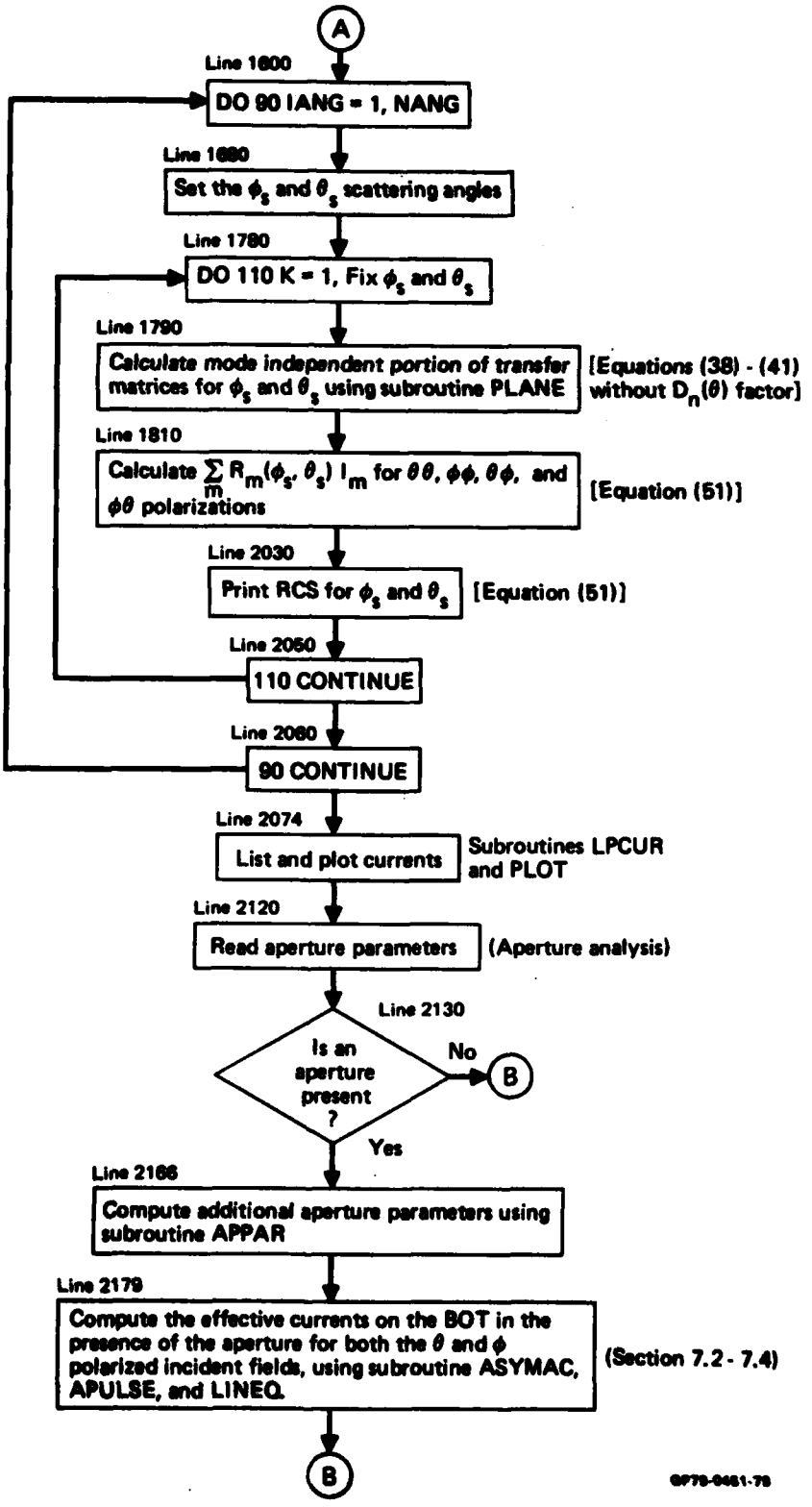

Figure 33. BOTSCB flow diagram. (continued)

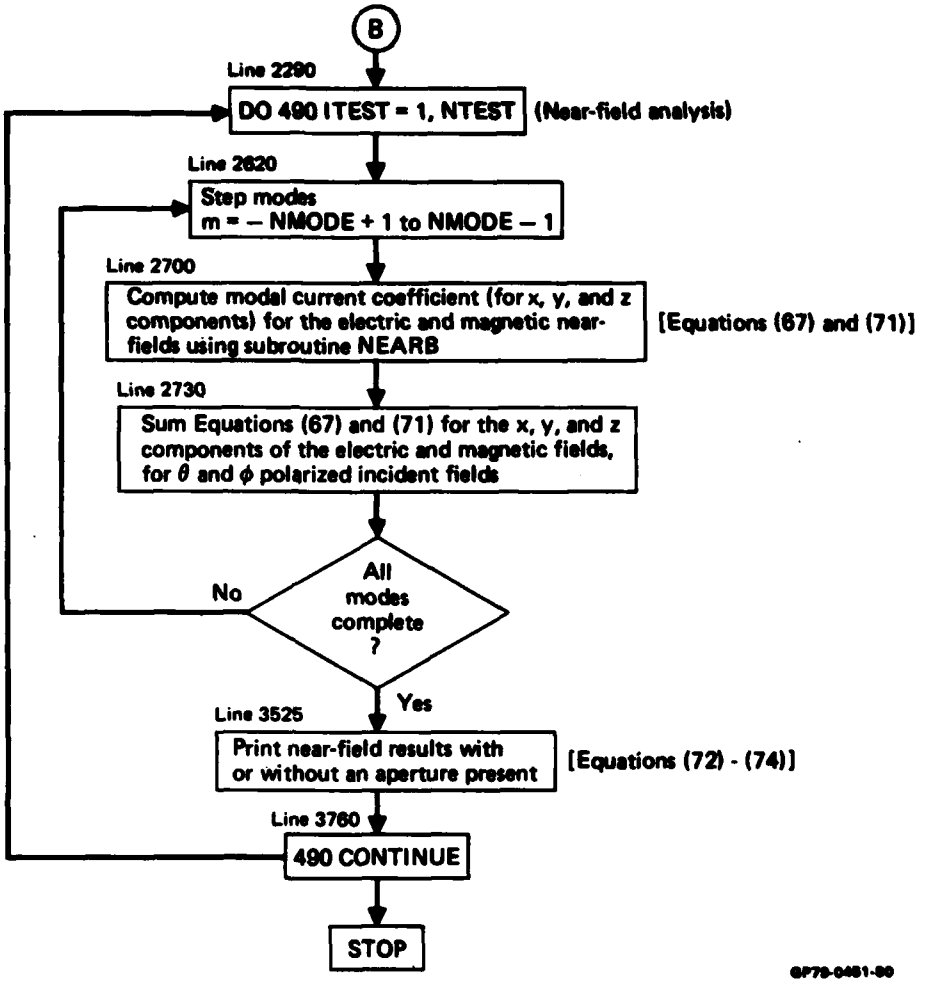

Figure 33. BOTSCB flow diagram. (concluded)

3.9.2 Subroutine APULSE

Subroutine APULSE computes the t- and z-directed aperture pulse functions. The calling statement and argument list is described below:

CALL APPAR(FPP(1,J),FPPZ(1,J),IT(J),LT(J),VLOW(J),VHGH(J),DH),

where

OUTPUT: FPP(1,J),FPP(2,J),FPP(3,J) - The three t-directed aperture pulse functions corresponding to aperture triangle function J are returned in these three successive storage

locations. See variable FPP in the appendix for storage details.

FPPZ(1,J),FPPZ(2,J),FPPZ(3,J) - The three z-directed aperture pulse functions corresponding to aperture triangle function J are returned in these three successive storage locations.

INPUT: IT(J),LT(J),VLOW(J),VHGH(J) - Aperture parameters corresponding to the J-th aperture triangle function, as described in Appendix A.

DH - Array containing BOT segment lengths.

3.9.3 Subroutine ASYMAC

Subroutine ASYMAC computes the equivalent BOT currents in the presence of an asymmetric aperture (the underlying analysis is given in Section 7 of Volume I). The flow diagram for ASYMAC is shown in Figure 34. The calling statement and argument list is described below:

CALL ASYMAC(NMODE,ZO,Z1,Y,CURT,CURP,VT,VP,NM,DH),

where

INPUT: NMODE, ZO, Z1 - Described in user input section.

Y - Work array of length LS^2 used to store the $Y_{m,n}$ submatrices as they are read from disk file.

CURT - Array of modal currents (resulting from a θ-polarized incident wave) on the BOT without an aperture present. On returning from ASYMAC, the array CURT will contain the modal currents on the BOT with the aperture present.

CURP - Array of modal currents (resulting from a ϕ-polarized incident wave) on the BOT without an aperture present. On returning from ASYMAC, the array CURP will contain the modal currents on the BOT with the aperture present.

VT - Work array of length LS.

VP - Work array of length LS.

NM, DH - Described in Appendix A.

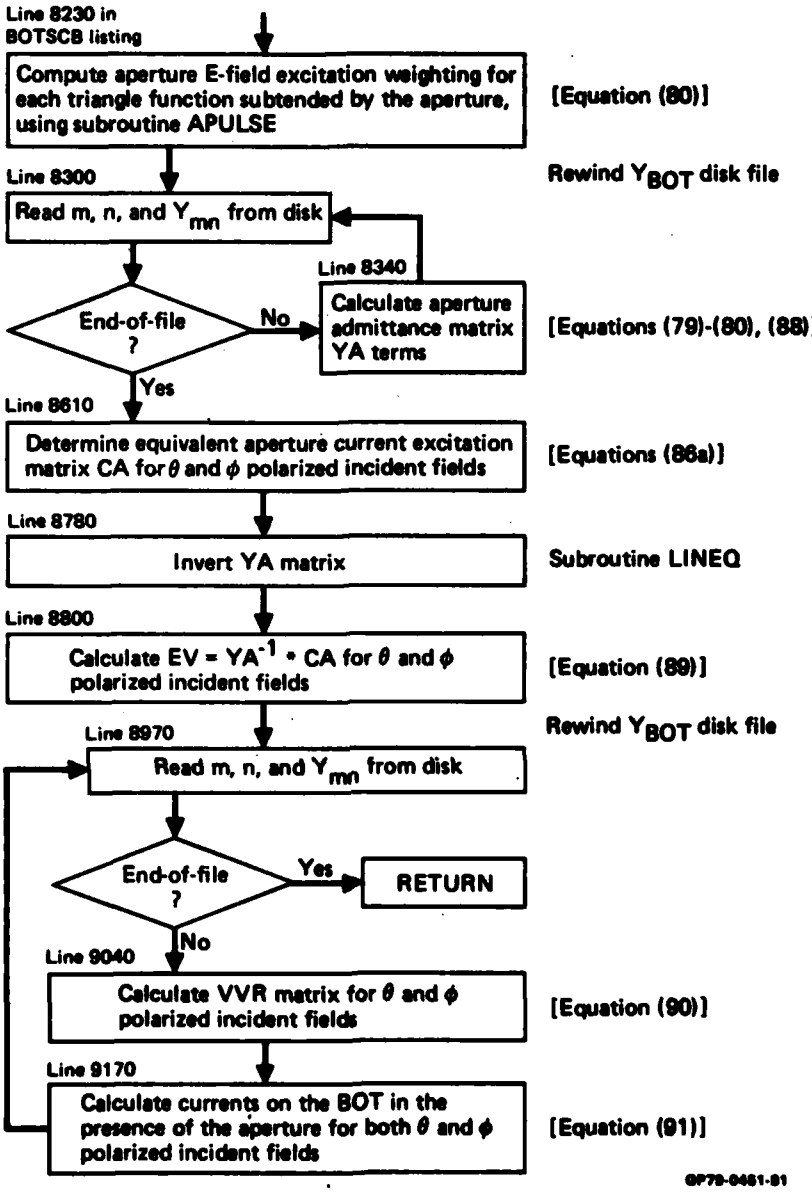

Figure 34. Subroutine ASYMAC flow diagram.

APPENDIX A: DICTIONARY OF COMMON PROGRAM VARIABLES

(Input variables are described in Section 2.3; equation numbers refer to expressions in Volume I; page numbers refer to Volume II)

ANG - Input array of fixed radiation or scattering angles (p. 8).

BK - Wave number (meters^{-1}).

BKL - BK*L.

CAP - Array containing equivalent aperture currents resulting from a ϕ-polarized incident wave [Equation (86)]. CAP(J) contains the t-directed current on the J-th aperture triangle function (i.e., C_{ap}^{t}). The z-directed current (i.e., C_{ap}^{z}) is stored in CAP(J + NAM).

CAT - Array containing equivalent aperture currents resulting from a θ-polarized incident wave [Equation (86)]. See variable CAP for storage details.

CP(I) - Cosine of ϕ angle for generating curve segment I. (See Figure 5 of Volume I.) Corresponds to $\cos\phi_q$ in Equations (38)-(41).

CUR - Array containing modal t- and z-directed currents on the BOT [Equation (10)]. CUR [(m + NMODE - 1)*LS + J] contains the t-directed current for mode m on triangle function J. The z-directed current is stored in CUR [(m + NMODE - 1)*LS + J + NM]. Used in BOTRA.

CURP - Array containing modal t- and z-directed currents on the BOT for a ϕ-polarized incident wave [Equation (10)]. See variable CUR for storage details. Used in BOTSCB.

CURT - Array containing modal t- and z-directed currents on the BOT for a θ-polarized incident wave [Equation (10)]. See variable CUR for storage details. Used in BOTSCB.

CV(I) - Cosine of ν_p angle for generating curve segment I. (See Figure 5 of Volume I.) [Equation (17)]. CV(J) corresponds to ν_q on segment J.

DELTA - GAMMA/L.

DH(I) - Length of generating curve segment I (meters).

DTOR - $\pi/180°$.

ESC - Array containing electric near-field radiation components of $\vec{E}(r')$ in the x, y, and z directions [Equation (67)], stored in ESC(1-3), respectively. Used in BOTRA.

ESCP - Array containing electric near-field scattering components resulting from a ϕ-polarized incident wave [Equation (67)]. Used in BOTSCB.

ESCT - Array containing electric near-field scattering components resulting from a θ-polarized incident wave [Equation (67)]. Used in BOTSCB.

EO - Input array for slot antenna excitation [Equation (46)]. (p. 9)

ETA - $\eta = \sqrt{\mu_o/\varepsilon_o} = 376.707\ \Omega$.

EVP - Array containing aperture E-fields resulting from a ϕ-polarized incident wave [Equation (89)]. EVP(J) contains the t-directed E-field on the J-th aperture triangle function. The z-directed E-field is stored in EVP(J + NAM). EVP(J) = EV^t_q; EVP(J + NAM) = EV^z_q.

EVT - Array containing aperture E-fields resulting from a θ-polarized incident wave [Equation (89)]. See variable EVP for storage details.

FPP - Matrix containing the t-directed pulse functions on the aperture, $F^{\alpha}_{j,q}$ with α = t [Equation (80)]. FPP(I = 1 to 3, J) contains the three pulse functions $F^t_{j-1,p}$, $F^t_{j,p}$, and $F^t_{j+1,p}$ for the J-th aperture triangle function.

FPPZ - Matrix containing the z-directed pulse functions on the aperture, $F^{\alpha}_{j,q}$ with α = z [Equation (80)]. See variable FPP for storage details.

G - Array containing the integrated Green's function kernel $G_{m,n}$ [Equation (21)]. In BOTZSS, G is symmetric with only the upper triangular portion stored by columns from index 1 to (NP - 1)* NP/2. $G_{i,j}$ is stored in location G[i + (j - 1)*j/2] when $i \leq j$.

GAMMA - Half length of a triangle function base (meters).

GP - Array containing the fields for the NT radiation angles [Equation (43)] to compute ϕ-polarized gain.

GT - Array containing the fields for the NT radiation angles [Equation (43)] to compute θ-polarized gain.

HO - Array containing the integrated Green's function kernel $H_n^o(q)$, ($\gamma = 0$) [Equation (63)] for the magnetic near fields [Equations (63)-(66)].

H1 - Array containing the integrated Green's function kernel $H_n^{'}(q)$, ($\gamma = 1$) [Equation (63)] for the magnetic near fields [Equations (63)-(66)].

HSC - Array containing magnetic near-field radiation components in the x, y, and z directions [Equation (71)]. HSC = $\vec{H}(r')$, used in BOTRA.

HSCP - Array containing magnetic near-field scattering components resulting from a ϕ-polarized incident wave [Equation (71)]. HSCP = $\vec{H}(r')$, used in BOTSCB.

HSCT - Array containing magnetic near-field scattering components resulting from a θ-polarized incident wave [Equation (71)]. HSCT = $\vec{H}(r')$, used in BOTSCB.

IEDGE - Indicates whether the generating curve is open or closed. IEDGE = 0 for closed and 1 for open.

IPLANE - Input array indicating whether corresponding element of array ANG is a θ or ϕ angle. (p. 8).

IS - Input array for specifying location of slot antennas. [See Equations (46)-(49).] (p. 9).

IT(K) - Indicates whether aperture segment K starts or terminates the aperture. IT = - 1 for the start, IT = 0 for interior, and IT = + 1 for termination.

KG - NP - 1.

L - Half length of the BOT (meters).

LS - Order of each $Z_{m,n}$ submatrix. LS = NP - 3.

LSS - LS*LS

LT(K) - Triangle function peak number for aperture segment K.

M - Mode number m.

MC - Input variable. M in Equation (26). (p. 7).

N - Mode number n.

NAM - Number of triangle function peaks on the aperture portion of the generating curve. NAM should be greater than 1, if an aperture is present.

NAM2 - NAM*2.

NANG - Input variable. Number of fixed radiation or scattering angles. (p. 8).

NBAND - Input variable. Number of submatrix diagonal bands used in Z_{BOT}^{-1}. (p. 7).

NM - Number of triangle functions on the BOT generating curve. NM = (NP - 3)/2.

NMODE - Input variable. Number of non-negative modes. (p. 6).

NM2 - Order of each $Z_{m,n}$ submatrix. NM2 = NP - 3.

NM4 - NM*4.

NP - Number of points on the BOT generating curve. (See Section 2.4.)

NPT - Input variable. Number of diagonal bands used in impedance matrices. (p. 7).

NSA - Number of slot antennas on the BOT.

NT - Input variable. Number of radiation and scattering angles. (p. 8).

NTEST - Input variable. Number of test points for near-fields. (p. 10).

PHII - ϕ angle for the incident wave (degrees). PHII = ϕ_i in Equation (51).

PHIR(K) - ϕ angle for the radiated fields (degrees). PHIR(K) = ϕ_r in Equation (38).

PHIS(K) - ϕ angle for the scattered fields (degrees). PHIS(K) = ϕ_s in Equation (51).

R(I) - Distance from origin ρ_q to generating curve segment I (meters) [used in A_q^r in Equations (38)-(41)].

RP - Array containing the mode independent portion of the $R_n^{t\phi}$ and $R_n^{z\phi}$ matrices (i.e., with the α term removed), resulting from a ϕ-polarized incident wave [Equations (40)-(41)]. The order of storage is

$\left\{(R_n^{t\phi})_i,\ i = 1 \text{ to } NM\right\}$ followed by

$\left\{(R_n^{z\phi})_i,\ i = 1 \text{ to } NM\right\}$

RP may contain the transfer matrices for several (ϕ, θ) angles. In this case, the starting index is off-set by a multiple of 2*NM.

RT - Array containing the mode-independent portion of the $R_n^{t\theta}$ and $R_n^{z\theta}$ matrices (i.e., with the α term removed), resulting from a θ-polarized incident wave [Equations (38)-(39)]. The order of storage is

$\left\{(R_n^{t\theta})_i,\ i = 1 \text{ to } NM\right\}$ followed by

$\left\{(R_n^{z\theta})_i,\ i = 1 \text{ to } NM\right\}$

As in RP, the starting index may be off-set by a multiple of 2*NM.

SP(I) - Sine of ϕ angle for generating curve segment I. (See Figure 5 of Volume I.) Corresponds to $\sin\phi_q$ in Equations (38), (40).

SPP - Array containing $\sigma^{\phi\phi}$ for the NT scattering angles [Equation (51)].

SPT - Array containing $\sigma^{\phi\theta}$ for the NT scattering angles [Equation (51)].

STP - Array containing $\sigma^{\theta\phi}$ for the NT scattering angles [Equation (51)].

STT - Array containing $\sigma^{\theta\theta}$ for the NT scattering angles [Equation (51)].

SV(I) - Sine of ν_p angle for generating curve segment I. (See Figure 5 of Volume I.) [Equation (17).] SV(J) corresponds to ν_q on segment J.

T - Array containing the values of the triangle functions T_p^t. T[(K - 1)*4 + p] contains the values of the kth triangle function over the p-th segment forming it. $1 \leq p \leq 4$. [Equations (17)-(20).] (p. 6).

TEXC - Input array indicates t-excitation on slot antenna. (p. 9).

THI - θ angle for the incident wave (degrees). THI = θ_i in Equation (51).

THR(K) - θ angle for the radiated fields (degrees). THR(K) = θ_r in Equation (43).

THS(K) - θ angle for the scattered fields (degrees) [Equation (51)].

TP - Array containing the values of $\dot{T}_p^t$. The storage method is the same as for T [Equations (17)-(20)]. (p. 6)

TZ - Array containing the values of T_p^z. The storage method is the same as for T [Equations (17)-(20)].

U - Imaginary number i.

UMN - Array containing values of the u_{mn} function [Equation (23)] needed in numerical integration of the Green's function kernel. [See Equation (27).]

VHGH(I) - Upper "part" width associated with I-th aperture port.

VLOW(I) - Lower "part" width associated with I-th aperture port.

VM - Array of voltages corresponding to mode M. VM(K) contains t-directed voltages V_{mi}^{t} on triangle function K. VM(K + NM) contains z-directed voltages V_{mi}^{z} on triangle function K [Equation (11)].

VN - Array of voltages corresponding to mode N. The storage method is the same as for VM [Equation (11)].

VP - Array containing the equivalent BOT voltages with an aperture present, resulting from a ϕ-polarized incident wave [Equation (90)]. VP(J) is V_{mj}^{t} and contains the t-directed voltage on the BOT triangle function J. The z-directed voltage V_{mj}^{z} is stored in VP(J + NM).

VT - Array containing the equivalent BOT voltages with an aperture present, resulting from a θ-polarized incident wave [Equation (90)]. VT(J) contains the t-directed voltage on the BOT triangle function J. The z-directed voltage is stored in VT(J + NM).

XO - Starting x coordinate for aperture. (p. 10).

X1 - Ending x coordinate for aperture. (p. 10).

XH - Input array of x coordinates for BOT. (p. 7).

XS(I) - x coordinate for generating curve segment I (meters) [Equation (28)].

XTEST - Input variable for near-field test point x' in r' [Equations (67), (71)]. (p. 10).

Y - Array containing the $Y_{m,n}$ submatrix [Equations (43), (51)]. In the near-field analysis, however, Y contains the measurement matrix ZM. $Y_{m,n}$ is stored by columns.

YO - Starting y coordinate for aperture. (p. 10).

Y1 - Ending y coordinate for aperture. (p. 10).

YA - Array containing the aperture admittance matrix, stored by columns [Equation (88)]. YA is of order NAM.

YH - Input array of y coordinates for BOT. (p. 7).

YP - Array used as intermediate storage, containing $R_{m}^{\phi}(\phi_s, \phi_s)\, Y_{m,n}$ for a given m, n, and scattering angle [Equation (51)].

YS(I) - y coordinate for generating curve segment I (meters) [Equation (28)].

YT - Array used as intermediate storage, containing $R_m^{\theta}(\phi_s, \theta_s)\, Y_{m,n}$ for a given m, n, and scattering angle [Equation (51)].

YTEST - Input variable for near-field test point y' in r' [Equations (67), (71)]. (p. 10).

Z - Array containing the $Z_{m,n}$ submatrix [Equations (10), (17)-(20)]. In the program BOTINV, however, Z contains the entire Z_{BOT} matrix. $Z_{m,n}$ is stored by columns.

ZEXC - Input array [Equation (48)].

ZM - Array containing the electric and magnetic modal current coefficients for near-field calculations [Equations (67), (71)]. ZM uses the same storage location as the Y matrix, which is of order LS, stored by columns. Rows 1 through 3 of ZM contain the M-th modal current coefficients for the electric near-field components in the x, y, and z, respectively, at the point (XTEST, YTEST, ZTEST). Similarly, rows 4 through 6 of ZM contain the M-th modal current coefficients for the magnetic near-field components in the x, y, and z directions, respectively.

ZTEST - Input variable for near-field test point z' in r' [Equations (67), (71)]. (p. 10).

ZO - Input. ZO has different definitions in the programs BOTRA and BOTSCB [Equation (49)]. (p. 10).

Z1 - Input. Z1 has different definitions in the programs BOTRA and BOTSCB [Equation (49)]. (p. 10).

APPENDIX B: SUBROUTINE CALLING PROGRAMS (BOTZSS, BOTINV, BOTRA, BOTSCM, AND BOTSCB ARE MAIN PROGRAMS)

Subroutine	Calling program
APPAR	BOTSCB
APULSE	ASYMAC
ASYMAC	BOTSCB
CSIMP	BOTZSS
DBCON	BOTRA, BOTSCB, BOTSCM
FUNC	CSIMP
INVBAN	BOTINV
LINEQ	ASYMAC, BOTINV, INVBAN
LIST	BOTINV, INVBAN
LPCUR	BOTRA, BOTSCB
MULT	INVBAN
MULTS	INVBAN
NEARB	BOTRA, BOTSCB
PLANE	BOTRA, BORSCB, BOTSCM
PLOT	LPCUR
PLOTB	BOTZSS
REPLACE	INVBAN
SINC	BOTRA, BOTSCB, BOTSCM
ZERO	INVBAN

GP78-0461-82